PhD degree in Systems Medicine (curriculum in Molecular Oncology)

European School of Molecular Medicine (SEMM),

University of Milan and University of Naples "Federico II"

Settore disciplinare: BIO/11

Crosstalk between PRC1 and PRC2 in intestinal lineage commitment and cell identity

Amato Simona

IEO, Milan

Matricola n. R12429

Supervisor: Dr. / Prof. Pasini Diego

European Institute of Oncology (IEO), Milan

Anno accademico 2021-2022

TABLE OF CONTENTS

LIST OF ABBREVIATIONS

APC	Adenomatous Polyposis Coli
ATOH1	Atonal BHLH Transcription Factor 1
AUTS2	Activator of Transcription and Developmental Regulator
BAP1	BRCA1 Associated Protein 1
BCOR	BCL6 Corepressor
BMP	Bone Morphogenetic Protein
BRD4	Bromodomain containing 4
CBX	Chromobox
ChIP	Chromatin Immunoprecipitation
cPRC1	canonical Polycomb Repressive Complex 1
CRC	Colorectal Cancer
dKO	double knockout
DUB	DeUbiquitinase
EED	Embryonic Ectoderm Development
EGF	Epidermal Growth Factor
EPOP	Elongin BC and Polycomb Repressive Complex 2 Associated Protein
EZH	Enhancer of Zeste
EZHIP	EZH Inhibitory Protein
FBS	Fetal Bovine Serum
GFI1	Growth Factor Independent 1 Transcriptional Repressor
GFP	Green Fluorescent Protein
HES	Hairy/Enhancer of Split
HOTAIR	HOX transcript antisense RNA
HOX	Homeobox
HSC	Human Stem Cell
ICM	Inner Cell Mass
IFN	Interferon
IP	Immunoprecipitation
ISC	Intestinal Stem Cell
JARID2	Jumonji and AT-Rich Interaction Domain Containing

	2
KDM2B	Lysine-specific Demethylase 2B
KO	Knockout
LoxP	Locus of Crossover in Phage P1
LGR5	Leucine-Rich Repeat Containing G Protein- Coupled Receptor 5
MAPK	Mitogen-activated Protein Kinase
ME	Methylation
MEDS	Mosaic Ends Double-Stranded oligonucleotides
mESC	mouse Embryonic Stem Cell
MPNST	Malignant Peripheral Nerve Sheath Tumors
MS	Mass Spectrometry
NICD	Notch Intracellular Domain
NDD	Neurodevelopmental Disorders
OCT	Optimal Cutting Temperature
OCT4	Octamer-binding transcription factor 4
PALI	PRC2-associated LCOR isoform 1
PcG	Polycomb Group of Proteins
PCGF	Polycomb Group Ring Finger protein
PCL	Polycomb-like Protein
PCR	Polymerase Chain Reaction
PHC	Polyhomeotic-like protein
PHF	PHD finger protein
PTM	Post-Translational Modification
PRC1	Polycomb Repressive Complex 1
PRC2	Polycomb Repressive Complex 2
qKO	quadruple Knockout
QPCR	Real Time quantitative PCR
RAWUL	Ring finger and WD40 Ubiquitin-Like
RBBP	Retinoblastoma-associated Protein
RBPJ	Recombination Signal Binding Protein for Immunoglobulin Kappa J Region
RING1	Really Interesting New Gene 1
RT	Room Temperature
RYBP	Ring and YY1 Binding Protein

SAM	Sterile Alpha Motif
SOX2	SRY (Sex Determining Region Y)-box 2
SUZ12	Suppressor of Zeste 12
TCF/LEF	T-cell factor/lymphoid Enhancer Factor
TF	Transcription Factor
tKO	tryple Knockout
TMA	Tissue MicroArray
TN5	Transposase 5
TSS	Transcription Start Site
UB	Ubiquitin
vPRC1	Variant Polycomb Repressive Complex 1
WNT	Wingless Integration site
YY1	Yin Yang 1
XIST	X Inactive Specific Transcript
ZGA	Zygote-Genome Activation
ZIC	Zing fingers of the Cerebullum

FIGURE INDEX

1. INTRODUCTION

2. MATERIALS AND METHODS

3. RESULTS

ABSTRACT

Polycomb Repressive Complexes 1 and 2 (PRC1 and PRC2) control cell identity by establishing facultative heterochromatin repressive domains at common sets of target genes, from the early stages of development to adulthood.

How they functionally preserve transcriptional silencing has been deeply explored in embryonic stem cells (ESC), but remains poorly described in an *in vivo* context.

Taking advantage of Cre-dependent conditional knockout mouse models targeting distinct Polycomb activities in the intestinal epithelium, the present work proposes to characterize the interplay among the PRC1 subcomplexes and their relationship with PRC2 activity. In particular, it functionally dissects how PRC1 and PRC2 cooperate or have independent roles to establish the epigenetic signature of intestinal cells.

Since catalytic inactivation of PRC1 (RING1A/B double knockout) affects intestinal homeostasis by exhausting the stem cell pool, we have ablated single PCGF activities (PRC1.1-1.6) to determine the role of variant (vPRC1) and canonical PRC1 (cPRC1) subcomplexes in the transcriptional identity of intestinal epithelial cells. By coupling *in vivo* studies with genome-wide analyses, we have found that none of them reproduces the effects of RING1A/B loss of function, resulting in the compensation of H2AK119ub1 deposition and gene repression.

Moreover, we have evaluated the dependency of PRC2 function on the downstream cPRC1 activity, demonstrating that PRC2 acts autonomously to control transcriptional silencing and secretory lineage commitment.

Unexpectedly, we have found that removal of PRC1.1 rescued the effects of PRC2 inactivation in lineage skewing while maintaining extensive transcriptional derepression, revealing an intimate connection between distinct Polycomb activities in the control of intestinal cell plasticity and identity.

Finally, by validating in parallel some of these *in vivo* findings in the mouse ESC model, we have also observed that promiscuous interactions between vPRC1 and cPRC1 occur, identifying a novel mechanism of functional compensation among Polycomb subcomplexes.

1. INTRODUCTION

1.1 Role of Polycomb group proteins during development

Mammalian development is a complex process in which a single totipotent cell proliferates and differentiates to produce all the different cell types composing the adult organism. The initiation of the pathways regulating these events implies the loss of pluripotency, followed by the progressive cellular commitment towards a specific cell lineage during differentiation. Such process requires an exquisite control of the gene programs in a spatiotemporal fashion. Indeed, genes that in many cases have been maintained as silent must be expressed, while a set of transcriptionally competent genes must be repressed [1].

Despite tissue-specific transcription factors play an essential role in regulating gene expression, they are not sufficient to prime differentiation cues. Changes of the chromatin structure both at the higher-order level and at lineage-specific genes are required to allow the activity of tissue-specific regulators [2].

Dynamic changes in the chromatin state, intended as the packaging of DNA with both histone and non-histone proteins, accompany developmental transitions and contribute to the establishment and maintenance of cellular identities [3].

The assembly and the compaction of chromatin are regulated by several mechanisms, including DNA modifications (for example, cytosine methylation), post-translational modifications (PTMs) of histones (such as methylation, acetylation, ubiquitylation and phosphorylation), the incorporation of histone variants (for example, H2A.Z and H3.3) and the activity of chromatin remodelers [4].

Among the chromatin regulators acting from the earliest stages of development, a pivotal role is played by Polycomb group (PcG) of proteins [5].

So far, embryonic stem cells (ESCs) have represented an excellent model to unravel the key features of cell differentiation and the role of Polycomb-mediated epigenetic regulation.

Derived from the inner cell mass (ICM) of the pre-implantation embryo at the stage of blastocyst (4 days post coitum), ESCs are pluripotent stem cells with unique properties of self-renewal. They can divide indefinitely *in vitro*, while maintaining the capacity to differentiate into any cell type of the adult organism [6,7].

Stem cells are present also in adult organisms, in which they play key functions to ensure proper tissue homeostasis and repair responses [8,9]. However, adult stem cells are

technically more difficult to obtain and maintain in the laboratory than ESCs, limiting the study of Polycomb activity in this system.

1.1.1 Overview of PcG proteins

First discovered in *Drosophila melanogaster*, PcG proteins were found to be essential for the regulation of Hox genes and normal development [10-12]. They play also important roles in several biological processes, comprising cell cycle progression, genomic imprinting, X-inactivation, differentiation and tissue homeostasis.

PcG proteins are organized in two distinct biochemical complexes, the Polycomb Repressive Complex 1 (PRC1) and the Polycomb Repressive Complex 2 (PRC2), which largely overlap in their genomic binding and cooperate to establish repressive chromatin domains. Both complexes are assembled around a catalytic core, which binds auxiliary proteins to create distinct PRC1 and PRC2 assemblies.

1.1.1.1 Polycomb Repressive Complex 1

PRC1 is composed by the catalytic subunit RING1B, or its paralogue RING1A, and one of six Polycomb group ring-finger (PCGF) proteins (PCGF1-6) [13]. RING1 and PCGFs share a similar protein structure, with an N-terminal RING domain and C-terminal RING-finger and WD40-associated ubiquitin-like (RAWUL) domain. These RING domains allow RING1 protein and PCGF dimerization, thus promoting their interaction with an E2 conjugating enzyme to enable histone ubiquitylation [14-16]. The RAWUL domain, instead, can bind to different auxiliary subunits, modulating the catalytic activity of PRC1 and its target specificity through the genome [17]. Finally, the PCGF proteins define which auxiliary subunits are included into the PRC1 complex, allowing the biochemical distinction between canonical PRC1 (cPRC1) and variant PRC1 (vPRC1) subcomplexes.

cPRC1 complexes, which were the first to be identified [18,19], contain either PCGF2 or PCGF4 along with one of five chromodomain-containing paralogues (CBX2, 4, 6, 7 or 8) and one of three Polyhomeotic subunits (PHC1, 2 or 3). On the other hand, vPRC1 complexes include one of the six PCGF proteins (PCGF1–6) with RING1 and YY1 binding protein (RYBP), or its paralogue YAF2, and other additional components according to which PCGF is present in the complex (Fig. 1.1).

Genome-wide analyses in ESCs have revealed that only the 10% of PRC1 chromatin associations depend on the RYBP/YAF2-containing complexes, while about 90% of PRC1 complexes at the chromatin assemble around CBXs, with CBX7 being the most abundant.

However, this classification should consider also PRC1 complexes in which PCGF2 and PCGF4 are associated with RYBP-RING1B, as previously identified by proteomic analysis performed in human cells [13].

The key role of PRC1 is to mono-ubiquitylate histone H2A on lysine 119. Such specificity is provided by the allosteric interaction between PRC1 and the E2 enzyme, which contacts the N-terminus of RING1B and the DNA at the nucleosome acidic path, as extensively described in independent studies [20,21].

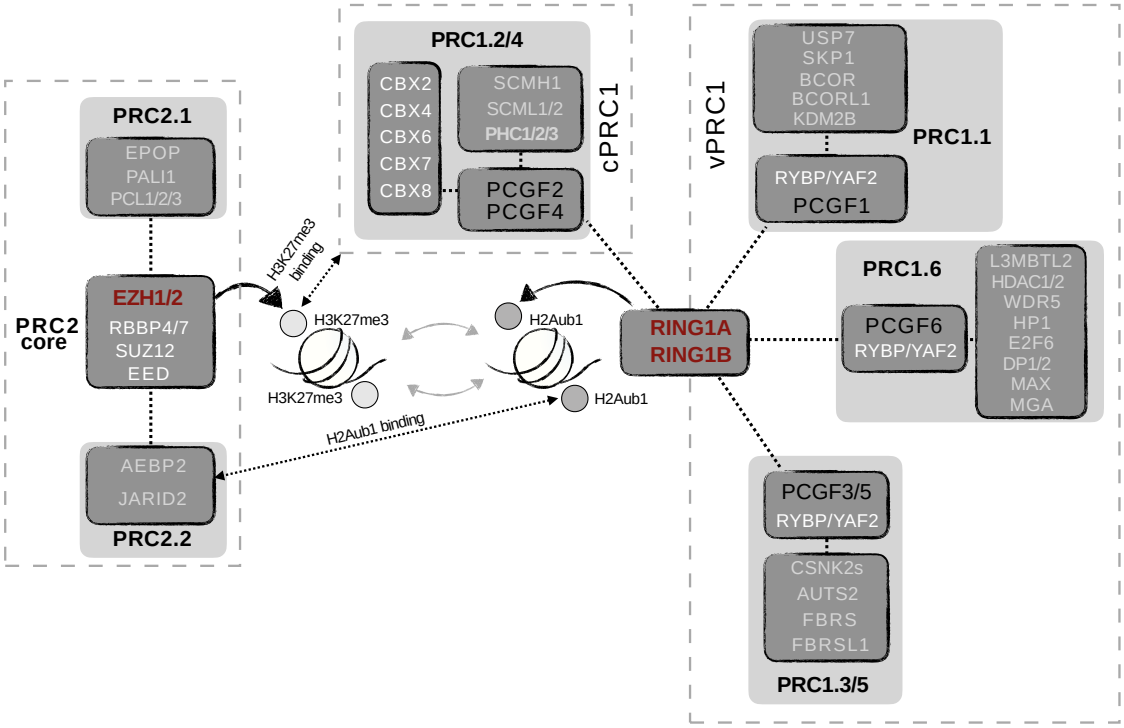

Fig. 1.1 Composition and interdependence of Polycomb Repressive Complexes

Biochemical composition of PRC1 and PRC2 complexes, highlighting their interplay in the deposition of H3K27me3 and H2AK119ub1. The figure further represents the subunits of PRC2 that provide affinity for H2AK119ub1 binding (AEBP2 and JARID2) and the subunits of PRC1 (CBX proteins) that recognize H3K27me3, allowing the distinction between cPRC1 and vPRC1 complexes (adapted from *Trends in Genetics*, Tamburri et al. 2019).

1.1.1.2 Polycomb Repressive Complex 2

PRC2 has a methyltransferase function responsible for mono-, di- and tri-methylation of lysine 27 on histone H3 (H3K27me1, H3K27me2 and H3K27me3). It is composed of one catalytic subunit, enhancer of zeste homologue 1 (EZH1) or its paralogue EZH2, and two additional core members, embryonic ectoderm development (EED) and suppressor of zeste 12 (SUZ12). All these three core components are critical for the catalytic activity of

PRC2, together with RB binding protein 4 or 7 (RBBP4/7), which bind to histone proteins [22].

Comprehensive proteomic studies have identified two mutually exclusive subcomplexes within the mammalian PRC2, PRC2.1 and PRC2.2, according their biochemical composition (Fig. 1.1) [23].

PRC2.1 contains one of three Polycomb-like proteins (PCL1/PHF1, PCL2/MTF2, or PCL3/PHF19), as well as one of the two accessory proteins Elongin BC and Polycomb Repressive Complex 2 Associated Protein (EPOP) and either PRC2-associated LCOR isoform 1 (PALI1), PALI2 or Elongin BC [24,25]. PRC2.2, instead, contains the Jumonji AT rich interactive domain 2 (JARID2) and the AE Binding Protein 2 (AEBP2) [26].

Recently, it has been shown that EZH inhibitory protein (EZHIP), a protein that is mainly expressed in germ-cells, is able to interact with the PRC2 core, inhibiting its methyltransferase activity and also blocking specific interactions with PRC2.1 and PRC2.2 subunits [27,28]. Such discovery suggests that cell type-specific regulators can modulate PRC2 functions during development.

1.1.2 Mechanisms of Polycomb recruitment to target loci

Genome-wide studies have revealed that Polycomb complexes are enriched at gene promoters and other gene regulatory elements, such as enhancers and super-enhancers [29,30].

The investigation of the mechanisms regulating PcG recruitment at specific target loci is one of the hotly debated and still undefined issues. Such mechanisms, ultimately leading to gene silencing and establishment of correct transcriptional programs, have been deeply characterized in *Drosophila*, but seem to be less conserved in vertebrates where alternative modes of recruitment have been proposed.

The primary mechanisms of Polycomb recruitment to target loci in mammals rely on CpG islands (CGIs) recognition, activity of sequence-specific DNA-binding factors and RNA-dependent mechanisms.

After having been recruited, PRC1 and PRC2 work in concert, as the catalytic activity of one complex influences the chromatin occupancy of the other and the resulting establishment of Polycomb chromatin repressive domains.

Although in some specific cases transcription factors and lncRNAs contribute to locus-specific recruitment of PRCs, these generic targeting mechanisms can limitedly explain the widespread, and often tissue-specific, PcG binding patterns that are observed *in vivo*.

1.1.2.1 Targeting to CpG islands

By performing genome-wide mapping studies, it has been discovered that Polycomb complexes associate primarily with CGIs [31]. CGIs are short regions (1–2 kb) containing a large number of CpG dinucleotide repeats that are associated with approximately 70% of mammalian gene promoters [32]. Such regions are absent in non-vertebrate model organisms, such as *Drosophila*. In CGIs, CpG dinucleotides lack DNA methylation, but are heavily methylated elsewhere in the genome where they serve to maintain heterochromatin and silence the expression of parasitic DNA elements [33]. The presence of methylated sites in CpG dinucleotides antagonizes the contact with the PRC2, since the binding of EED is prevented when a methylated CGI is incorporated in nucleosomes [34].

The first evidence that binding to CGIs may be crucial for Polycomb recruitment comes from the biochemical isolation of the PCGF1-vPRC1 complex, stably incorporating lysine-specific demethylase 2B (KDM2B) [35]. KDM2B specifically binds to non-methylated CGIs through its zinc finger-CxxC domain [36]. Recruitment of KDM2B to promoters leads to H2AK119ub1 deposition, followed by PRC2 binding and H3K27me3-mediated silencing [37]. In addition, removal of the ZF-CxxC domain of KDM2B halves the number of RING1B binding sites in mouse ESCs. CGI binding is also central to target-site identification by PRC2 since PCL proteins of PRC2.1 complexes can bind to non-methylated CGIs through a winged-helix domain [38].

1.1.2.2 Target site recognition through DNA-binding factors

Despite the high degree of conservation of PcG proteins between species, the consensus sequences required for Polycomb recruitment to chromatin can vary significantly. In *Drosophila*, the targeting of PRCs to their specific genomic sites is mediated by Polycomb Response Elements (PREs) [39]. Such sequences are absent in mammals, where Polycomb recruitment can be influenced by a variety of transcription factors (TFs), as suggested by the co-localization of PcG subunits with the pluripotency factors OCT4, SOX2 and NANOG [40-42].

It has been recently demonstrated that the TFs MGA and E2F6 can promote PCGF6 recruitment to chromatin and that the interaction between PCGF3 and USF1 mediates PRC1 tethering on the chromatin [43,44].

Other DNA-binding factors including REST, RUNX1 and SNAIL1 have been proposed to contribute to PRC1 or PRC2 targeting in cell-specific context [45-47].

1.1.2.3 Target site identification through long-non coding RNA

In the last few years an increasing number of long-non coding RNAs (lncRNAs) have been proposed to functionally interact with Polycomb Repressive Complexes.

The most characterized PcG-lncRNA interactions include (a) the recruitment of Polycomb complexes to the inactivating X-chromosome through *Xist*; (b) the Polycomb-mediated transcriptional silencing of the *HoxD* locus via direct interaction with HOTAIR; (c) the PRC1 recruitment to the *Ink4a-Arf* locus by the ANRIL ncRNA.

Both PRC1 and PRC2 complexes decorate the inactive X-chromosome (Xi) in mammals depositing H2AK119ub1 and H3K27me3, respectively.

PRC2 coating of the Xi is mediated by its ability to interact with two antagonistic ncRNAs transcribed from the X-chromosome inactivation centre, RepA and Tsix. This induces the full transcriptional activation of one *Xist* allele, which interacts with PRC2 and spreads in *cis* to promote mono-allelic chromosomal gene silencing [48].

PRC1 recruitment at Xi is mediated by the RNA-binding protein heterogeneous nuclear ribonucleoprotein K (hnRNPK), which specifically interacts with the PCGF3/5-vPRC1 complex, leading to its enrichment on the inactive X chromosome [49,50].

The lncRNA HOX transcript antisense RNA (HOTAIR) has been proposed to interact with PRC2, mediating its recruitment and serving as a trans-acting repressor of the *HoxD* locus [51].

However, it has been recently proposed that HOTAIR-mediated transcriptional silencing is PRC2-independent, and that PRC2 recruitment to the *HoxD* locus occurs primarily in response to gene repression, without directly involving HOTAIR [52]. Such observations are reinforced by *in vivo* studies showing that HOTAIR deletion has no effect on *HoxD* expression during mouse development [53].

Finally, it has been proposed that the PRC1 complex represses the *Ink4a/Arf* locus in part by interacting with ANRIL, a long antisense non-coding transcript originating from the *Cdkn2a* locus [54].

However, *in vitro* studies have demonstrated that PRC2 binds to RNA promiscuously with little sequence specificity, and that more than 9000 different RNAs are putative PRC2 partners in mESCs [55].

In conclusion, for the vast majority of lncRNAs proposed as Polycomb-interacting molecules are unclear the mechanisms mediating PcG recruitment, making quite speculative the functional relevance of such interactions in gene regulation.

1.1.3 Interdependence of PRC1 and PRC2 in the formation of PcG repressive domains

Once PRC1 and PRC2 are engaged on their target sites, this primary recruitment is converted into the stable formation of Polycomb repressive chromatin domains, which can extend up to tens of kilobases. During the last decades, several tethering experiments have been performed to define the sequentiality of Polycomb action, giving rise to the classical and the alternative models of Polycomb recruitment.

1.1.3.1 Classical model of Polycomb recruitment

The classical model of Polycomb recruitment to chromatin posits that the PRC2-deposited H3K27me3 is recognized by the CBX subunit of the cPRC1 through its chromodomain (Fig. 1.2a).

In support of this model, removal of PRC2 activity affects the binding of CBX7, which is the most abundant member of the CBX family in ESCs, preventing cPRC1 recruitment to chromatin [56].

Consistent with their low E3 ligase activity *in vitro*, cPRC1 complexes contribute only minimally to H2AK119ub1 levels *in vivo* and in tethering experiments, indicating their inability to efficiently drive *de novo* formation of Polycomb repressive domains [57,58].

Moreover, PRC2 can bind its terminal enzymatic product, H3K27me3, through a WD40-repeat domain in EED. This mechanism promotes the allosteric activation of the methyltransferase activity and the spreading of H3K27me3 through the genome [59,60].

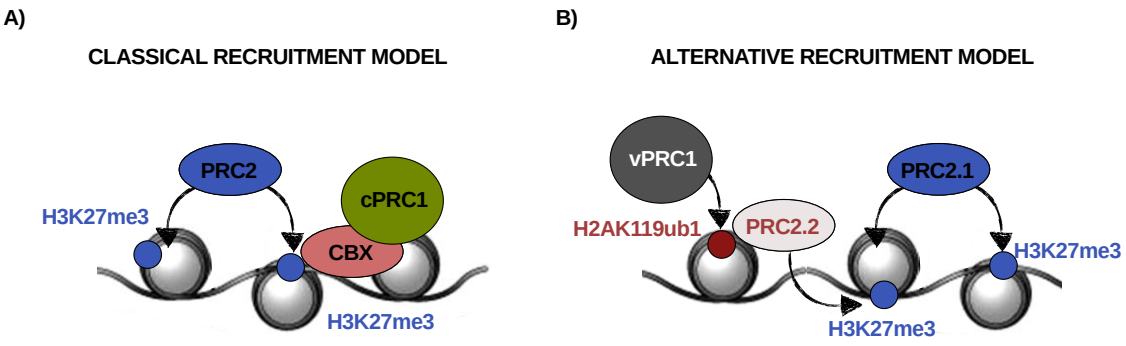

Fig. 1.2 Models of Polycomb recruitment to chromatin

Schematic representation of the two proposed models of Polycomb tethering to genomic loci: (a) cPRC1 is recruited via the PRC2-dependent deposition of H3K27me3; (b) vPRC1 catalyzes H2AK119ub1 deposition, leading to the subsequent engagement of PRC2.

1.1.3.2 Alternative model of Polycomb recruitment

The alternative model of Polycomb recruitment supports that PRC1 is engaged to chromatin as first and with an H3K27me3-independent mechanism (Fig. 1.2b). Such hypothesis derives from genome-wide studies showing that not all PRC1 co-localizes with PRC2 [61]. This activity is restricted to vPRC1 complexes, since they have shown to be more catalytically active compared to their cPRC1 counterpart. Indeed, several experiments have revealed that the engagement of vPRC1 is able to promote *de novo* recruitment of PRC2, deposition of H3K27me3 and wide spreading of Polycomb repressive domains [62-64]. Moreover, PRC1 can still deposit H2AK119ub1 and repress gene transcription in PRC2-deficient mouse ESCs [65].

Another biochemical link between H2AK119ub1 deposition and PRC2 recruitment has been provided by a study revealing the ability of JARID2 to directly bind to H2AK119ub1 through a ubiquitin binding motif [66]. Such interaction also triggers the catalytic activity of PRC2 [67].

The pivotal role of vPRC1 in recruiting PRC2 by H2AK119ub1 deposition, and thus in establishing Polycomb repressive domains, has been also demonstrated through detailed genetic perturbation studies in mouse ESCs. Indeed, combined removal of RING1A and RING1B induces not only the loss of H2AK119ub1 but also the depletion of PRC2 binding [64].

H2AK119ub1 deposition not only affects PRC2.2 activity, but also reinforces chromatin binding and vPRC1 activity through a zinc finger in RYBP, which can directly bind H2AK119ub1. Such interaction supports the spreading of this histone mark onto close nucleosomes via mechanism that appears to be mediated by histone H1 [62,66].

1.1.3.3 cPRC1 mediates long-range interactions between Polycomb respressive domains

cPRC1 complexes have evolved non-ubiquitylating mechanisms to promote gene repression, as revealed by biochemical assays in which cPRC1 complexes show to undergo liquid–liquid phase separation *in vitro* and to produce nuclear condensates *in vivo*. The liquid–liquid phase separation property relies on CBX2, which contains a positively charged disordered region, and on the sterile alpha motif (SAM) of PHC proteins, which mediates their polymerization [68-70]. Condensates formed by CBX2 or PHC have shown to retain nucleosomes and nucleic acids, while also enhancing entry of other Polycomb complexes [70]. This suggests that condensates could promote Polycomb activities on chromatin or limit the access of other factors to such repressive chromatin domains.

Additionally, the polymerization of PHC proteins can produce long filaments that enable the creation of long-range interactions between distal Polycomb domains [71,72]. These interactions can be observed with imaging experiments: they appear as focal condensates of Polycomb proteins and are known as Polycomb bodies [73]. The mechanisms by which these filaments support three-dimensional chromatin interactions are unclear, but it has been reported that the binding of Polycomb proteins at these sites is highly dynamic and that the activity of cohesin antagonizes such interactions.

1.1.4 Somatic and transgenerational inheritance of Polycomb chromatin domains

The two processes allowing epigenetic inheritance during cell proliferation are DNA replication and cell division. Several studies have demonstrated that the Polycomb machinery may promote the transmission of chromatin states when these events occur. Indeed, it has been demonstrated that PcG proteins are present on mammalian mitotic chromosomes and that they remain bound to DNA templates during replication, both in *in vitro* assays [74,75] and *in vivo* [76,77].

Although H3K27me3 is diluted during DNA replication, it can mediate short-term memory of repressed chromatin states [78] and, after DNA replication, PRC2 recognizes the already deposited H3K27me3 on parental nucleosomes to restore pre-replicative H3K27me3 levels [79]. In this context, recent studies have shown that H3K27me3-containing nucleosomes are acquired by daughter DNA strands almost in the same position in which they were deposited in the template DNA, providing an example of somatic inheritance of PRC2-marked chromatin domains [80,81].

Polycomb chromatin states are also transmitted across multiple generations.

In mammals, the mechanisms underlying transgenerational epigenetic inheritance require specific pathways responsible for resetting the state of the epigenome during germline development. ChIP-seq analyses performed in gametes have showed that sperm and oocytes contain several bivalent domains, which are genomic regions enriched with both H3K4me3 and H3K27me3. Such bivalency is extensively reprogrammed upon fertilization and during the early cell division cycles of the embryo [82,83]. However, a significant number of bivalent domains is retained during early embryogenesis [84], suggesting that a precise epigenetic control is required in germ cells for the correct definition of the embryonic transcriptional programs.

Upon fertilization, several epigenetic changes occur in parental nuclei, since protamines are completely lost by the sperm nucleus and rapidly replaced by maternally provided histones [85]. Moreover, a wave of DNA demethylation affects the male pronucleus and the

deposition of the H3.3 histone variant takes place [86]. Alongside, the maternal transcription program is turned off to promote the zygote-genome activation (ZGA). In this context, Posfai and colleagues have showed that combined deletion of RING1A and RING1B in oocytes results in developmental arrest of embryos at the two-cell stage due to defective replication and impaired ZGA [87].

Moreover, it has been recently found that deletion of the PRC2 cofactor EZHIP in mice leads to a global increase in H3K27me2/3 deposition both during spermatogenesis and at late stages of oocyte maturation, further stressing the requirement of Polycomb activity in gametes [27].

1.1.5 PcG functions in mammalian embryogenesis

Studies of germline loss-of-function mutations in mice have revealed that dysregulation of PRC1 or PRC2 activity severely impairs mammalian embryogenesis. Ablation of one of the three PRC2 core components (EZH2, EED and SUZ12) invariably induces gastrulation defects and lethality around embryonic day (E) 7.5-8.5, during early post implantation stages [88-90].

Although EZH1 is the catalytic PRC2 subunit, EZH1 knockout (KO) mice are viable [91], suggesting that EZH2 can compensate for its loss during development. Similarly, RING1B$^{-/-}$ mice die around 7.5-9.5 days post coitum (dpc), but RING1A$^{-/-}$ mice are healthy, showing only minor defects [92,93].

Several studies have also reported the requirement of cPRC1 function for proper embryonic development. Although removal of PCGF2 (alias MEL18) or PCGF4 (alias BM1) causes defects in anterior-posterior specification of the axial skeleton [94,95], MEL18/BMI1 double-KO mice die at around 9.5 dpc due to severe developmental defects[95]. This result supports the hypothesis that PCGF2 and PCGF4 can act redundantly. However, this interpretation is in part challenged by the unique phenotypes observed in the single KO mice, suggesting potential different functions.

Similarly, also vPRC1 components are required during embryonic development, since RYBP KO embryos die at the early post-implantation stage [97] and KDM2B loss impairs embryonic neural development [98]. Contrarily, CBX proteins are dispensable during embryonic development as mutants for CBX2 or CBX4 displayed postnatal lethality [99,100].

1.1.6 Role of PcG in stem cell renewal and differentiation

1.1.6.1 PRC2 cooperates with transcription factors to maintain ESCs self-renewal

Among the epigenetic players regulating the self-renewal ability of ESCs, PcG complexes ensure the maintenance of cellular identity preventing cell differentiation by cooperatively repressing the transcription of key developmental and lineage-specific genes. Indeed, both PRC1 and PRC2 occupy the promoters of a large cohort of developmental genes in ESCs, such as the members of the Hox, Pou, Sox, Fox, Pax, Tbx and Wnt gene families [101-103].
The three transcription factors mainly required for ES cells self-renewal are OCT4, SOX2 and NANOG. By performing motif analyses, in 2015 Müller and colleagues found that OCT4 co-binds with SOX2 and NANOG at promoters of genes that are silenced via H3K27me3 deposition during differentiation, suggesting the role of PRC2 in regulating self-renewal properties of ESCs [104].
OCT4 is a member of the POU family of TFs with a highly conserved role in the maintenance of pluripotency [105]. Expression levels of OCT4 define ESC fate and ICM production [106] and seem to be regulated by the activity of SOX2, another crucial TF whose deficiency in mouse embryos induces die shortly after implantation [107,108]. It has been suggested that these transcription factors cooperate to promote the expression of a set of self-renewal genes, maintaining the 'stemness' of ES cells [41,42, 109].

1.1.6.2 PRC1 and PRC2 work in concert to preserve ESC identity

Despite PRC2 cooperates with a network of TFs for the maintenance of cell identity, it is dispensable for self-renewal properties since ESCs can be still derived from EED or SUZ12 mutant embryos and maintained in vitro [110-114]. Such ES cells show transcriptional derepression of all major pluripotent and developmental genes that are otherwise repressed in normal ESCs, suggesting that the self-renewal program is dominant in maintaining ESC fate even if differentiation programs are activated.
Contrarily, RING1A/B double-deficient ESCs exhibit severely impaired self-renewal capacity. As each single KO preserves ESCs growth, such phenotype suggests the redundant role of RING1A and RING1B proteins in pluripotency maintenance.
Among the PCGF proteins only PCGF6, which is the most abundant in mESCs, is required for the maintenance of cell identity via the repression of germ-cell related genes [115].

Despite the co-occupancy of PRC1 and PRC2 at most established Polycomb sites *in vivo*, some reports [116] suggest that the two complexes are, at least in part, independent and act

redundantly. Indeed, in RING1B/EED double KO ESCs, the number of derepressed genes, which are direct Polycomb targets, shows a two-fold increase, compared with the single EED or RING1B knockout. Half of these genes are transcriptionally reactivated only after the loss of both complexes, and remain silenced in each single KO, suggesting that PRC1 and PRC2 act redundantly for the repression of these genes. Such observation is corroborated by the "rescue" of transcriptional silencing when EED expression is induced in double KO cells.

In addition to the role of PcG in self-renewal of mESCs, PRC1 and PRC2 complexes are also implied in their proper differentiation.

Indeed, the removal of RING1B impairs the correct expression of differentiation markers when ESCs are grown as embryoid bodies [117]. Loss of other PRC1 components, such as CBX proteins or RYBP, affects ESC differentiation [56,65,118,119].

Moreover, EZH2 is required for mesendodermal lineage segregation [113] and removal of SUZ12 impairs ESCs differentiation towards the endodermal lineages [111]. Contrarily, EED KO ESCs can give rise to the three germ layers and contribute to chimera formation [112]. Other PRC2 members, such as JARID2 and the PCL proteins, are required for proper differentiation [120-123].

However, ESCs lacking either RING1B or EED form small teratomas compared to the wild-type counterpart, with an increase in the ectodermal or endodermal fraction, respectively [116]. Only combined removal of EED and RING1B abolish teratoma formation, further confirming their partially independent functions, as reported above.

1.1.6.3 PcG complexes regulate bivalent genes in mouse ESCs

Genome-wide studies have revealed that a subset of developmental genes in mESCs is enriched by both H3K27me3 and H3K4me3, a combination of histone modifications known as bivalency. In addition to the deposition of an active H3K4me3 mark, bivalent genes present poised RNA polymerase II [124]. Despite that, they are transcriptionally silent, but can be rapidly transcribed in response to specific signals. In fact, upon ESC differentiation, bivalent domains are resolved to either H3K27me3 or H3K4me3 regions, depending on the expression state of the associated gene in a given differentiated cell type [125,126]. Genes that need to be stably repressed upon differentiation are in general exposed to DNA methylation [127,128]. This transition to a more repressed state is also promoted by the activity of specific histone demethylases that selectively remove H3K4me3 [129,130]. Conversely, genes that must be activated for lineage commitment lose H3K27me3.

Collectively, the relevance of bivalent domains is still matter of debate since they are not unique to ESCs and their establishment can be affected by growth conditions. Indeed, bivalency is a feature also of other multipotent stem cells, such as hematopoietic stem cells [131,132], and it has been reported that the number of bivalent domains is three-fold reduced in ESCs grown in 2i-containing medium compared to ESCs maintained in presence of serum [133].

1.1.7 Regulation of gene transcription by Polycomb complexes

Although the PRC2-cPRC1 axis may contribute to gene repression, ESCs depleted of PRC2 components or cPRC1 subunits exhibit relatively few gene expression changes [134]. This suggests that, at least in ESCs, alternative mechanisms of Polycomb-mediated transcriptional silencing must exist.

In agreement with this hypothesis, recent studies have pointed out a central role for H2AK119ub1 and vPRC1 activity. Indeed, combined removal of PCGF1/3/5/6 results in the transcriptional derepression of thousands of Polycomb target genes [134]. Such effect is reproduced by the loss of RING1A and RING1B, despite vPRC1 binding is preserved at its target sites, indicating that gene repression by PRC1 in this context depends on H2AK119 ubiquitylation [135,136].

The central role of H2AK119ub1 in transcriptional silencing may be explained by the high dynamicity of PRC1 binding to chromatin, as revealed by its low target site occupancy [137,138].

To date, the precise mechanisms by which H2AK119ub1 affects gene expression remain to be elucidated, but they seem to be PRC2-independent [139]. A possibility is that PRC1 and H2AK119ub1 affect transcription initiation, as acute disruption of PRC1 and loss of H2AK119ub1 rapidly recruit Pol II on new binding sites and elevate the frequency of transcription bursts. Such observation is concordant with previous works claiming that PRC1 prevents the assembly or activity of the transcription pre-initiation complex [140,141].

Although H2AK119ub1 and H3K27me3 are mainly concentrated on Polycomb chromatin domains, they are also found everywhere in the genome and several studies posit that these alternative sites of histone marks may influence gene expression. In this context, it has been demonstrated that the PRC1.3/5 complex, although having the lowest number of target genes, is the major determinant of global H2AK119ub1 deposition [134]. Such “blanket” of ubiquitination is prevented by the deubiquitinase BAP1, whose loss increases

H2AK119ub1 levels and strongly represses thousands of genes that are not normally controlled by PRC1 activity [142,143].

1.2 Role of Polycomb complexes in adult stem cells

Adult stem cells (SCs) are a special population of undifferentiated cells that reside within specific tissues to maintain proper homeostasis, by constantly replenishing damaged cells, and to confer cellular plasticity in response to stress or other perturbations.
In the last years several studies, including the work of our laboratory, have demonstrated the role of PRC1 and PRC2 in regulating cell-type specific transcriptional programs during tissue homeostasis and regeneration [144,145].
In contrast to ESCs, where key developmental genes exist in a bivalent state, adult SCs have very few genes exhibiting this "poised" behavior [146]. This suggests that bivalency may be less critical once tissue lineages have been defined and cell type options have been selected. By using distinct adult compartments as models (such as bone marrow, skin, liver, intestine, brain), it has been demonstrated that coupling PcG-mediated silencing with the activity of cell-type specific transcriptional activators ensures the maintenance of cell identity during homeostasis and the acquisition of alternative lineage choices only upon environmental cues.

1.2.1 Control of adult intestinal identity by the Polycomb machinery

1.2.1.1 The architecture of the intestinal epithelium

The intestinal epithelium exerts several important functions in the organism. Besides allowing efficient digestion and nutrients absorption, it serves also as barrier against microorganisms and potentially genotoxic molecules.
The epithelium of the small intestine is structured in functional modules, the crypt–villus units [8]. Differentiated cells are mainly located in the villi, finger-like protrusions that notably expand the absorptive area of the intestinal epithelium. The base of each villus is surrounded by several epithelial invaginations, called crypts of Lieberkühn (Fig 1.3a).
The harsh content of the gut lumen, to which the intestinal cells are exposed, impose a high regenerative rate. Indeed, the intestinal epithelium is replenished every 3-4 days, representing the fastest renewing tissue of the body. This impressive turnover is ensured by a pool of rapidly dividing $Lgr5^+$ intestinal stem cells (ISCs), which reside at the crypt bottom. ISCs proliferate every 24 hours and their progeny gradually migrate at the middle of the crypt, entering the transit-amplifying (TA) compartment. Here the cells reside for

48–72 hours undergoing up to 6 rounds of cell division and, while migrating toward the top of the villus, gradually differentiate [147]. Once reached the tip of the villus, they undergo apoptosis and are shed into the intestinal lumen. Only Paneth cells escape this high epithelial turnover, as they are renewed every 3–6 weeks (Fig. 1.3b).
In addition to the fast-cycling $Lgr5^+$ ISCs, there is also a population of quiescent stem cells capable of mounting a regenerative response when the pool of active-cycling stem cells is ablated by injuries [148]. So far, almost all the lineage progenitors and maturely differentiated cells have been demonstrated to re-enter cell cycle, reacquire stemness and replenish the loss of $Lgr5^+$ stem cells [149-152], highlighting the plasticity of the intestinal epithelium.

The three tracts of the small intestinal epithelium (duodenum, jejunum, ileum) display specific functional activities, which are mirrored by a different cell composition. The length of the villi decreases along the rostro-caudal axis, being longest in the duodenum, and absorptive enterocytes represent the largest population. The number of secretory goblet cells increases along the small intestine, being prevalent in the ileal tract, where they release mucins to facilitate the motility of colonic content. Along the whole small intestine, Paneth cells are the only differentiated cells residing at the crypt bottom, specialized in the secretion of antimicrobial peptides and of the hydrolytic enzyme lysozyme. Scattered enteroendocrine cells produce hormones required to interact with the other organs of the digestive system, and a small population of Tuft cells can be rapidly amplified to activate type 2 immune response during helminth infections [153,154].
In the colon, where the predominant activity is stool compaction and water absorption, villi are completely absent, goblet cells are the prevalent cell type and no Paneth cells are detected.
Function and activity of the intestinal epithelium can be faithfully reproduced *in vitro* with the organoid model, a three-dimensional cell culture system that can be established either from purified $Lgr5^+$ stem cells or small intestinal crypts (Fig. 1.3c).

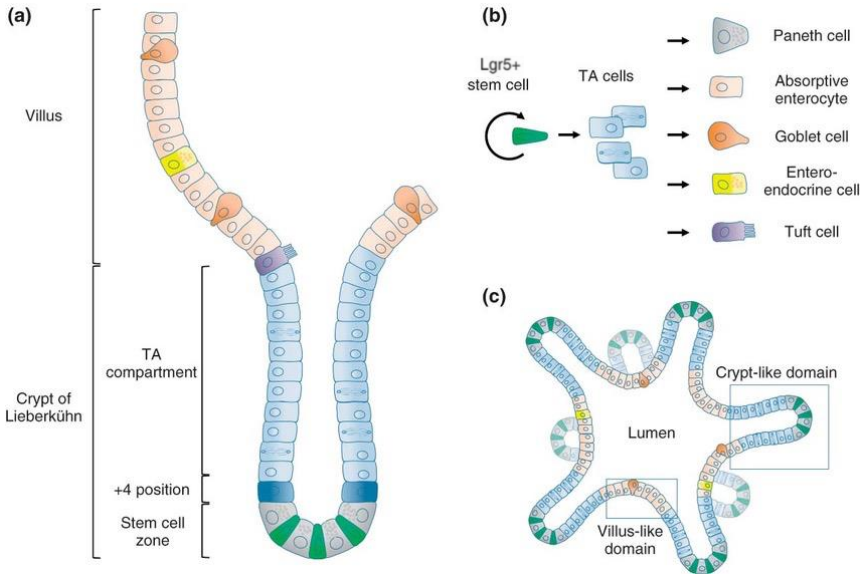

Fig. 1.3 Cellular composition of the small intestinal epithelium

A cartoon depicting the cross-sectional structure of the small intestinal epithelium (a) with its major cell-types, including enterocytes, goblet, Paneth, tuft and stem cells (b). The physiology of the intestinal epithelium is faithfully reproduced *in vitro* using the organoid model (c) (adapted from *Wiley Interdisciplinary Rev Syst Biol Med*, Rizk & Barker 2012).

1.2.1.2 Signaling pathways regulating intestinal homeostasis

Self-renewal of ISCs as well as proper intestinal differentiation and development are tightly controlled by four signaling pathways: WNT, BMP/TGFβ, NOTCH and EGF.

The WNT pathway

The WNT/β-Catenin signaling pathway is responsible for intestinal stem cell maintenance [155]. Its activation requires the binding of the WNT ligands to the Frizzled receptor. Such event initiates a signaling cascade with the recruitment of a multiprotein complex, called the "destruction complex," on the membrane. In absence of ligands, β-catenin is sequestered by the destruction complex, where it is phosphorylated and degraded. When the binding occurs, the destruction complex is recruited to the cell membrane inhibiting β-catenin degradation, which can in turn accumulate in the cytoplasm and then move into the nucleus. Here, β-catenin binds TCF/LEF1 transcription factors, promoting transcriptional activation of specific target genes (Fig. 1.4a).

WNT signaling is heavily involved in differentiation and maturation of Paneth cells which subsequently become one of the main sources of WNT ligands [156,157]. Such property is

reflected by a gradient of WNT concentration, highest at the crypt bottom and lessening towards the gut lumen.

Inhibition of WNT signaling severely impairs intestinal morphology leading to stem cell exhaustion. Moreover, loss-of-function mutations in members of the destruction complex (mainly APC) or mutations in the residues required for β-catenin degradation cause the constitutive activation of the pathway and are a common feature of intestinal tumors [158].

The BMP pathway

In the intestinal epithelium, the BMP signaling can be considered the alter ego of the WNT pathway [159]. Expressed in the opposite gradient, from the villus to the crypt, BMP ligands prevent the expansion of the intestinal stem cell compartment by repressing stemness-related genes [160]. The activity of BMP inhibitors, such as Noggin, counteracts the effects of BMP signaling activation, avoiding stem cell exhaustion (Fig. 1.4b).

The NOTCH pathway

The NOTCH pathway is one of the most short-range forms of cell-to-cell communication with highly pleiotropic effects, ranging from proliferation and differentiation to apoptosis [161]. In mammals, five ligands (DLL1, -3 and -4; JAG1 and -2) and four NOTCH receptors (NOTCH1–4) have been identified. Their binding activates the γ-secretase protease which cleaves NOTCH, releasing the NOTCH intracellular domain (NICD). Once freed, NICD moves into the nucleus, where it binds the transcriptional factor RBPJ to promote gene expression of different targets. Among them, the HES family of transcriptional repressors inhibits the activity of *Atoh1*, which is the master regulator of secretory cell fate commitment (Fig. 1.4c).

In the small intestine, the main source of NOTCH ligands are secretory precursors and Paneth cells [162]. $LGR5^+$ stem cells express NOTCH1 and -2 that act redundantly. The acquisition of a Paneth cell fate and, in general, the specification towards the secretory lineage, triggers the expression of DLL1 and DLL4 that activate NOTCH signaling in $LGR5^+$ cells inhibiting their premature differentiation. Inhibition of γ-secretase activity, genetic ablation of NOTCH receptors or DLL1 and -4 expression induces an improper skewing toward the secretory lineage. This compromises the absorptive functions of the intestine leading to death.

The EGF pathway

The EGF pathway is required for intestinal cell growth and proliferation [163]. It comprises four transmembrane receptors tyrosine kinase (ERBB1/EGFR, ERBB2-4) and several

ligands sharing the epidermal growth factor domain. The binding of the ligand induces the dimerization of the receptor and its activation, triggering a signaling cascade which culminates with the RAS GTPase recruitment and mitogen-activated-protein-kinase (MAPK) activation (Fig. 1.4d).

Lack or depletion of EGF signaling in the small intestine profoundly affects its homeostatic processes. EGFR null animals die perinatally due to a disrupted epithelial morphology [164].

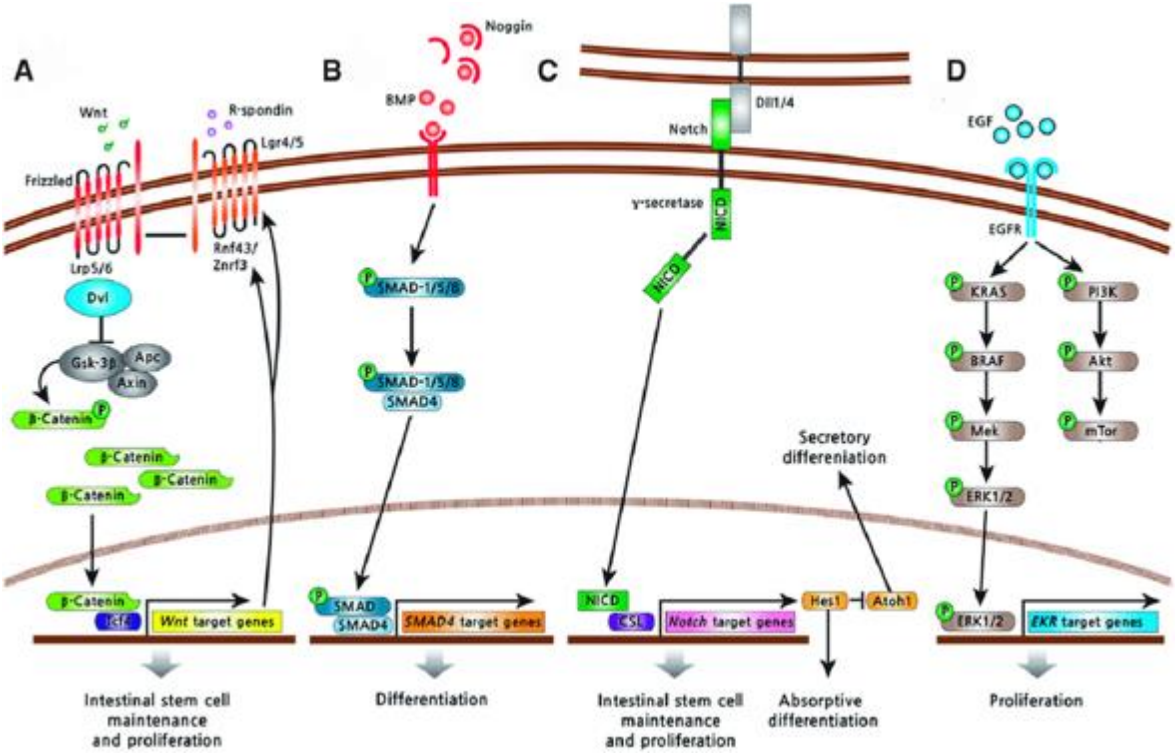

Fig. 1.4 Main signaling pathways in intestinal homeostasis

Representation of the major signaling pathways regulating the activity of intestinal cells: WNT cascade promotes self-renewal and proliferation of ISCs (A); BMP molecules induce intestinal cell differentiation, antagonizing WNT activity (B); NOTCH signaling regulates stem cell proliferation and skewing towards the secretory lineage (C); EGF pathway positively regulates cell proliferation by activation of the MAPK cascade (D) (adapted from *Stem Cells Transl Med*, Hong et al. 2017).

1.2.1.3 Role of PRC1 and PRC2 in intestinal stem cell identity and epithelial regeneration

Recently, it has been revealed that Polycomb complexes preserve intestinal stem cell identity and the ability of progenitor cells to proliferate during intestinal regeneration.

By knocking-out EED, we have previously found that loss of PRC2 activity in the intestinal epithelium is associated with a skewing towards the secretory lineage and cell cycle defects in the TA compartment [144]. Such anomalies are well tolerated during homeostasis, but severely affect the ability to mount a reparative response when the pool of $Lgr5^+$ stem cells is depleted by whole-body irradiation. This regenerative defect depends on the cell cycle arrest induced by the transcriptional reactivation of the *Cdkn2a* locus (or *INK4A-ARF*), normally kept silent by PRC1 and PRC2 to control cell proliferation. *Cdkn2a* encodes for the tumor suppressors *p16INK4A* and *p19ARF*, two central proteins involved in negative cell cycle regulation. In EED null progenitors the expression of *p16* and *p19* compromises their ability to revert to stem cells and promote intestinal regeneration. Indeed, removal of *Cdkn2a* in the EED null background fully rescues the regenerative potential.

While the plasticity of intestinal progenitors depends on the transcriptional reactivation of *Cdkn2a*, the accumulation of goblet cells after PRC2 inactivation derives from a loss of direct transcriptional control of *Atoh1* and *Gfi1*, the two master regulators of secretory lineage specification.

In contrast to PRC2 loss of function, depletion of PRC1 activity severely affects intestinal homeostasis. By using a mouse model that couples a constitutive null allele of RING1A and a Cre-dependent conditional KO allele for RING1B, we have previously found that inducible loss of PRC1 catalytic function results in degenerating crypt architecture, weight loss and morbidity [145]. Despite combined removal of RING1A and RING1B completely abrogates H2AK119ub1 deposition, global levels of H3K27me3 are not affected, indicating that PRC1 function acts independently of PRC2 in the intestinal epithelium.

Notably, PRC1 activity is required for self-renewal of ISCs and the maintenance of their transcriptional identity. Indeed, PRC1 loss leads to derepression of non-lineage specific genes, mainly belonging to the ZIC family of TFs, which control cell fate determination in other tissues. By interfering with TCF7L2/β-catenin, these ectopically expressed TFs force stem cells to exit from their niche without activating a specific differentiation program. This loss of stem cell identity is not rescued by WNT hyperactivation, further confirming impaired TCF7L2/β-catenin transcriptional activity.

1.2.2 Role of Polycomb complexes in other adult stem cell systems

In line with the findings in ISCs (discussed above), our group has showed that loss of PRC1 function in $LGR5^+$ cells impairs also hair follicle regeneration by transcriptional reactivating several Polycomb targets and a subset of non-lineage specific genes [165].

However, it has been demonstrated that both PRC1 and PRC2 control self-renewal properties of tissue stem cells also via *Cdkn2a*-dependent mechanisms. Indeed, ectopic expression of PcG subunits, such as BMI1, EZH2, CBX7 and CBX8, suppresses *INK4a* and *ARF* expression to bypass senescence [166,167]. In contrast, depletion of Polycomb components reactivates this locus, resulting in cell growth inhibition and senescence.

For example, constitutive expression of BMI1 promotes proliferation of hematopoietic stem cells (HSCs) and confers stress resistance to HSCs during serial transplantation [168]. Contrarily, BMI1 null mice exhibit reduction in bone marrow cellularity and hematopoietic progenitor cells [169]. Consistent with this notion, BMI1 has been shown to promote expansion of muscle satellite cells (MuSCs), since its depletion induces an irreversible senescent-like fate and prevents satellite-cell-mediated regeneration [170].

In addition, several evidences highlight the importance of PRC2 activity during neurodevelopment. As pluripotent ESCs undergo neural fate commitment, bivalent developmental genes that must be activated in neural progenitors lose H3K27me3 [131,171]. Once specified, neural progenitors are restrained from further differentiation by Polycomb-mediated repression of genes specified in neurons or glial cells. This involves both the maintenance of bivalent domains originally established in ESCs as well as a new acquired bivalency at previously unmarked genes in neural progenitors [131]. Furthermore, during cortical neuron differentiation, expression levels of EZH1 and EZH2 are up- and down-regulated respectively, controlling not only the timing of neuronal maturation but also the neurogenic-to-astrogenic switch [172].

Similarly, EZH2 regulates cell fate commitment of embryonic endoderm towards pancreatic or hepatic buds and is required for hepatoblast proliferation. More than 3000 genes differentially expressed in hepatocytes, from postnatal day 14 to month 2 after birth, are under the control of PRC2. Indeed, combined loss of EZH1 and EZH2 in livers promotes early differentiation of perinatal hepatocytes, as they express genes at postnatal day 14 that would normally be induced later, resulting in liver fibrosis [173].

1.3 Polycomb deregulation and disease

During the last decades, several studies have reported the deregulation of PRC1 and PRC2 activities in tumors, and the requirement of both complexes for proliferation of cancer cells. Differently from PRC2, which frequently exhibits gain- or loss-of-function mutations in cancers, impairment of PRC1 activity mainly involves epigenetic changes rather than genetic alterations (Fig. 1.5).

The first association between PRC1 disfunction and cancer derived from the identification of PCGF4 (alias BMI1) as a proto-oncogene, which cooperates with c-Myc during lymphomagenesis via direct silencing of *Cdkn2a* [166].

A similar oncogenic role has been reported for CBX7, which is overexpressed in human leukemias, prostate cancer and ovarian carcinoma [174].

More recently, a functional dysregulation in the catalytic activity of PRC1 has been reported in breast cancer, where a cooperation between RING1B, the estrogen receptor and BRD4 occurs to regulate active enhancers [175].

Additionally, specific mutations and gene fusions in the vPRC1 ancillary subunits have been identified in several tumors. For example, AUTS2 (PRC1.3/5) is implicated in lung adenocarcinoma, prostate cancer and leukemia [176], whereas BCOR (PRC1.1) is mutated in sarcomas, gliomas and hematological malignancies [177].

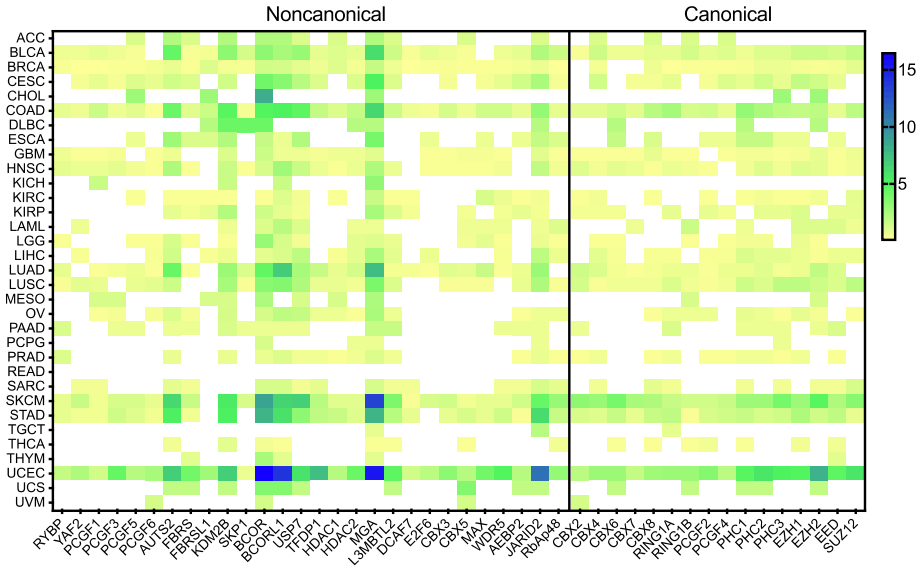

Fig. 1.5 PcG subunits mutated in cancer

Heatmap showing the percentage of tumors with Polycomb Group gene mutations (adapted from *NAR*, S. Wang, 2021)

Among the first evidences correlating PRC2 function and cancer, the Chinnaiyan lab has reported high levels of EZH2 and H3K27me3 in prostate tumors with poor prognosis [178].

Later, Morin and colleagues have identified a correlation between a gain-of-function mono-allelic mutation in the catalytic pocket of EZH2 (Y641) and lymphomas [179]. Despite this missense mutation impairs mono- and di-methylation of H3K27, deposition of H3K27me3 is not affected. Mechanistically, EZH2 expressed from the wild-type allele ensures the conversion of unmethylated H3K27 into H3K27me1/2, while mutated EZH2 activity induces aberrant deposition of H3K27me3 in tumors. These data suggest that

hypermethylation at H3K27 acts as a driver in several human cancers, promoting cell invasion and metastasis. Based on these observations, several EZH2 inhibitors have been developed, some of them already in use in clinical practice [180].
Despite that, also inactivating mutations in EZH2, EED and SUZ12 have been reported, specifically in myelodysplastic syndrome and malignant peripheral nerve sheath tumors (MPNST) [181]. These loss-of-function mutations lead to reduced levels of H3K27me2/3, challenging the concept that PRC2 acts as an oncogene.

Alongside several evidences linking Polycomb to cancer, large-scale whole-exome studies have identified *de novo* mutations in both PRC1 and PRC2 components in patients with neurodevelopmental disorders (NDDs). For example, AUTS2 results frequently mutated and some PcG-related genes, including RING1B, are associated with neurodevelopmental or neurological phenotypes upon loss of function in distinct mouse models [176].

AIM OF THE PROJECT

Despite tumorigenesis is caused by a set of multiple mutations, a pan-cancer analysis has revealed that about 5% of tumors do not have driver mutations, suggesting that genetics alone could not explain cancer onset. Non-genetic alterations have been involved in development, progression and drug resistance of cancer cells. For example, metastases arising from pancreatic ductal adenocarcinomas do not show driver gene mutations but are widely exposed to epigenomic reprogramming, implying the involvement of chromatin modifiers.

Beside their role in cell identity, PcG proteins represent a hallmark of tumorigenesis. A fascinating part of the oncogenic function of Polycomb components resides on their ability to act both dependently or independently on Polycomb complexes.

By analyzing the crosstalk existing between PRC1 and PRC2 at the cellular and molecular level, this project aims to define a whole picture of their mode of action. Determining how these dependencies take place *in vivo* is not a mere academic exercise but is essential to fully characterize oncogenic conditions in which Polycomb activities are altered.

Considering that deregulation of Polycomb proteins can produce opposing effects in different cancer types, identifying the molecular pathways regulating their context-dependent activity, as we did in the adult intestine, will be crucial to improve cancer diagnosis, prognosis and therapy.

2. MATERIALS AND METHODS

2.1 Mouse models

Animal housing was performed adhering to the guidelines set out in Commission Recommendation 2007/526/EC, 18 June 2007, for the accommodation and care of animals used for experimental and other scientific purposes. *In vivo* experiments were carried out in accordance with the Italian Laws (D.L.vo 116/92 and following additions), which applies EU Directive 86/609 (Council Directive 86/609/EEC of 24 November 1986 regulating the protection of animals employed for experimental and other scientific purposes).

PCGFs conditional KO strains were generated by mating *Pcgf1*$^{fl/fl}$, *Pcgf3/5*$^{fl/fl}$ and *Pcgf6*$^{fl/fl}$ mice (generated in Haruhiko Koseki's lab, [49]) with the *AhCre* (kindly provided by Douglas Winton) [182] or the *LGR5-GFP-ires-CreERT2* [183] transgenic strain (Fig. 2.1). These mice were crossed with *Rosa26 lox-stop-lox LacZ* transgenic mice for in vivo lineage tracing [184].

With the *AhCre* model, Cre expression was induced in the small intestine (except the colonic epithelium and Paneth cells), with four intraperitoneal injections of β-naphthoflavone (Santa Cruz Biotechnology), dissolved in corn oil (Sigma) at 80 mg/kg. By using the *LGR5-GFP-ires-CreERT2* transgene, gene deletion was achieved specifically in the intestinal stem cell compartment via four consecutive tamoxifen (Sigma) injections per day, resuspended at 75 mg/kg in corn oil.

For *Pcgf1*$^{fl/fl}$ mice loxP sites spanned the beginning of exon 2 and the end of exon 7, for *Pcgf3 knockout* Cre recombinase activity allowed the deletion of exon 4, for Pcgf5 inactivation only the exon 2 was removed and in *Pcgf6*$^{fl/fl}$ mice loxP sites were positioned between exons 2-3.

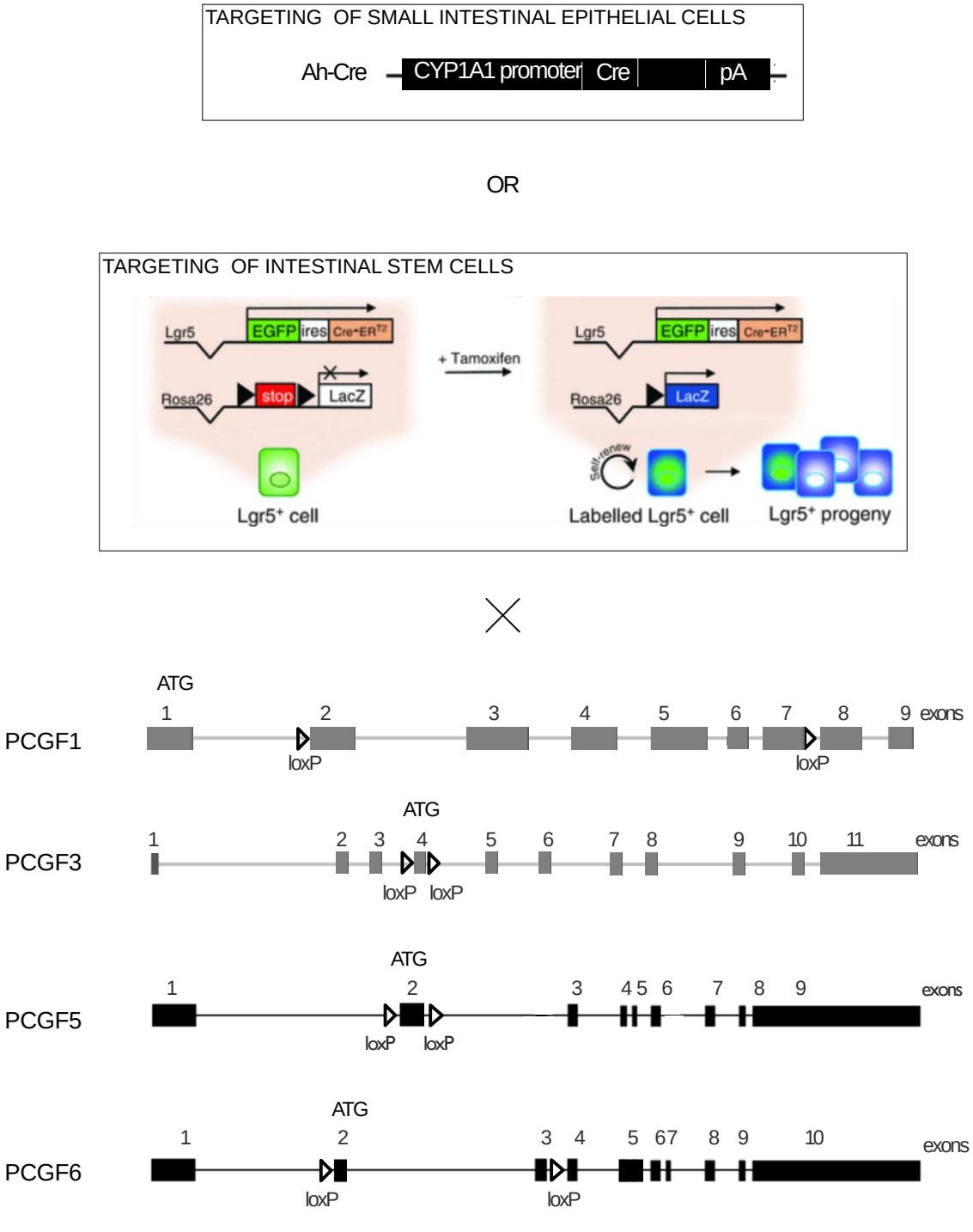

Fig. 2.1 *In vivo* targeting of PcG subunits (I)

Schematic representation of *in vivo* targeting of vPRC1-associated PCGF proteins, achieved with *AhCre* or *LGR5-GFP-ires-CreERT2* transgenes (adapted from *Cell Biology of the Ovary*, Barker, 2018).

PCGF1 was deleted also in the *Villin-CreERT2* background, as well as PCGF2/4 and EED in *Pcgf2/4*$^{fl/fl}$, *Eed*$^{fl/fl}$ and *Eed/Pcgf1*$^{fl/fl}$ mice (Fig. 2.2). With the *Villin-CreERT2* promoter, gene deletion was achieved in the whole intestine, including the colonic epithelium, by four consecutive intraperitoneal injection of tamoxifen [185].

Genotyping was confirmed by PCR of tail or ear skin DNA, as described in the next paragraph.

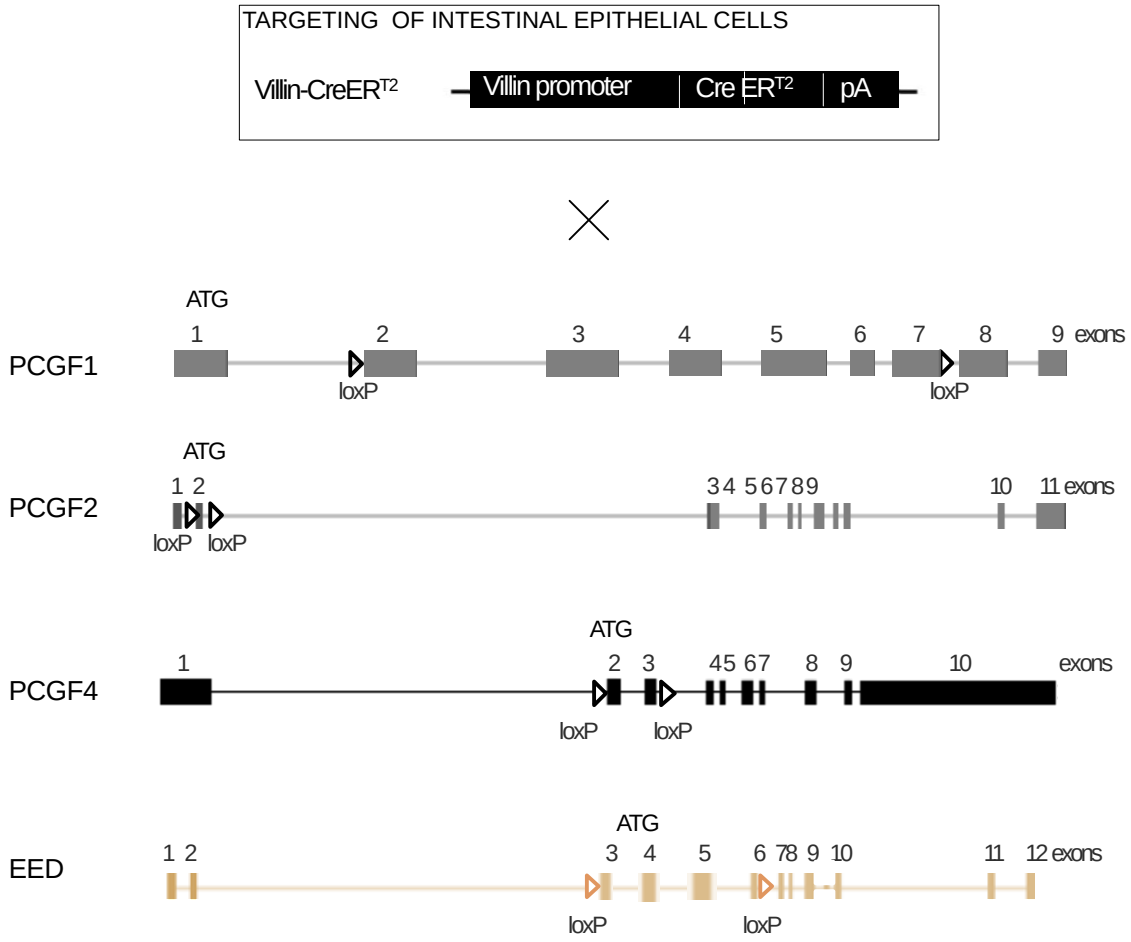

Fig. 2.2 *In vivo* targeting of PcG subunits (II)

Schematic representation of *in vivo* targeting of vPRC1-associated PCGF proteins, achieved with the *Villin-CreERT2* promoter.

2.2 Mouse genotyping

Skin from tails or ears were maintained in 100% ethanol until the extraction. Ethanol was discarded and the samples were washed with 1X PBS to remove remaining traces of alcohol. Samples were digested in 200 µL of Digestion buffer (10 mM TRIS-HCl pH 7,5, 10 mM EDTA pH8, 10 mM NaCl, SDS 0,5%) with 0,5 mg/ml proteinase K at 52°C

overnight in thermomixer. After digestion, tissues were purified by adding 1 volume of guanidine thiocyanate solution (0,345 g/ml guanidine thiocyanate, 10 mM EDTA pH8, 10 mM TRIS-HCl pH 7,5, 10 mM NaCl) and 1 volume of 75% ethanol. The mixture was vortexed, loaded on an EconoSpinTM Spin Column for DNA (Epoch Life Science), centrifuged at 13000 RPM for 3' at room temperature (RT). Once discarded the flow-through, the column was washed first with 500 μL of Washing Buffer (25% ethanol, 25% 2-propanol, 100 mM NaCl, 10 mM TRIS-HCl pH8) and then with 600 μL of 75% ethanol. The flow-through was removed at the end of each wash. The column was centrifuged for 5' at 13000 RPM at RT in order to remove potential residues of ethanol. Finally, the DNA was eluted in 50 μl of DNase-RNase free water and 5 μL of the eluate were used for each PCR.

2.3 Histology

Intestinal tissues were isolated from treated mice at the indicated time points according to the experimental flow. Samples were fixed overnight at 4°C in formaldehyde, flattened in biopsy cassettes. Tissues were then dehydrated in ethanol, at increasing concentrations to substitute the aqueous content of the tissue, and incubated in xylene. Finally, the samples were embedded in paraffin and cut with microtome at 5 μm thickness. Once dried, the slices were rehydrated and stained.

For Hematoxylin\Eosin Y staining, tissues were first incubated in Hematoxylin (Harris Hematoxylin Solution, Sigma Aldrich) for 2' at RT and the excess of colorant was removed with three washes in source water. Then, cell cytoplasm was counterstained with Eosin Y, washed with 95% ethanol to remove the excess of colorant.

For Alcian Blue staining, tissues were incubated in the staining solution (Alcian Blue, Sigma Aldrich) for 30' at RT and the excess of colorant was removed with three washes in source water.

Stained sections were dehydrated in 100% ethanol and then incubated in xylene. Finally, slides were mounted with Eukitt (Bio-Optica) and the images were acquired with either Olympus BX51 or Leica DM6 widefield microscopes.

2.4 Immunofluorescence, Immunohistochemistry and LacZ staining

For immunofluorescence experiments, isolated small intestines were longitudinally opened and fixed for one hour in paraformaldehyde (PFA) 4% (in 1X PBS) at 4°C, flattened in the biopsy cassettes. After an overnight incubation in 25% sucrose (in 1X PBS), intestinal

samples were washed twice in 1X PBS and embedded in OCT (Tissue-Tek 4583), suitable for frozen sectioning on a cryostat. Prior sectioning, frozen slides were equilibrated at RT, washed twice in 1X PBS and blocked with 1% BSA+10% goat serum in PBS containing 0.5% Triton X-100 for one hour at RT. Incubation with primary antibodies was performed in 1X PBS containing 0.1% Triton X-100, 1% BSA and 10% goat serum (antibody solution) at 4° C overnight. After three washes in 1X PBS, intestinal slides were incubated with the secondary antibody [1:500 (in antibody dilution)] for one hour at room temperature. After washing of the unbound antibody, nuclei were stained with DAPI (32670, Sigma- Aldrich) for 3' at RT. Slides were mounted in Mowiol 4-88 (81381, Sigma Aldrich) and the images were acquired with Leica DM6B microscope.

For immunohistochemistry, paraffin-embedded tissues were exposed to proteinase K–mediated antigen unmasking or heat-induced antigen retrieval using 10 mM sodium citrate. Anti-Ki-67 (1:400 - Abcam, ab16667) and anti-lyz1 (1:5000 - Dako, A0099) were used as primary antibodies.

For LacZ staining, fresh intestinal tissues were washed once in ice cold PBS and incubated in a fixing solution (containing Gluteraldehyde 0.2%, NP-40 0,02% and PFA 2% in PBS), rocking for 3 hours at 4°C. After three washes of 10' in PBS at RT, the samples were soaked in the Equilibration Buffer (2mM MgCl2, NP-40 0,02% and sodium deoxycholate 0,1% in PBS) and leaved in the orbital shaker for 30' at RT. Then, intestinal tissues were stained overnight at RT with 5 mM K3Fe(CN)6, 5 mM K4Fe(CN)6 and 1mg/ml X-Gal (5-bromo-4-chloro-3-indolyl- beta-D-galactopyranoside), directly added to the Equilibration Buffer. The day after, stained tissues were washed three times with PBS for 10' and fixed in PFA 4% for 6 hours at RT, while rocking. Then, the fixative was removed and the tissues were immersed in 70% ethanol, ready for paraffin-embedding and the downstream histological analyses, as described in the Histology section.

2.5 Intestinal crypts purification

Murine small intestines were *ex vivo* isolated and flushed with ice-cold PBS. The epithelium was longitudinally opened with scissors and the villi were scraped using a glass coverslip. Intestines were then chopped into around 5mm pieces and incubated in 30 ml of cold PBS containing 1mM EDTA, and kept on ice for 20'. After this incubation, the falcon was gently inverted twice in order to release remaining villi in the supernatant, which was carefully removed. Intestinal fragments were further incubated in PBS containing 5mM EDTA for 45' at 4°C, while rocking. Then, the supernatant was discarded and fragments including crypts, present at the bottom of the falcon, were resuspended in 20 ml of ice-cold

PBS containing 1% of FBS and vigorously shacked ten times. The supernatant, containing the released crypts, was filtered using a 70 μM cell strainer. This step was performed three times with new 20 ml of PBS-FBS 1% solution. Crypts were pelleted at 1000 RPM for 5' at 4°C and, after a wash with ice-cold PBS-FBS 1%, centrifuged again at 800 RPM for 5' at 4°C. The pellet of purified crypts was used for downstream applications, such as minigut culture, lysate preparation or genome-wide analyses (ChIP-seq, RNA-seq).

2.6 Mini-gut culture

Intestinal organoids were cultured in Matrigel (Corning), by embedding purified small intestinal crypts in sitting drop of 50 μl. Organoids were then cultured with a basal medium containing Advanced Dulbecco Modified Eagle Medium (DMEM)/F12 (Invitrogen), 2mM Glutamine (Lonza), 10 mM Hepes, 100 U/ml penicillin and 0,1 mg/ml streptomycin, 1.25 mM N-acetyl-cysteine (Sigma-Aldrich), N2 (Invitrogen), B27 (Invitrogen). This medium was supplemented with Recombinant Wnt3a (homemade), Recombinant R-spondin1 (homemade), 0,1 μg/ml Noggin (PeproTech), 0,05 μg/ml Egf (Thermo Fisher Scientific). Growth factors were added daily and the medium was replaced every 2 days.

2.7 Cell lines and cell culture

Conditional mESC lines, previously generated in our laboratory [43, 186], were grown on 0,1% gelatin-coated dishes in GMEM medium (Euroclone) supplemented with 20% fetal calf serum (Euroclone), 2 mM glutamine (GIBCO), 100 U/ml penicillin, 0,1 mg/ml streptomycin (GIBCO), 0,1 mM non-essential amino acids (GIBCO), 1 mM sodium pyruvate (GIBCO), 50 μM β-mercaptoethanol phosphate buffered saline (GIBCO), 1000 U/ml leukemia inhibitory factor (LIF; homemade), 3 μM of GSK3β and 1 μM of MEK1/2 inhibitors (Selleckchem).

To generate stable CBX7 KO cell lines, 10 μg pX458 2.0 plasmids (Addgene) encoding Cas9 and sgRNAs were transfected with Lipofectamine 2000 (Thermo Fisher Scientific), following the manufacturer's instruction. GFP positive cells were purified by sorting 30 hours post transfection and 2000 cells were seeded into a 15 cm dish. Clones were isolated 10 days later and screened by Western Blotting for protein lysates.

The following gRNA guides were used for targeting: *CBX7* Exon 1 CACCGCATCCGGAAGAAGCGCGTG and AAACCACGCGCTTCTTCCGGATGC; *CBX7* Exon 6 CACCGCGTCACCGTCACCTTCCGCG and AAACCGCGGAAGGTGACGGTGACGC.

For rescue clone generation, mESCs *Pcgf1 KO*, previously generated in our laboratory [43], were transfected with 10ug pCAG vectors encoding 2xFlag-HA-tagged PCGF1 wild type using Lipofectamine 2000 (Thermo Fisher Scientific), according to manufacturer's instructions. 24 hours later cells were selected with puromycin (1μg/mL), which was added for further 24 hours. Cells were then split to clonal density (~1:40) onto a 15 cm plate. Clones were isolated 10 days later and grown further before screening for rescue allele expression by Western blotting.

2.8 Western Blotting

Western Blotting analyses were performed on pellets of purified crypts or cultured mESCs. Pellets were lysed with S300 extraction buffer (20 mM TRIS-HCl pH 8, 300 mM NaCl, Glycerol 10%, Igepal 0,2%) in presence of protease inhibitors, maintaining the samples on ice for 30'. After the centrifugation at 16000g for 20' at 4° C, the supernatant, representing the soluble fraction, was separated from the pellet and quantified with the Bradford assay. The pellet, containing histones, was washed once with S300 buffer and then lysed in 8M Urea buffer, supplemented with 100 mM ammonium bicarbonate, 150mM NaCl and protease inhibitors. Then, it was sonicated and centrifuged at 16000g for 20' at 4° C. The resulting supernatant was collected and quantified with the Bradford assay.

Both soluble and insoluble fractions were independently diluted and preserved with 1X LAEMLLI buffer to achieve the desired protein concentration, usually 1 or 2 μg/μL. 30ug of the soluble fraction and 5 ug of histones were separated through SDS-PAGE and transferred on nitrocellulose membrane. Then, the membrane was saturated with 5% low-fat dried milk in TBS-Tween 0,01% and incubated with the specific primer antibody, as reported in Table 1.

After primary antibody binding, membranes were washed three times in TBS-Tween 0,01% for 10' and incubated with the required secondary antibody. The secondary antibody was washed away prior to signal detection, which was performed with ClarityTM Western ECL Substrate (Bio Rad). Images were acquired with ChemiDoc XRS+ (Bio Rad).

2.9 Sample preparation and mass spectrometry analysis

Proteins purified from mESCs stably expressing FLAG-HA (F/HA)-tagged PCGF1 using M2 affinity gel beads (Sigma A2220) were separated for 2 cm by SDS–PAGE, using 4%–12% NuPAGE Novex Bis–Tris gels (Invitrogen) and NuPAGE MES SDS running buffer

(Invitrogen). Then, the gels were stained with Coomassie Blue using InstantBlue Comassie (Expedeon). Gel pieces were cut and digested with trypsin (Promega) overnight at 37°C. Then, peptides extraction was performed and the mix of resulting peptides was desalted and concentrated using StageTip (Proxeon Biosystems) columns. After a wash with 30mL of formic acid (FA) 0,1%, cleaned peptides were eluted with 40µL of 80% MeCN in FA 0,1%. The samples were concentrated in vacuum concentrator (Eppendorf concentrator 5301) and peptides were resuspended in 7µL of 0,1% FA. 6 µL of purified peptide mixture were loaded on a LC–ESI–MS-MS Q-Exactive HF hybrid quadrupole-Orbitrap mass spectrometer (Thermo Fisher Scientific), using a gradient of 80' with a flow of 250 nL/min. The resulting full scan MS spectra were acquired in a range of m/z 300–1650.
Raw data were analyzed with MaxQuant software (version 1.5.2.8) using default parameters and performing searches against the Uniprot mouse ID:UP000000589. Other evaluated factors were label-free quantification (LFQ), match-between-runs, and IBAQ. iBAQ intensity values, calculated by MaxQuant, were used to estimate relative abundance of proteins.

2.10 RNA isolation and Real-Time qPCR

RNA was extracted from small intestinal crypts using the Rneasy Total Rna Kit (Qiagen) and quantified by NanoDrop. 500 or 1000 nanograms of purified RNA were retrotranscribed to obtain cDNA. RT was performed with ImProm-IITM Reverse Transcriptase reagents, according the protocol provided by Promega.
Retrotranscribed cDNA was analyzed by qPCR with Gotaq(r) Qpcr Master Mix (Promega). Primers for amplification were designed with Primer3 Plus using the following parameters: amplicon length 80-150 bp; primer size 18-23 bp; primer Tm 57°C -63°C; spanning at least two exons, in order to prevent amplification of genomic DNA. All the primers employed in the present study are reported in Table 2.

2.11 RNA-sequencing

For RNA-sequencing, the total RNA was processed following Smart-seq2 protocol (Switching Mechanism at the 5' end of the RNA Transcript) (Fig. 2.3) [187], once checked for quality with Total RNA assay of Bioanalyzer instrument (Invitrogen). 5 nanograms of RNA were incubated for 3' at 72°C with one µL of 10 mM oligo-dT30Vn and one µL of 10 mM deoxynucleotide triphosphate. This step was performed to allow RNA unfolding and oligo annealing with the polyA tail of mRNA. Then, reverse transcription coupled with

template switching was carried out according the publishing protocol, by adding a mix containing the enzyme SuperScript III reverse transcriptase 100U/μL (Invitrogen) and its First-strand Buffer, RNase Inhibitor 10U/μL, 1M betaine, 5 mM DTT, 6 mM MgCl2 and 1 μM TSO (Template Switching Oligo). cDNA was pre-amplified by incubating the samples with 15 μL of the preamplification mix (KAPA HotStart Taq, KAPA High Fidelity Buffer, 0,5 mM MgCl2, 0,3 mM dNTPs, 0,1 μM ISPCR primer) in the thermal cycler, following the program of the published protocol.

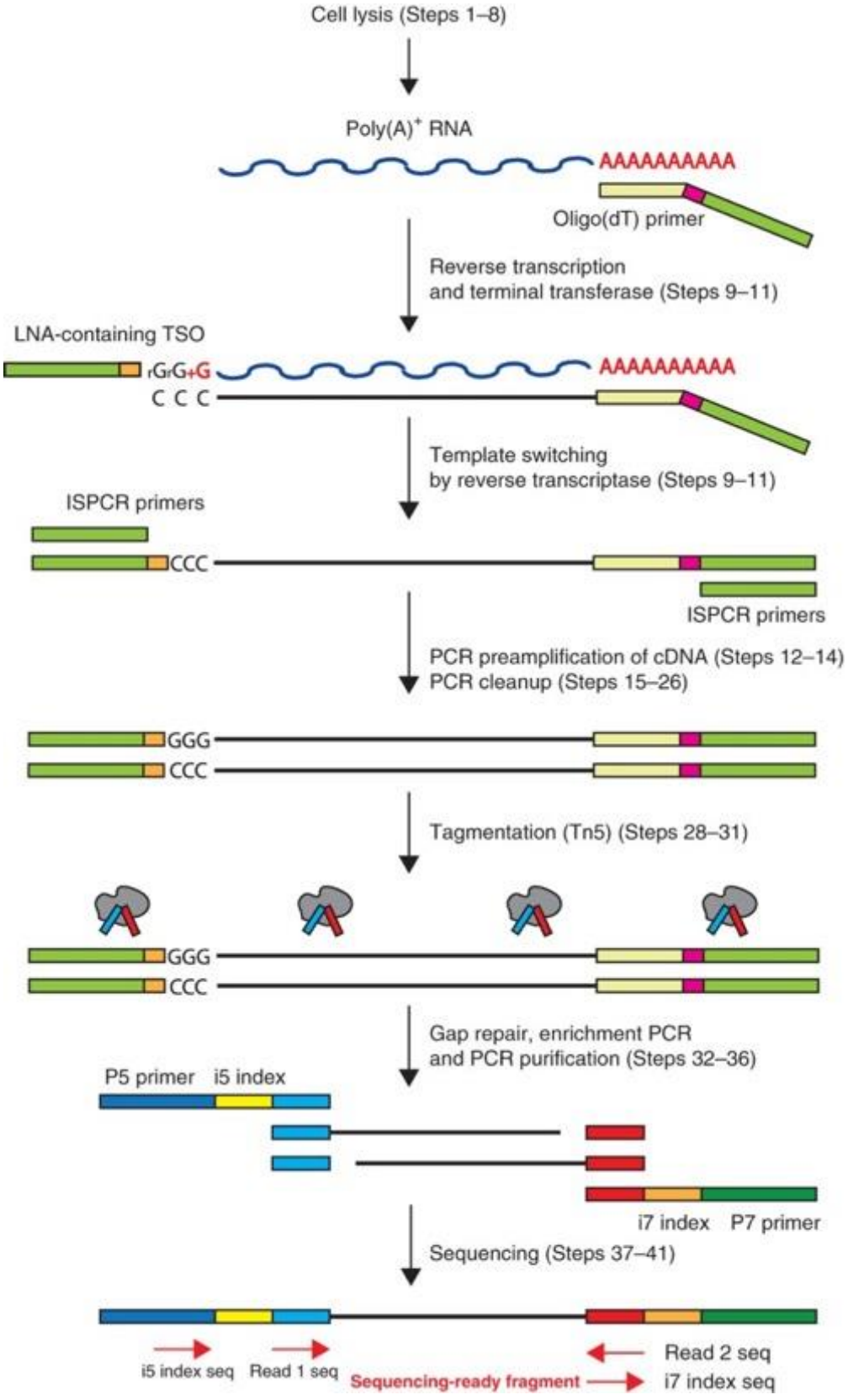

Fig. 2.3 Overview of the Smart-seq2 protocol

Schematic workflow of SMART-seq2 protocol highlighting the principal steps for library preparation (adapted from *Nature Protocol*, Picelli et al., 2014).

Samples were then purified with an equal volume of AMPure XP beads (Agencourt AMPure
XP, Beckman Coulter) and the mix was incubated at RT for 8’ to allow the binding of DNA to the beads. Beads were immobilized with a magnet and washed with 100 μL of 80% ethanol and dried for 5’ to remove alcohol residues. cDNA was eluted in 20 μL of sterile water and stored at -20°C. Eluted cDNA was quantified with Qubit colorimetric quantitation assay (Thermo Fisher Scientific, Q32854), and the quality was checked with High-sensitivity DNA assay of Bioanalyzer instrument. 1 nanogram of good quality cDNA was tagmented with 100 ng of homemade Tn5 enzyme pre-annealed with A/B-MEDS (Mosaic End Double-Stranded) oligonucleotides in working buffer containing 5mM TAPS-NaOH pH 8.5 and PEG 8000 8% for 5’ at 55°C. After tagmentation, the samples were put on ice to stop the reaction and the enzyme was stripped 5’ at RT by adding 5 μl of SDS 0,2%. Enzyme and buffer were removed by a quick AMPure purification and the eluted DNA was amplified according to the KAPA Hifi PCR protocol, adding a sample-specific primer for Illumina sequencing. The tagmented DNA was amplified according the published protocol and purified with AMPure beads. Finally, libraries were quantified with Qubit and checked for quality with High-sensitivity DNA assay of Bioanalyzer. Libraries showing an enrichment of DNA fragments with a length of 200-800 bp were sequenced using Illumina HiSeq 2000.

2.12 RNA-sequencing analysis

Raw fastq reads were aligned to the mouse genome mm10 using STAR with default parameters, except for the removal of multimapping reads using the flag -outFilterMultimapNmax 1. PCR duplicates were removed using Samblaster with default parameters [188]. PCR duplicate-free bam files were used to quantify gene expression with featureCounts with parameters -s 0 -t exon -g gene_name with GRCm38 annotation (Gencode M21) [189]. Once gene counts were quantified, the R package DESeq2 was used to perform library normalization and differential gene expression [190]. Log2 fold changes calculated by DESeq2 were corrected using the R package apeglm in order to optimize the calculation for genes with high variance [191]. To increase the statistical power of differential expression testing, while controlling the false discovery rate (FDR), the package IHW was used [192]. This allows to correct the p-values calculated by DESeq2, which improves the performance for lowly expressed genes. A threshold of Log2Fold Change of 1,5 and FDR of 0,05 was applied to annotate genes as differentially expressed. Gene Ontology analysis

of differentially expressed genes was performed using the R package clusterProfiler [193], setting as threshold a q-value and p-value of 0,01.

2.13 ChIP-sequencing

ChIP assays were carried out as described previously [194].

Purified intestinal crypts or mESCs were crosslinked in 1% formaldehyde for 10' at RT and incubated for 5' in 0,125 M Glycine. After two washes in PBS, cells were pelleted and resuspended in IP buffer, composed of two volumes of SDS buffer (100 mM NaCl, 50 mM Tris-HCl pH8.1, 5 mM EDTA pH8.0, SDS 0.5% in water) and 1 volume of Triton dilution buffer (100 mM NaCl, 100 mM Tris-HCl pH8.6, 5 mM EDTA pH8.0, Triton X-100 5% in water).

Cells were lysed 20' on ice and sonicated to get fragments long around 500 bp with the Branson sonicator. Sonicated cells were then pelleted, and the supernatant was used for immunoprecipitation. The correct amount of antibody (listed in Table 1) was added to the chromatin, and the IPs were performed overnight. For histone modifications (H2AK119ub1, H3K27me3) ChIPs, chromatin was supplemented with 5% spike-in of S2 Drosophila chromatin (prepared in the same manner).

The day after, the immunocomplexes were recovered with protein A sepharose beads (GE Healthcare) for 3 hours rocking at 4°C, and then washed three times with washing buffer containing 150 mM salt, and once with 500 mM salt (150 or 500 mM NaCl, 20 mM Tris-HCl pH 8.0, 2 mM EDTA pH 8.0, SDS 0,1%, Triton X-100 1%). Samples were decrosslinked in TE 1X with SDS 2% and 2µl of proteinase K, shacking overnight at 65°C. Decrosslinked DNA was purified with PCR purification Kit (Qiagen) and sequenced with Illumina HiSeq2000.

2.14 ChIP-sequencing analysis

Paired-end DNA reads (PE) were processed using fastp v0.20.0 to trim adapters and to remove low quality nucleotides at read ends [195]. High-quality DNA reads were aligned to the mouse reference genome mm10, or mm10 and fly reference genome (dm6) for histone ChIP-Rx using Bowtie v1.2.2 retaining only uniquely aligned reads (-m 1) and using the parameters --best and -I 10 -X 1000 for PE reads [196]. Reads mapped to both mm10 and dm6 were discarded. Peaks were identified using MACS2 v2.1.1 in narrow mode with parameters --format BAMPE--keep-dup all -m 3 30 -p 1e-10 [197]. Peaks were annotated using the R package ChIPpeakAnno v3.15 [198] and the intensity of ChIPseq signal of

histone modifications was represented with boxplots and heatmaps, both generated from BigWig files obtained using the function bamCoverage from deepTools 3.1.1 [199] with parameters --binSize 50 --extendReads. To normalize for differences in sample library size, a scaling factor for each sample was calculated as (1/total mapped reads)*1,000,000 and applied during the generation of BigWig files, through the parameter –scaleFactors from bamCoverage function. For ChIP-Rx samples, the scaling factor was calculated as previously described [200]. For the spike-in samples, a second scaling factor was calculated based on the ratio mm10/dm6 reads in the input samples. A particular scaling factor calculated from a certain input, is applied to all its respective ChIP-Rx samples. This allows to correct any potential difference in the amount of spike-in added to the different batches of chromatin. Heatmaps were produced using the function computeMatrix from deepTools, to compute a matrix of scores across regions with parameters reference-point --referencePoint TSS/center -a 5000/10000 -b 5000/10000 -bs 50, and then plotted with the function plotHeatmap from the same package, excluding blacklisted regions by the Encode Project Consortium. Boxplots were obtained using the function multiBigWigSummary, with BED-file and -outRawCounts parameters, from deepTools to compute average scores at gene promoters. Scores where then plotted in R v4.0.3 using the package ggplot2 v3.3.3. Promoters of mm10 genes were defined as the ±2.5 kb region around their TSS. A file containing coordinates for all known CpG islands in mm10, was retrieved from UCSC table browser and used to annotate promoters. ChIPseq tracks were visualized using IGV v2.12.2.

2.15 Antibodies list

Table 1: List of primary antibodies used in this study

Name	**Identifier**	**IF**	**ChIP (*in vivo*)**	**ChIP (*mESC*)**	**Western Blot**
Histone H2A	Cat. 07-146, Merck	/			1:1000; 5% milk in TBS\T; Rabbit; o/n 4°C
H2AK119ub1	Cat. 8240, Cell Signaling Technology	1:100	6µg		1:1000; 5% milk in TBS\T; Rabbit; o/n 4°C

Histone H3	Cat. 1791, Abcam				1:8000; 5% milk in TBS\T; Rabbit; o/n 4°C
H3K27ac	Ab 4729, Abcam				1:1000; 5% milk in TBS\T; Rabbit; o/n 4°C
H3K27me3	Cat. 9733, Cell Signaling Technology		6μg		1:1000; 5% milk in TBS\T; Rabbit; o/n 4°C
RING1B	Home made (for ChIP) MBL, D139-3 (for WB)		10 ug		1:1000; 5% milk in TBS\T; Rabbit; o/n 4°C
PCGF1	Home made	/	/		1:500; 5% milk in TBS\T; Rabbit; o/n 4°C
PCGF2	Home made	/	/		1:500; 5% milk in TBS\T; Rabbit; o/n 4°C
PCGF4	Home made	/	/		1:500; 5% milk in TBS\T; Rabbit; o/n 4°C
CD45	NB100-77417G, Novus Biologicals	1:200	/	/	/
CBX7	Ab21873, Abcam (for		8ug	6ug	1:1000; 5% milk in TBS\T; Rabbit; o/n

	ChIP) Cat. 07-146, Merck (for WB)				4°C
GAPDH	SC-32233, Santa Cruz				1:1000; 5% milk in TBS\T; Mouse; o/n 4°C
EED	Home made				1:10; 5% milk in TBS\T; Mouse; o/n 4°C
EZH2	Home made				1:10; 5% milk in TBS\T; Mouse; o/n 4°C
SUZ12	Cat. 3737, Cell Signaling Technology		10 ug		1:1000; 5% milk in TBS\T; Rabbit; o/n 4°C
VINCULIN	V9131, Sigma Aldrich				1:20000; 5% milk in TBS\T; Mouse; o/n 4°C
Rabbit IgG control antibody	Cat. I5006, Merck (Sigma-Aldrich)		Equal to the respective amount of ChIP antibody	Equal to the respective amount of ChIP antibody	

2.16 Primers list

Table 2: qPCR primers list

Name	**Sequence**	**Genomic position**

PCGF1 Fw	GGCTGAGTTCTGGCAAAGAC	Spanning exons 5-8
PCGF1 Rv	GGAGCTGTACATGCTGTGGA	
PCGF2 Fw	AATCACGGAGCTGAACCCTC	Spanning exons 2-3
PCGF2 Rv	AGCGTACGATGCAGGTTTTG	
PCGF3 Fw	TCCAGAGGAGAAGCCAAAGA	Spanning exons 3-4
PCGF3 Rv	ACTGTGGTTGCGTCAATGAG	
PCGF4 Fw	TGTCCAGGTTCACAAAACCA	Spanning exons 3-5
PCGF4 Rv	CGGGTGAGCTGCATAAAAAT	
PCGF5 Fw	CTGATCAAGCCCACGACAGT	Spanning exons 2-3
PCGF5 Rv	TGAACTTGGTTGCCACACCT	
PCGF6 Fw	TCCACCAGACTCAGCCTCTT	Spanning exons 3-5
PCGF6 Rv	GGCTTGGGGACTTCTAGACC	
EED Fw	TGTGAACAGCCTCAAGGAAGAT	Spanning exons 2-3
EED Rv	CCCACAGTTGCAAACACCAG	
Rplp0 Fw	GCATCACCACGAAAATCTCC	Spanning exons 4-5
Rplp0 Rv	TCAGCATGTTCAGCAGTGTG	
Lyz1 Fw	GCCCAGGCCAAGGTCTACAAT	Spanning exons 1-2
Lyz1 Rv	CACACCCAGTCAGCCAGCTT	

3. RESULTS

3.1 Variant PRC1 subcomplexes are dispensable for intestinal homeostasis and transcriptional identity

Variant PRC1 (vPRC1) complexes represent the most active H2AK119 ubiquitin ligases *in vitro* and have been proposed to control transcriptional silencing in different contexts [62-64,134].

Given the fundamental role of both RING1A and RING1B in preserving the identity of intestinal stem cells [145], we unveiled whether vPRC1 subcomplexes contribute to H2AK119ub1 deposition and gene repression in the adult intestine.

The expression levels of vPRC1-associated PCGF proteins suggested that PCGF1 was the most abundant, followed by PCGF3, PCGF5 and PCGF6, in small intestinal crypts (Fig. 3.1A).

Since the inactivation of both RING1A and RING1B disrupts all PRC1 activities [145], we took advantage of a series of Cre-dependent conditional knockout (KO) mouse models to target PCGF1, PCGF3, PCGF5 and PCGF6 functions. PCGF3 and PCGF5 were deleted together to avoid any potential compensatory effects of redundant PCGF proteins.

These mice were crossed with a transgenic line expressing a Cyp1a1 promoter-driven Cre recombinase (*AhCre*), which is activated by β-naphthoflavone (βNF), an aryl hydrocarbon receptor agonist to achieve intestinal tissue specificity [182].

Acute loss of vPRC1 activity in *AhCre Pcgf1*$^{fl/fl}$, *AhCre Pcgf3/5*$^{fl/fl}$ and *AhCre Pcgf6*$^{fl/fl}$ mice was confirmed by quantitative Real-time PCR and Western Blot (qPCR) (Fig. 3.1B, C).

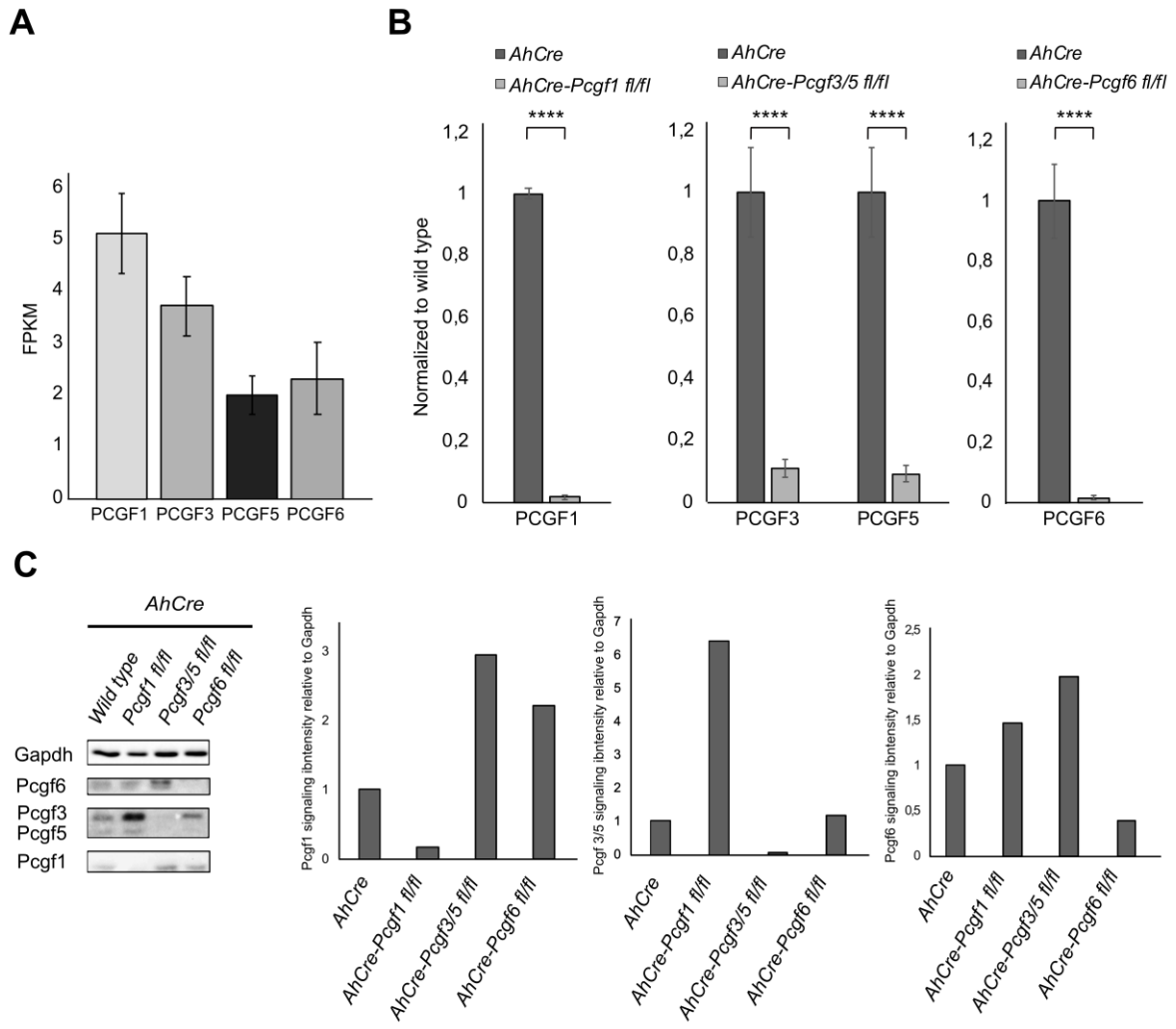

Fig. 3.1 Efficient inactivation of vPRC1-associated PCGFs in the intestinal epithelium

A) Bar plots showing the expression levels obtained from RNA-seq analyses performed in wild type intestinal crypts (n = 2) for the indicated PCGF genes. Error bars represent ± SD.

B) Expression analysis by qPCR of PCGF1, PCGF3, PCGF5, PCGF6 in the relative *AhCre* knockout mice (n = 2, n = 3, n = 2) fifteen days after the first βNF injection. Rplp0 expression was used as normalizing control. Error bars represent ± SD. The p values were determined by 2 tailed student's t-test (**** P<0.0001).

C) Western Blot and quantification graphs of Pcgf1, Pcgf3/5 and Pcgf6 protein levels in intestinal crypts isolated fifteen days post tamoxifen injection in the indicated *AhCre* mice (n = 1). Gapdh was used as loading control.

Histological analysis and immunohistochemical staining of Ki-67 positive cells showed normal homeostasis and proficient proliferation of intestinal epithelial cells upon loss distinct vPRC1- associated PCGFs (Fig. 3.2).

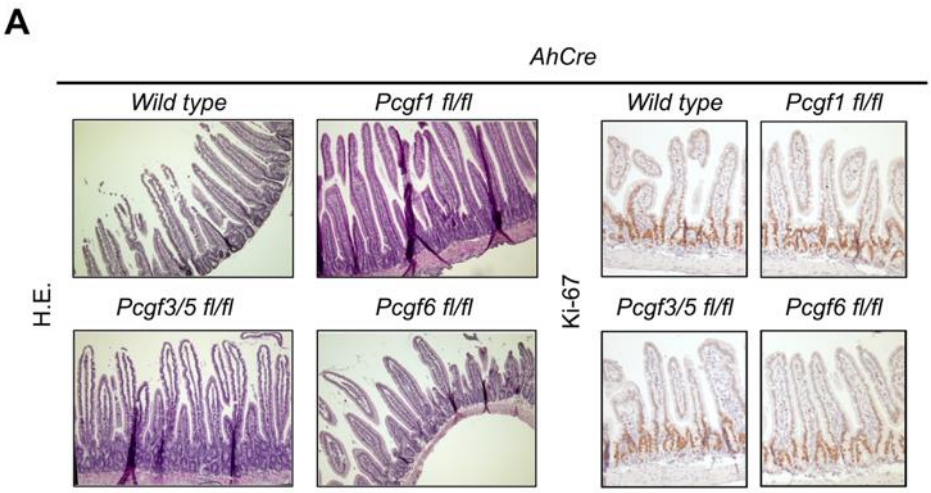

Fig. 3.2 Loss of vPRC1 subcomplexes preserves intestinal proliferation

Haematoxylin and eosin (H.E.) staining and immunohistochemical staining using anti-Ki67 on intestinal sections prepared from the indicated *AhCre* mice (n = 1) fifteen days after the first βNF injection.

Therefore, we evaluated the potential effects of vPRC1 function in ISC self-renewal, by taking advantage of a knock-in transgenic mouse strain developed by the H. Clevers laboratory, in which expression of both GFP and CreERT2 are controlled by the ISC-specific Lgr5 promoter (*Lgr5*$^{GFP\text{-}CreERT2}$) [183]. This model displays an heterogenous GFP and CreERT2 expression that allows to perform functional analyses preserving the overall functionality of the intestinal epithelium. Moreover, the introduction of a Cre-induced reporter into the *Rosa26* locus marks the ISCs progeny with constitutive LacZ expression [184]. After thirty days from the first βNF administration, the β-galactosidase activity was fully maintained in the entire tissue (Fig. 3.3). Considering the fast renewal time of the intestinal epithelium, these results strongly confirmed that vPRC1 complexes were dispensable for intestinal self-renewal.

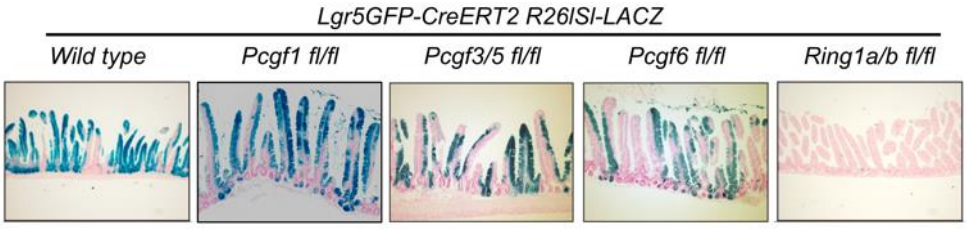

Fig. 3.3 Intestinal stem cell self-renewal is maintained upon vPRC1 loss

ISC lineage tracing in the indicated mice (n = 1) thirty days post Cre recombinase activation. Intestinal sections were stained with X-GAL and nuclei were counterstained using Nuclear Fast Red.

These results were substantiated by RNA-seq analyses (RNA-seq), showing few changes in gene expression as well as the absence of the aberrant transcriptional derepression observed in *Ring1a/b double knockout* (dKO) mice (Fig. 3.4A, B).

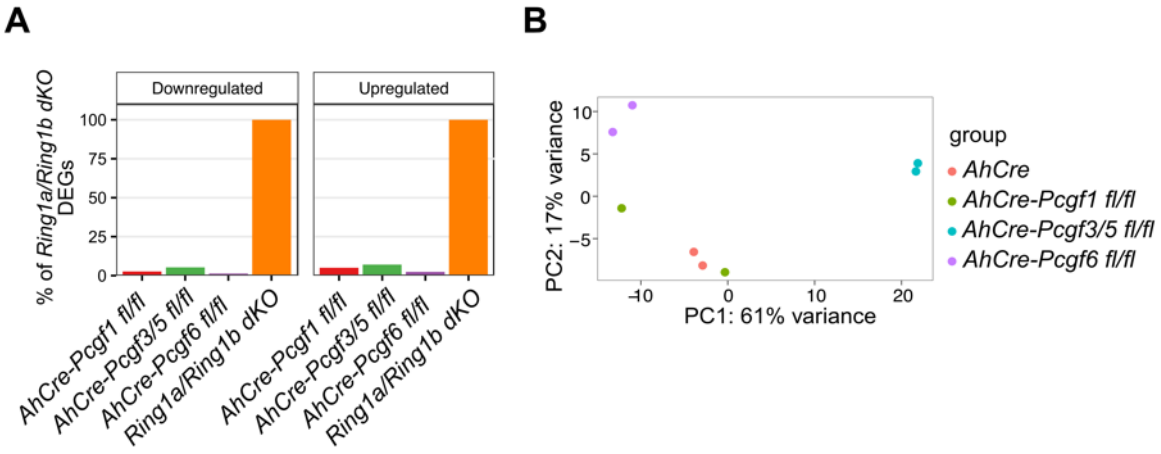

Fig. 3.4 vPRC1 subcomplexes compensate for Polycomb-mediated transcriptional repression

A) Bar plots showing the percentage of *Ring1a/Ring1b dKO* differentially expressed genes in the RNA-seq dataset of the indicated KO mice (n = 2), using small intestinal crypts samples.

B) Principal component analysis of gene expression levels from RNA-seq analysis performed in wild type and KO intestinal crypts. Experimental replicates are reported as dots of the same color.

Overall, these data strongly confirmed that loss of distinct vPRC1 activities did not recapitulate the effects of combined removal of RING1A and RING1B in the intestinal stem cell compartment.

3.2 PRC1.1, PRC1.3/5 and PRC1.6 compensate for H2AK119ub1 deposition

The maintenance of Polycomb-mediated gene repression following removal of individual PRC1 subcomplexes lead us to evaluate whether Polycomb chromatin domains were also retained.

We carried out ChIP-sequencing (ChIP-seq) for H2AK119ub1 and RING1B to identify genomic loci occupied by distinct PCGF-PRC1 complexes. Moreover, we analyzed the effects on PRC2 function upon inactivation of vPRC1 subcomplexes by evaluating H3K27me3 levels.

In mESCs, removal of PCGF1 has the largest effect on H2AK119ub1 deposition at PRC1-bound sites, resulting in a concomitant reduction of H3K27me3 levels and in the

reactivation of hundreds of genes [134]. Contrarily, *in vivo* removal of PCGF1-containing complexes preserved H2AK119ub1 deposition and RING1B occupancy at PRC1-bound sites (Fig. 3.5A-C, Fig. 3.6A), despite >50% of RING1B targets was decorated also by PCGF1 in intestinal crypts (Fig. 3.6B).

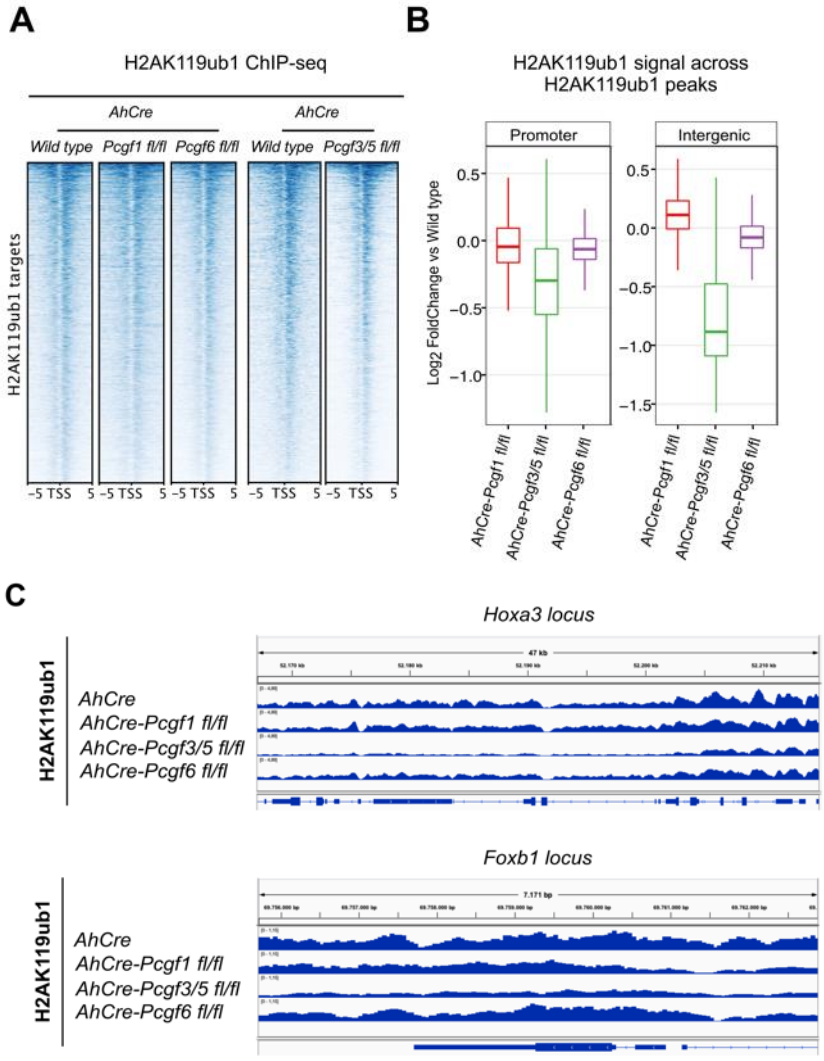

Fig. 3.5 PCGF1 and PCGF6 are not essential for H2AK119ub1 deposition at promoters

A) Heatmaps showing H2AK119ub1 ChIP-Rx enrichments ±5 kb around the TSS of H2AK119ub1 targets in the indicated *AhCre* mice (n = 1) fifteen days after the first tamoxifen injection.

B) Boxplots representing log2 fold change of H2AK119ub1 ChIP-seq signal between wild type and the indicated *AhCre* KO mice (n = 1) across H2AK119ub1 peaks.

C) Genomic snapshots of *Hoxa3* and *Foxb1* genomic loci showing H2AK119ub1 deposition at the promoter regions in the indicated *AhCre* mice (n = 1) fifteen days after Cre recombinase activation.

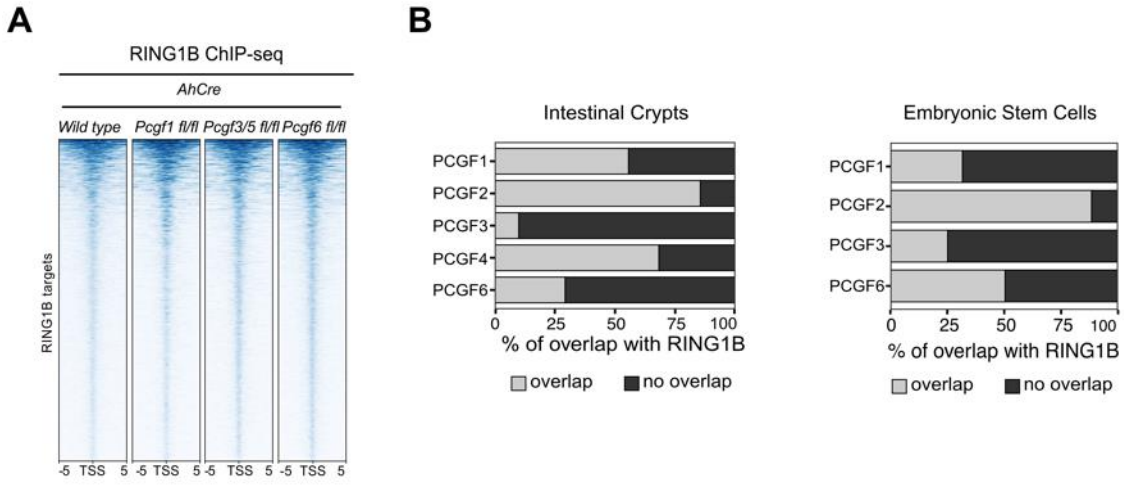

Fig. 3.6 RING1B occupancy is maintained upon loss of distinct vPRC1 activities

A) Heatmaps representing normalized RING1B ChIP-seq intensities ±5 kb around the TSS of RING1B targets in the indicated *AhCre* mice (n = 1) fifteen days after the first tamoxifen injection.

B) Percentage of overlap of the target genes identified for each indicated PCGF protein with respect to RING1B targets in replicates of wild type small intestinal crypts (left panel) and ESCs (right panel).

This was associated with an intact PRC2 activity, as the enrichment of H3K27me3 was preserved upon PCGF1 loss in the intestinal epithelium (Fig. 3.7A-C). This suggested that the remaining PCGF proteins were able to sustain normal H2AK119ub1 deposition and H3K27me3 levels in absence of PCGF1 activity.

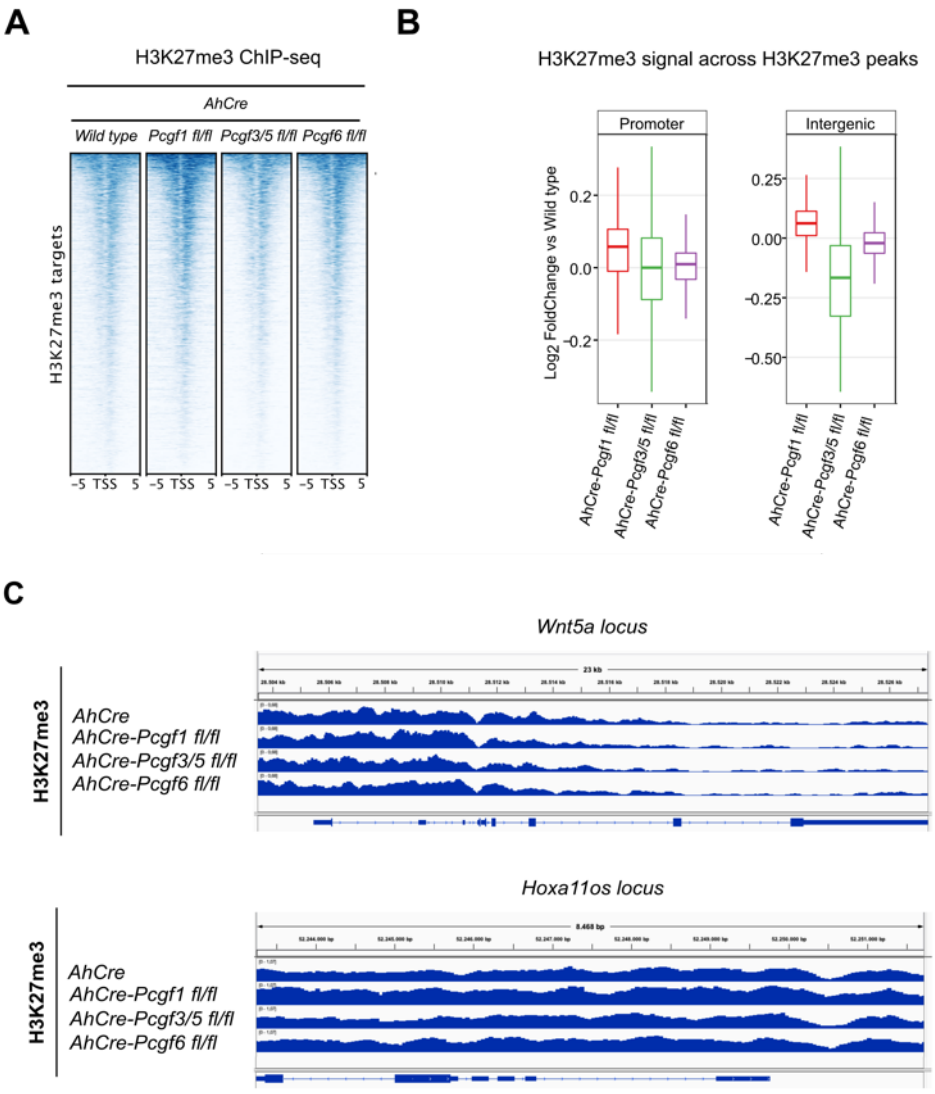

Fig. 3.7 PRC1.1, PRC1.3/5 and PRC1.6 complexes are dispensable for PRC2 activity

A) Heatmaps showing H3K27me3 ChIP-Rx enrichments ±5 kb around the TSS of H3K27me3 targets in the indicated *AhCre* mice (n = 1) fifteen days after the first tamoxifen injection.

B) Boxplots representing log2 fold change of H3K27me3 ChIP-seq signal between wild type and the indicated *AhCre* KO mice (n = 1) across H3K27me3 peaks.

C) Genomic snapshots of *Wnt5a* and *Hoxa11os* genomic loci showing H3K27me3 deposition at the promoter regions in the indicated *AhCre* mice (n = 1) fifteen days after Cre recombinase activation.

Therefore, we focused on PCGF3 and PCGF5, which display high sequence homology and produce similar protein complexes [13]. Combined loss of PCGF3 and PCGF5 resulted in a major reduction of H2AK119ub1 levels, as demonstrated by Western blot analysis as well as immunofluorescence staining of intestinal villi (Fig. 3.8A, B).

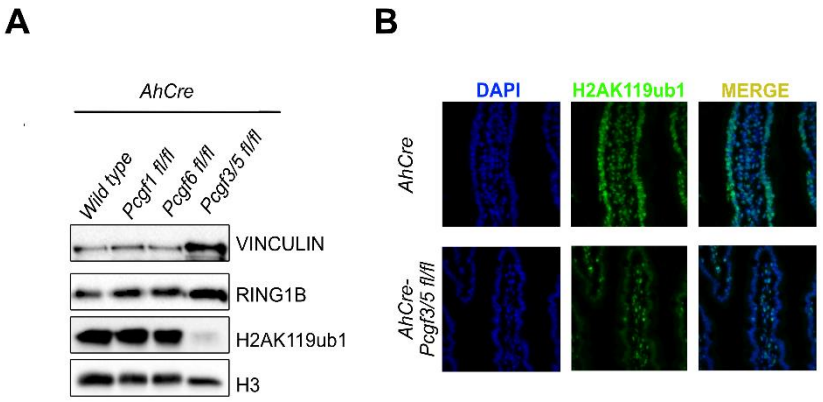

Fig. 3.8 Loss of PRC1.3/5 depletes H2AK119ub1 levels in bulk

A) Western Blot showing RING1B and H2AK119ub1 protein levels in intestinal crypts isolated fifteen days post tamoxifen injection from the indicated *AhCre* mice (n = 1). Vinculin and histone H3 were used as loading controls.

B) Immunofluorescence staining using anti-H2AK119ub1 antibody in intestinal sections isolated from wild type and *Ahcre-Pcgf3/5* $^{fl/fl}$ mice (n = 1) fifteen days after Cre recombinase activation.

Particularly, a profound depletion of H2AK119ub1 deposition occurred at intergenic regions, as revealed by ChIP-seq analysis (Fig. 3.5B). Such observation was in agreement with previous findings in the mESC model [134,142], highlighting the fundamental role of PCGF3/5-PRC1 in depositing a genome-wide "blanket" of H2AK119ub1 *in vivo*. Despite that, loss of PCGF3/5 preserved RING1B deposition and ubiquitination levels, as well as H3K27me3 enrichment (Fig. 3.5A, Fig. 3.6A, Fig. 3.7A-C), further supporting the moderate PCGF3/5-dependent effects on gene transcription (Fig. 3.4A).

Differently from the mESC model, where PCGF6 and RING1B occupancy largely overlap, *in vivo* only the 25% of PCGF6 targets was decorated also by RING1B (Fig. 3.6B). Consistent with this, loss of PCGF6 in the intestinal epithelium maintained H2AK119ub1 deposition (Fig. 3.5A-C), and preserved global levels of H3K27me3 (Fig. 3.7A-C).

Overall, our results proved that inactivation of independent vPRC1 functions *in vivo* activate compensatory mechanisms for preserving H2AK119ub1 deposition, resulting also in the maintenance of RING1B occupancy and PRC2 catalytic activity.

3.3 Canonical PRC1 preserves RING1B occupancy, but is not required for gene repression *in vivo*

Our results clearly demonstrated that vPRC1 subcomplexes compensate for H2AK119ub1 deposition and gene repression, raising the possibility that the canonical PRC1 (cPRC1) counterpart could be the main determinant of Polycomb-mediated transcriptional silencing *in vivo*.

By using the ESC model, it has been proposed that deposition of H3K27me3 by PRC2 recruits cPRC1 to Polycomb target genes through CBX7 in order to compact chromatin and drive Polycomb-dependent transcriptional repression [128,201].

We addressed this hypothesis by generating *Pcgf2/4 dKO* mice containing floxable alleles of both PCGF2 and PCGF4, which are functionally redundant. Germline homozygosity for the recombined alleles was associated with low rate of breeding when the Cre recombinase was expressed under the *AhCre* transgene. To overcome this limit, we used the *Villin* transgene (*Villin-CreERT2*), an intestine-specific promoter activated by tamoxifen administration [185].

Villin-Pcgf2/4$^{fl/fl}$ mice were injected with tamoxifen for four consecutive days and sacrificed seven and fifteen days after the first intraperitoneal injection. Efficient inactivation of cPRC1 activity was confirmed at both RNA and protein levels, without any sign of counterselection (fig. 3.9 A, B).

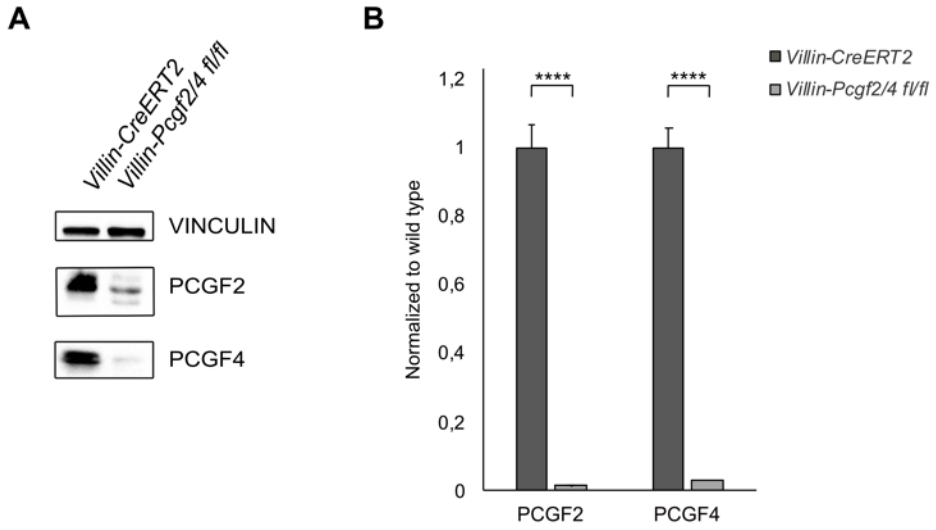

Fig. 3.9 Efficient inactivation of cPRC1 activity in the intestinal epithelium

A) Western Blot of PCGF2 and PCGF4 protein levels in intestinal crypts isolated seven days post tamoxifen injection (n = 1). Vinculin was used as loading control.

B) Expression analysis by qPCR of both PCGF2 and PCGF4 in wild type and *Villin-Pcgf2/4*$^{fl/fl}$ intestinal crypts (n = 4) fifteen days after the first tamoxifen injection.

Rplp0 expression was used as a normalizing control. Error bars represent ± SD. The p values were determined by 2 tailed student's t-test (**** P<0.0001).

Histological analyses revealed that epithelial morphology and cell proliferation were maintained upon loss of PCGF2 and PCGF4 activities over time (Fig. 3.10A, C), suggesting that cPRC1 function was dispensable for the homeostasis of the small intestinal epithelium. Consistent with this, *ex vivo* organoids derived from this model grew efficiently in a medium containing Wnt-3a, Egf, Noggin, R-spondin (Fig. 3.10B).

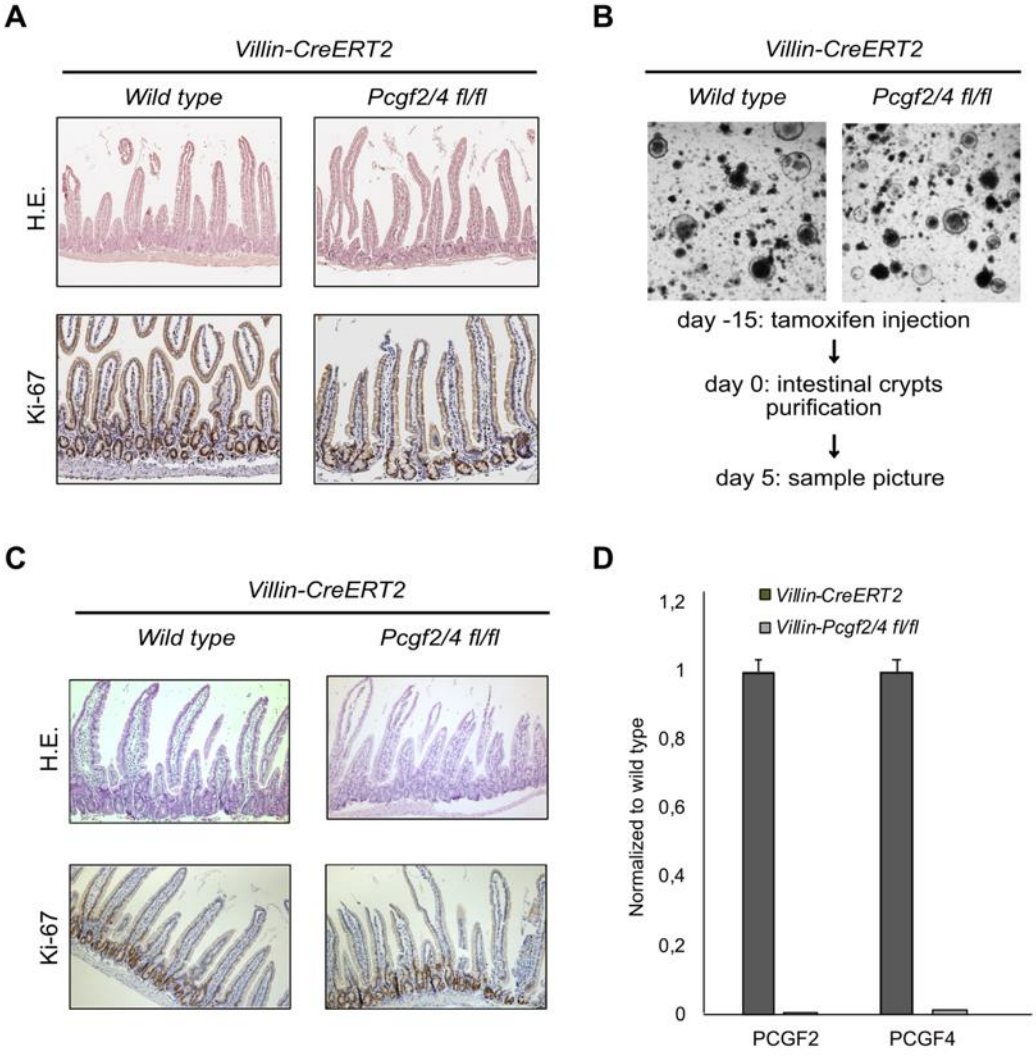

Fig. 3.10 cPRC1 is not required for intestinal homeostasis and gene repression

A) Haematoxylin and eosin (H.E.) staining and immunohistochemical staining using anti-Ki67 on intestinal sections prepared from the indicated *Villin-CreERT2* mice (n = 1) fifteen days after the first tamoxifen injection.

B) *In vitro* organoid formation using crypts isolated from wild type and *Pcgf2/Pcgf4* $^{fl/fl}$ mice (n = 2) fifteen days after the first tamoxifen injection. Pictures of organoids were taken five days later.

C) Haematoxylin and eosin (H.E.) staining and immunohistochemical staining using anti-Ki67 on intestinal sections prepared from the indicated *Villin-CreERT2* mice (n = 1) thirty days after the first tamoxifen injection.

D) Expression analysis by qPCR of both PCGF2 and PCGF4 in wild type and *Villin-Pcgf2/4* $^{fl/fl}$ intestinal crypts (n = 1) thirty days after the first tamoxifen injection. Rplp0 expression was used as a normalizing control. Error bars represent ± SD.

To investigate the transcriptional program regulated by cPRC1 in the small intestinal epithelium, we performed RNA-seq analyses from small intestinal crypts, finding few transcriptional changes upon loss of PCGF2/4 (Fig. 3.11A).

Thus, we have analyzed whether Polycomb chromatin domains were also retained, finding that the binding of RING1B was globally reduced at PRC1-repressed promoters (Fig. 3.11B). However, this did not translate into effects on H2AK119ub1 deposition as quantified by bulk Western blot analysis as well as ChIP-sequencing, which revealed normal levels and spatial deposition of H2AK119ub1 in crypts depleted of cPRC1 activity (Fig. 3.11C, D).

Overall, these observations implied that vPRC1 subcomplexes compensated for H2AK119ub1 deposition when cPRC1 function was compromised.

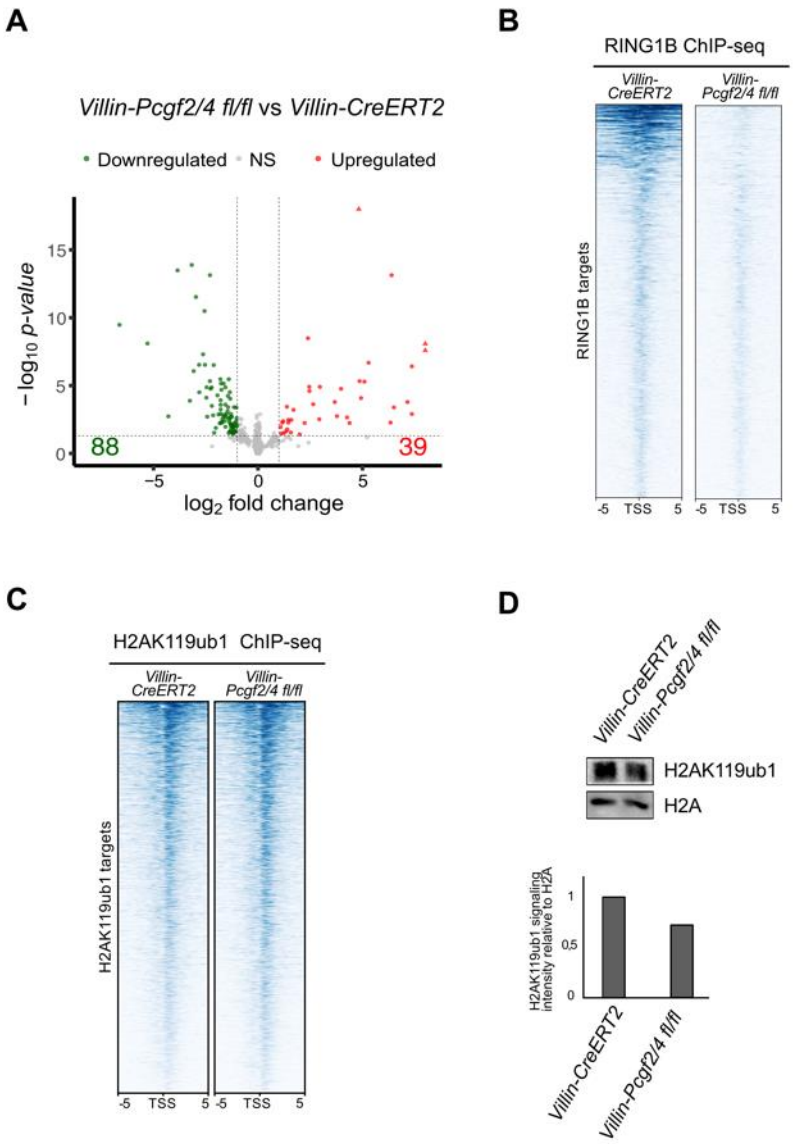

Fig. 3.11 PRC1 activity is globally maintained upon combined loss of PCGF2 and PCGF4

A) Volcano plots of –log10 (p value) against log2 fold change representing the differences in gene expression, related to RNA-seq analysis, between wild type and *Pcgf2/Pcgf4 dKO* small intestinal crypts (n = 2) isolated fifteen days post tamoxifen injection.

B) Heatmaps representing normalized RING1B ChIP-seq intensities ±5 kb around the TSS of RING1B targets in the indicated mice (n = 1) fifteen days after the first tamoxifen injection.

C) Heatmaps showing H2AK119ub1 ChIP-Rx enrichments ±5 kb around the TSS of H2AK119ub1 targets in the indicated *AhCre* mice (n = 1) fifteen days after the first tamoxifen injection.

D) Western Blot and quantification graphs of H2AK119ub1 protein levels in intestinal crypts isolated from the indicated mice (n = 1) fifteen days post tamoxifen injection. Histone H2A was used as loading control.

It has been previously proposed that the crosstalk between PRC1 and PRC2 at Polycomb chromatin domains resides on the capacity of PRC2 to recognize H2AK119ub1 [58,63,64]. Nevertheless, global levels of H3K27me3 and SUZ12 binding across RING1B targets were maintained upon loss of PCGF2/4 (Fig. 3.12A, B).

Collectively, these results demonstrated the role of cPRC1 in preserving RING1B occupancy, but its dispensability for H2AK119ub1 deposition, PRC2 recruitment and activity, and transcriptional silencing.

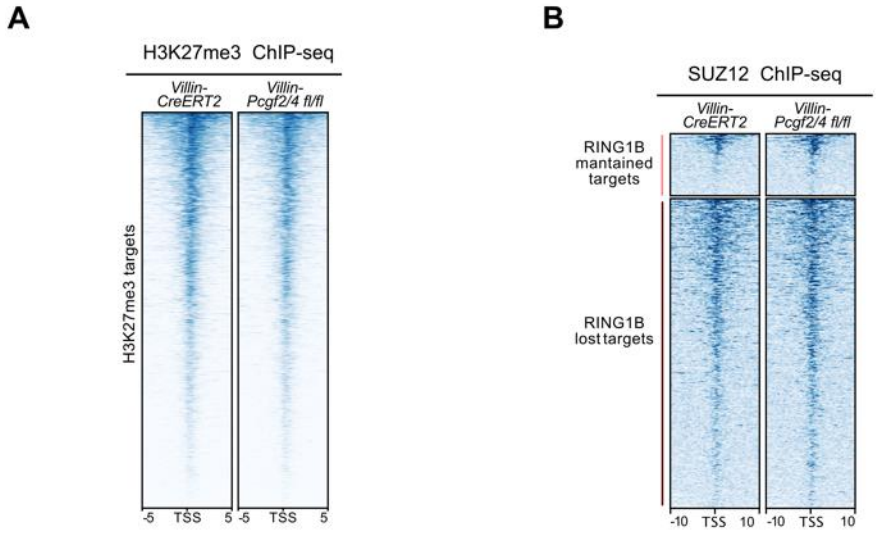

Fig. 3.12 PRC2 activity and recruitment are unaffected upon cPRC1 loss of function

A) Heatmaps showing H3K27me3 ChIP-Rx enrichments ±5 kb around the TSS of H3K27me3 targets in the indicated *AhCre* mice (n = 1) fifteen days after the first tamoxifen injection.

B) Heatmaps representing normalized SUZ12 ChIP-seq intensities ±10 kb in the indicated mice (n = 1) across RING1B targets, maintained and lost upon removal of PCGF2/4.

3.4 vPRC1 complexes contribute to CBX7 binding in absence of cPRC1 activity

It is well established that CBX7 acts as a central hub for cPRC1 targeting at PRC2-bound loci in mESCs, leading to the establishment of Polycomb-repressive domains.

Our RNA-seq analysis in wild type ESC revealed that, among PRC1-associated CBX proteins (CBX2, 4, 6, 7, 8), CBX7 was the most expressed, in agreement with previous

findings [56], and that CBX8 was almost absent (Fig. 3.13), coherent with its silencing in undifferentiated cellular systems [202].

We evaluated whether such expression pattern was conserved also in wild type intestinal crypts, finding that CBX8 was the most prominent, followed by CBX7 (Fig. 3.13). This result is probably due to the dualistic nature of the intestinal epithelium, in which stem cells coexist with more differentiated cell types.

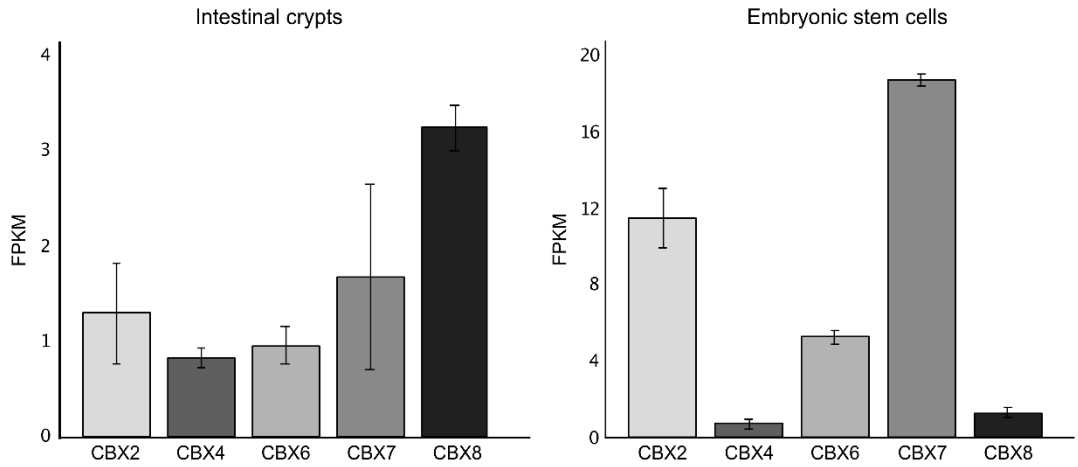

Fig. 3.13 Expression profiles of CBXs differ in intestinal crypts and ESCs

Bar plots showing the expression levels obtained from RNA-seq analyses performed in wild type intestinal crypts (n = 2) and ESCs (n = 3) for the indicated CBX genes. Error bars represent ± SD.

Considering that CBX7 has the highest affinity for H3K27me3 [203], we sought to determine its genomic distribution in intestinal crypts depleted of cPRC1 activity.

Despite our ChIP-seq analysis revealed that the vast majority of CBX7 binding was displaced upon PCGF2/4 loss, a residual occupancy still occurred *in vivo* (Fig. 3.14A). To exclude a possible failure of conditional gene deletion in achieving a full inactivation of cPRC1 and a potential compensatory effect of CBX8, we took advantage of *Pcgf2/4 dKO* mESCs, an isogenic clonal cell line previously generated in our laboratory [43]. Also in this context, we detected a residual binding of CBX7, whose specificity was confirmed by the absence of ChIP-seq signal in *Cbx7 KO* mESCs (Fig. 3.14B).

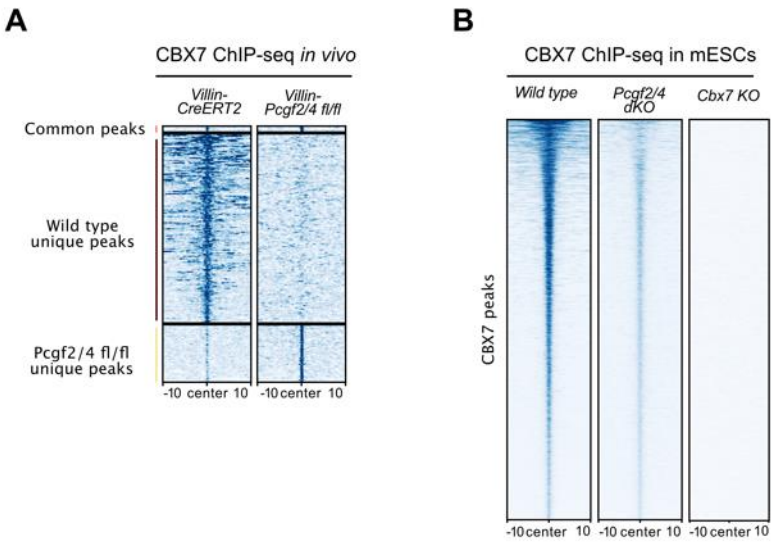

Fig. 3.14 CBX7 binding is partially retained upon cPRC1 inactivation *in vivo* and in ESCs

A) Heatmaps representing normalized CBX7 ChIP-seq intensities ±10 kb around the center of CBX7 peaks in the indicated mice (n = 1) across wild type and *Villin-Pcgf2/4* $^{fl/fl}$ unique and common peaks fifteen days after Cre recombinase activation.

B) Heatmaps representing normalized CBX7 ChIP-seq intensities ±10 kb around the center of CBX7 peaks in the indicated ESC lines.

By analyzing the percentage of retained peaks, we found that CBX7 occupancy *in vivo* was lost at cPRC1 targets but gained at vPRC1-unique sites upon PCGF2/4 removal, suggesting that vPRC1-associated PCGF proteins can contribute to CBX7 binding (Fig. 3.15A). Consistent with this, genome wide-analyses in mESCs revealed that almost all CBX7 peaks overlapped with PCGF1 and PCGF6-unique loci (Fig. 3.15B). This "promiscuous" interaction between vPRC1 and CBX7 was confirmed by tandem mass-spectrometry (MS/MS) analysis, which identified CBX7 as one of the PCGF1-interacting proteins, along with the classical vPRC1 components (Fig. 3.15C).

Despite loss of PCGF1 in the PCGF2/4 null background (*Pcgf1/2/4 tryple KO* mESCs) had no additive effects in CBX7 occupancy, combined removal of PCGF1 and PCGF6 (*Pcgf1/2/4/6 quadruple KO* mESCs) resulted in a strong displacement of CBX7 from chromatin (Fig. 3.15D). This effect was similar to what observed in the catalytically dead PRC2 mutant *Ezh1KO-Ezh2*Y726D, a cell line in which the catalytic pocket of EZH2 harbors a point mutation that prevents H3K27me3 deposition (Fig. 3.15D) [186].

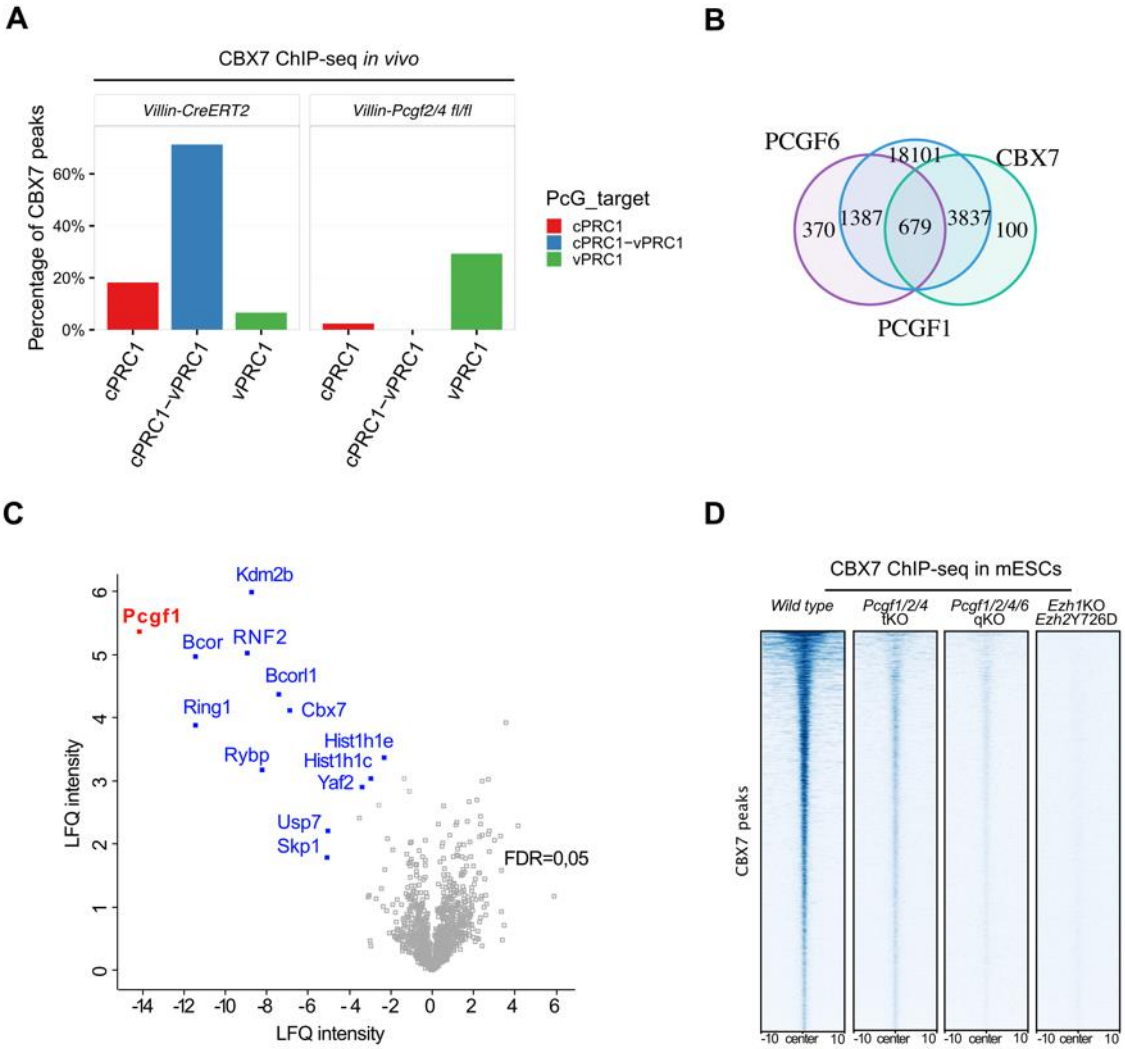

Fig. 3.15 CBX7 functionally interacts with PCGF1/PCGF6-containing complexes

A) Bar plots representing the percentage of CBX7 peaks in the indicated mice (n = 1) at unique and shared cPRC1 and vPRC1 target loci.

B) Venn diagrams showing the overlapping peaks between PCGF1, PCGF6 and CBX7 in wild type ESCs.

C) LFQ intensity obtained by tandem mass spectrometry (MS/MS) analyses in the PCGF1 immuno-purifications (anti-FLAG) from wild type mESCs stably expressing FLAG-HA (F/HA)-tagged PCGF1.

D) Heatmaps representing normalized CBX7 ChIP-seq intensities ±10 kb around the center of CBX7 peaks in the indicated ESC lines.

Overall, these findings revealed that, in absence of cPRC1 activity, a *de novo* co-occupancy of PCGF1/6 and CBX7 occurred, paving the way for a novel model of functional compensation between vPRC1 and cPRC1 that require further studies.

3.5 PRC2 preserves secretory lineage commitment and transcriptional silencing via cPRC1-independent mechanisms

Since the current model of Polycomb recruitment implies that cPRC1 acts downstream PRC2, we asked whether the effects induced by EED loss *in vivo* involved PCGF2/4 activities.

By deleting EED in the *AhCre* background, we have previously shown that PRC2 was required during intestinal homeostasis for preserving secretory lineage commitment [144].

As Paneth cells are spared by *AhCre*, we sought to exclude possible biases between the *AhCre* and the *Villin-CreERT2* models. Thus, we compared the effects of cPRC1 removal respect to PRC2 inactivation by knocking out EED also in the *Villin-CreERT2* background. Loss of EED prevented the ability of PRC2 to tri-methylate histone H3 at lysine 27 (H3K27me3), as quantified by bulk Western blot analysis as well as ChIP-sequencing, which showed a profound depletion of H3K27me3 across RING1B targets, suggesting that PRC1-bound loci were devoid of PRC2 catalytic activity (Fig. 3.16A, B). Moreover, the whole stability of the complex was affected, since the levels of the other PRC2 components, EZH2 and SUZ12, were strongly decreased (Fig. 3.16A, C).

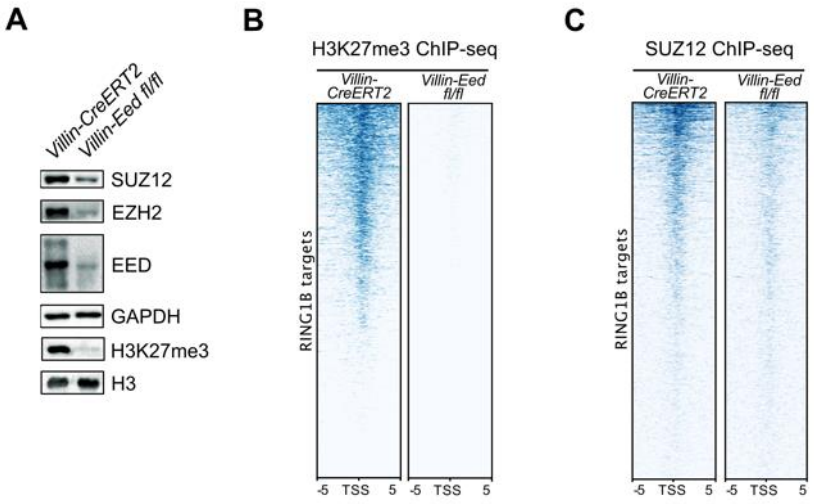

Fig. 3.16 EED inactivation prevents PRC2 activity and assembly

A) Western Blot showing SUZ12, EZH2, EED and H3K27me3 protein levels in intestinal crypts isolated from the indicated mice (n = 1) fifteen days after the first tamoxifen injection. GAPDH and Histone H3 were used as loading controls.

B) Heatmaps showing H3K27me3 ChIP-Rx enrichments ±5 kb around the TSS of RING1B targets in the indicated *AhCre* mice (n = 1) fifteen days after the first tamoxifen injection.

C) Heatmaps representing normalized SUZ12 ChIP-seq intensities ±5 kb around the TSS of RING1B targets in the indicated mice (n = 1) fifteen days after Cre recombinase activation.

Consistent with our previous findings in the *AhCre* model, the histological analysis of *Villin -Eed*$^{fl/fl}$ intestines revealed a marked alteration in the crypt–villus architecture fifteen days after Cre recombinase activation. A clear defect in cell proliferation, specifically restricted to the transit-amplifying compartment, was highlighted by Ki67 staining (Fig. 3.17A). In addition, we observed an increased number of mucus-secreting cells (Goblet cells) and scattered lysozyme1 positive cells (Paneth cells) at the crypt-villus junction (Fig. 3.17A). Such effects were cPRC1-independent, as goblet cell specification and Paneth cell positioning were preserved in intestines depleted of both PCGF2 and PCGF4 activities (Fig. 3.17B).

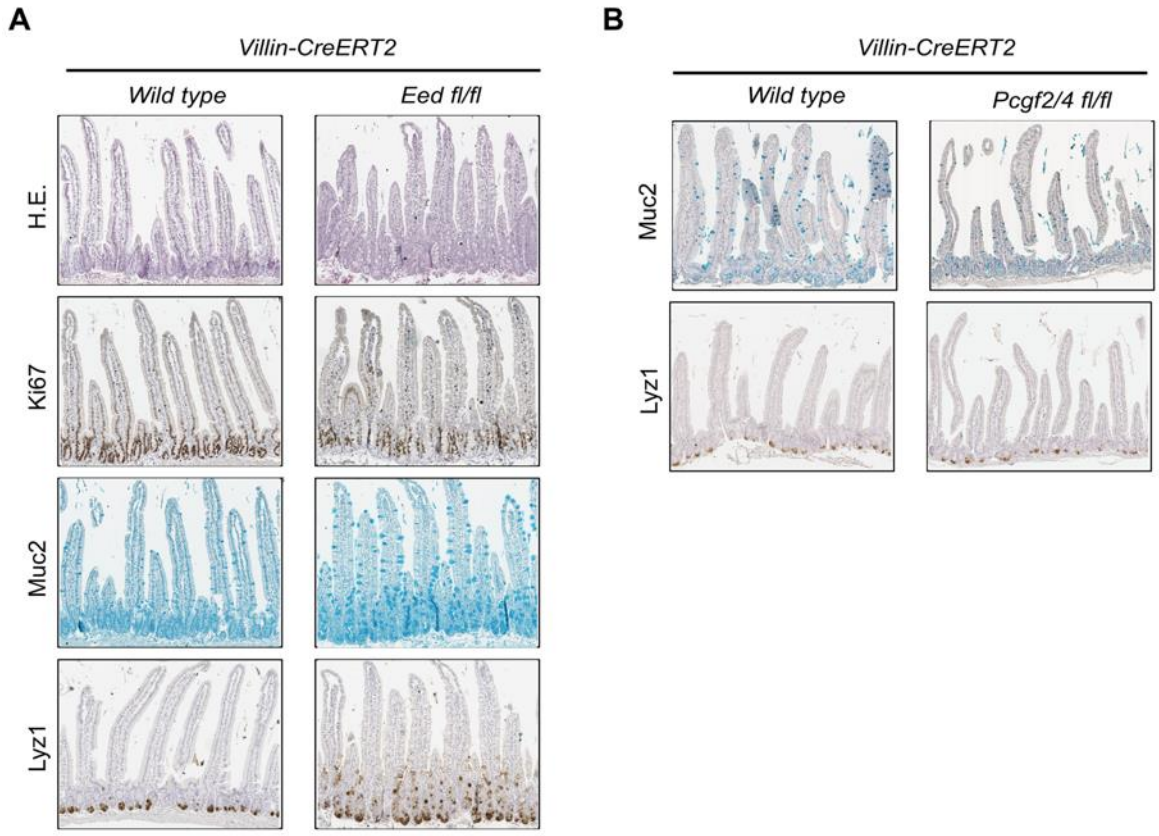

Fig. 3.17 PRC2 loss expands the secretory compartment independently from cPRC1 activity

A) Haematoxylin and eosin (H.E.) staining, Alcian Blue staining (showing Muc2 positive cells) and immunohistochemical staining using anti-Ki67 and anti-lysozyme1 (Lyz1) on intestinal sections prepared from wild type and *Villin-Eed* $^{fl/fl}$ mice (n = 2) fifteen days after the first tamoxifen injection.

B) Alcian Blue staining and immunohistochemical staining using anti-lysozyme1 on intestinal sections prepared from wild type and *Villin-Pcgff2/4*$^{fl/fl}$ mice (n = 2) fifteen days after the first tamoxifen injection.

Moreover, RNA-seq analyses showed global transcriptional changes upon EED removal (Fig. 3.18A), confirming that PRC2 acted as an autonomous repressive unit *in vivo*, uncoupled from cPRC1 function (Fig. 3.11A).
Consistent with the absence of H3K27me3 deposition at RING1B-bound loci (Fig. 3.16B), we found that the percentage of upregulated RING1B targets upon EED removal resembled the transcriptional reactivation observed after catalytic inactivation of PRC1 (Fig. 3.18B).

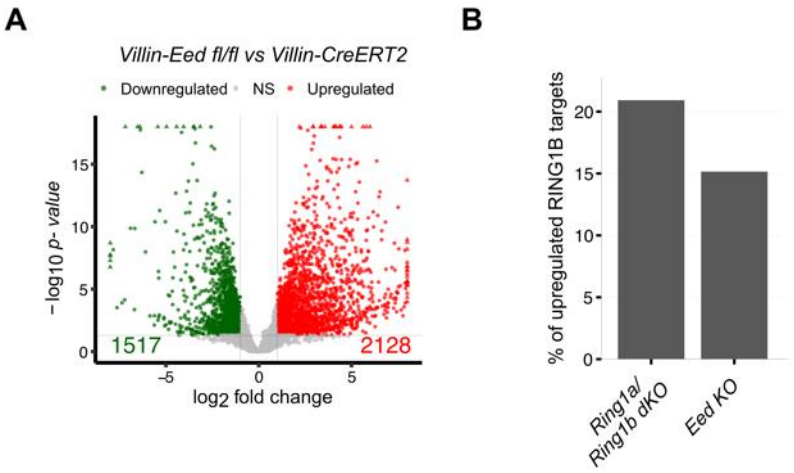

Fig. 3.18 EED loss results in extensive transcriptional changes

A) Volcano plots of –log10 (p value) against log2 fold change representing the differences in gene expression, related to RNA-seq analysis, between wild type and *Eed KO* small intestinal crypts (n = 2) fifteen days after the first tamoxifen injection.
B) Bar plots showing the percentage of RING1B upregulated targets in the RNA-seq dataset of the indicated knockout mice (n = 2).

Such effects in gene expression did not involve PRC1 catalytic activity, as ChIP-seq analyses revealed normal H2AK119ub1 deposition upon PRC2 loss (Fig. 3.19A), despite RING1B was displaced from its target sites with the same extent of cPRC1 inactivation (Fig. 3.19B, Fig. 3.11A).

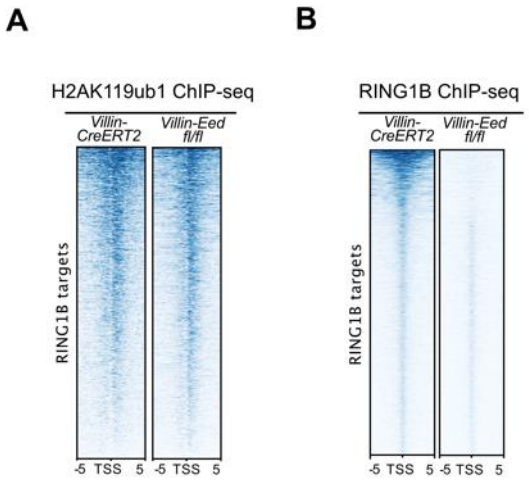

Fig. 3.19 PRC2 inactivation preserves H2AK119ub1 deposition, but impairs RING1B occupancy

A) Heatmaps showing H2AK119ub1 ChIP-Rx enrichments ±5 kb around the TSS of RING1B targets in the indicated *AhCre* mice (n = 1) fifteen days after the first tamoxifen injection.
B) Heatmaps representing normalized RING1B ChIP-seq intensities ±5 kb around the TSS of RING1B targets in the indicated mice fifteen days after Cre recombinase activation.

Collectively, these results strongly confirmed that PRC2 controls secretory lineage commitment and transcriptional identity of intestinal cells without involving the downstream PCGF2/4 activities.

3.6 PRC2 inactivation results in the accumulation of intermediate secretory cells by interfering with Notch and Wnt signaling pathways

To explore the molecular events behind the increased number of intestinal secretory cells induced by EED loss, we evaluated the activity of the Notch signaling, which is involved both in goblet and Paneth cells differentiation.

Notch signaling drives the absorptive cell fate over the default secretory cell fate by activating the transcription factor *Hes1*, which acts as transcriptional repressor of *Atoh1*, the master regulator of the secretory lineage.

The vast majority of the players acting within the Notch pathway (i.e., *Dll1*, *Dll2*, *Hes1*, *Rbpj*) were not perturbed by EED loss, with the exception of *Atoh1* and the downstream target *Spdef*, which underwent strong transcriptional activation (Fig. 3.20A). Indeed, our ChIP-seq analysis revealed a wide H3K27me3 deposition at the promoters of those genes,

which was lost after EED removal, further confirming the repressive control exerted by PRC2 (Fig. 3.20B).

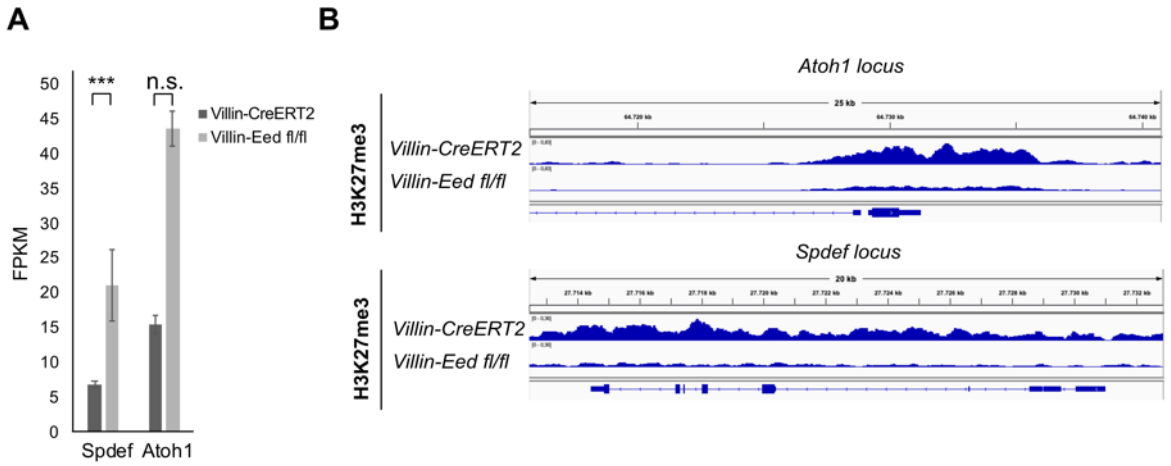

Fig. 3.20 PRC2 controls *Spdef* and *Atoh1* transcriptional silencing

A) Bar plots showing the expression levels obtained from RNA-seq analyses performed in wild type and *Villin-Eed*$^{fl/fl}$ intestinal crypts (n = 2) for *Atoh1* and *Spdef* genes, seven days post tamoxifen injection. Error bars represent ± SD. The p values were determined by Wilcoxon non-parametric statistical test (*** P< 0,001).

B) Genomic snapshots of *Atoh1* and *Spdef* genomic loci showing H3K27me3 deposition at the promoter regions in the wild type condition and fifteen days after EED loss.

Despite in line with our previous findings [144], these observations were not sufficient to explain the mislocalization of Paneth cells, as genes involved in their positioning (*Ephb3*, *Afdn*, *Prkci*) were transcriptionally unchanged upon EED loss. Moreover, our RNA seq data did not reveal an activation of the Paneth cell signature (*Lyz1*, *Mmp7*, *Ang4*, *Cd24a*) following PRC2 inactivation (data not shown).

In agreement with the growing evidence that Paneth and goblet cells share a common mechanism of differentiation [149,204], we hypothesized that secretory cells accumulating in the small intestine upon PRC2 inactivation represent a cell population sharing features of an undifferentiated cell as well as immature secretory cells. These dubbed “intermediate cells” co-express genes identifying Paneth cells and markers specific of goblet cells. Consistent with this, we noticed a strong upregulation of genes shared by Paneth and goblet cells, such as *cryptidin 2* (*Crip2*) and *hepatocyte growth factor activator* (*Hgfac*) (Fig. 3.21A). Moreover, we detected reduced levels of *serine/threonine kinase 11* (*Stk11*; also called *Lkb1*), a tumor suppressor gene whose absence triggers the acquisition of a

transcriptional signature associated with secretory cells in the intestinal epithelium (Fig. 3.21A) [205].

Intermediate cells have been shown to increase during the immune response against infective agents [206]. Not by chance, Gene Ontology analysis of the differentially expressed genes (DEGs) in intestinal crypts depleted of PRC2 activity revealed an enrichment of type I interferons (IFN) genes alpha and beta, indicating an active antiviral response (Fig. 3.21B).

To interrogate whether the appearance of intermediate cells was induced by inflammation we evaluated the expression of Cd45, marker of activated immune cells, finding no transcriptional changes in our RNAseq data (data not shown). This observation was corroborated by the absence of Cd45 positive cells in the colonic epithelium as well as inflammatory infiltrates (Fig.3.21C).

Overall, these results suggested that the transcriptional changes observed in inflammation-associated genes upon EED loss were not accompanied by an active recruitment of immune cells in the intestinal epithelium.

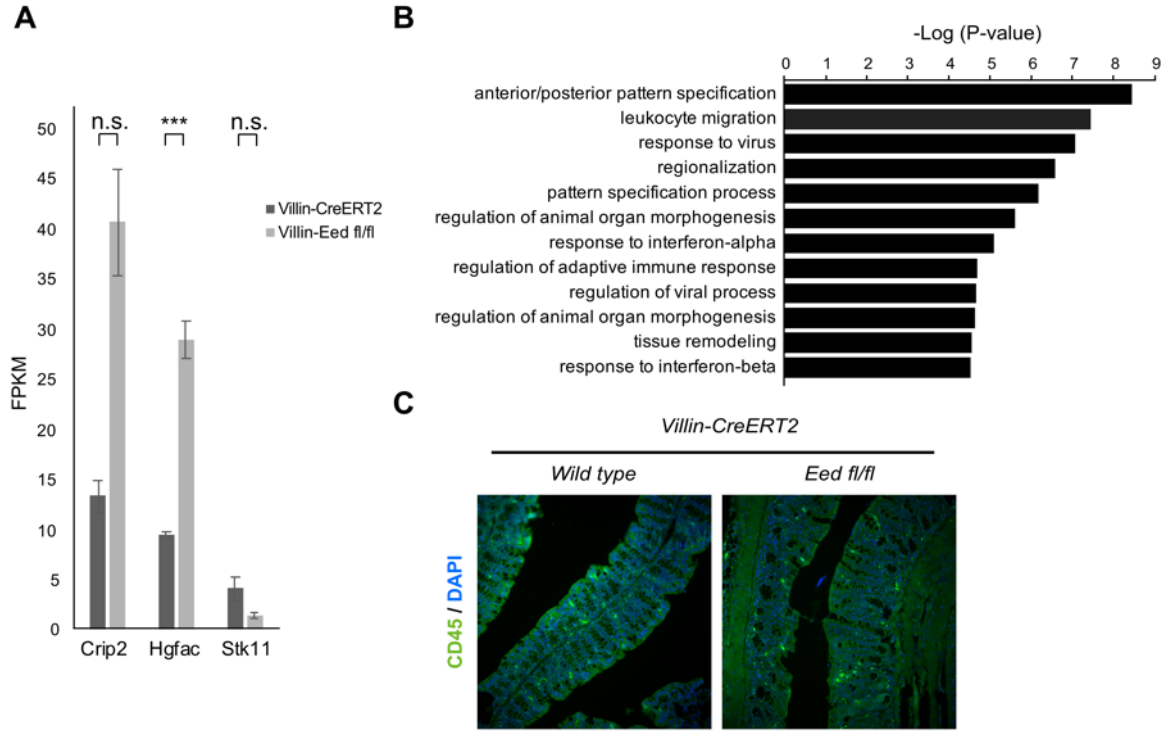

Fig. 3.21 EED loss activates the expression of "intermediate cells" markers and inflammation-associated genes

A) Bar plots showing the expression levels obtained from RNA-seq analyses performed in wild type and *Villin-Eed*$^{fl/fl}$ intestinal crypts (n = 2) for *Crip2*, *Hgfac* and *Stk11* genes, seven days post tamoxifen injection. Error bars represent ± SD.

The p values were determined by Wilcoxon non-parametric statistical test (*** P< 0,001).

B) Bar plot of affected biological processes in Eed KO intestines.

C) Immunofluorescence staining on wild type and *Villin-Eed*$^{fl/fl}$ intestinal sections (n = 1) using anti-Cd45 antibody (green) seven days after Cre recombinase activation. Nuclei were stained with Dapi (blue).

Transcriptional analysis of intestinal samples depleted of PRC2 activity showed a strong upregulation of several Wnt target genes, associated with decreased levels of *Axin2* and *Sp5*, which act as feedback inhibitors of the pathway (Fig. 3.22A).

Considering the documented role of Wnt signaling in Paneth cells differentiation and maturation [156,157], we hypothesized that Wnt activation triggered the appearance of lysozyme-expressing cells upon PRC2 inactivation.

Paneth cells are absent from the colonic epithelium in homeostatic conditions, but they can occur in disease states, such as colorectal cancer (CRC) [207]. Consistent with this, we found that oncogenic Wnt activation induced a robust transcriptional activation of lysozyme1 gene in colonic adenomas isolated from mice carrying a biallelic loss of function mutation in the *Apc* gene (Fig. 3.22B). Thus, we performed immunohistochemical staining for lysozyme1 in the colon of EED null mice, which revealed the presence of Paneth cells at the crypt bottom (Fig. 3.22C).

Overall, these results suggested that the activation of the Wnt pathway induced by PRC2 loss stimulated differentiation of Paneth cells.

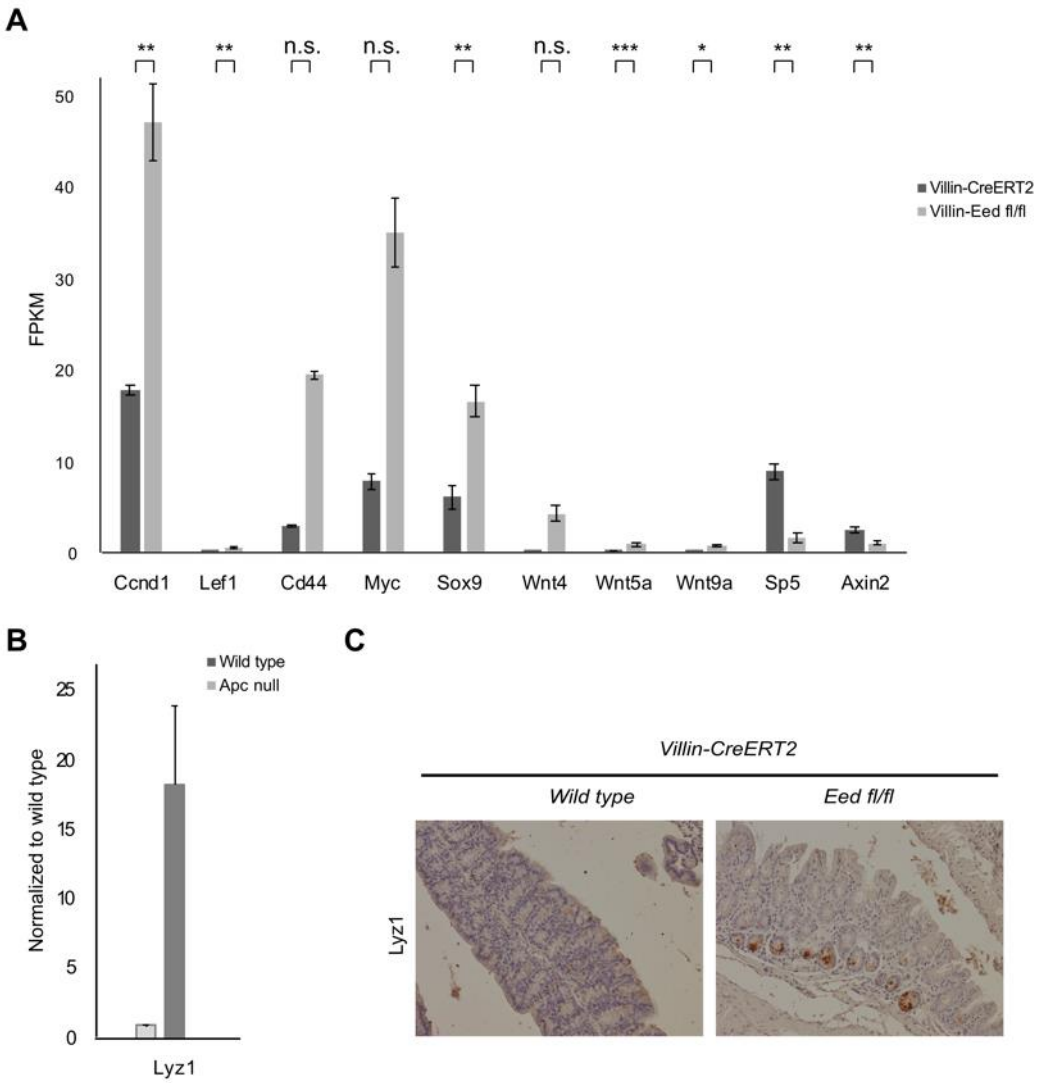

Fig. 3.22 Activation of Wnt signaling upon EED loss promotes the appearance of lysozyme1-expressing cells in the colonic epithelium

A) Bar plots showing the expression levels obtained from RNA-seq analyses performed in wild type and *Villin-Eed*$^{fl/fl}$ intestinal crypts (n = 2) for a set of Wnt target genes, seven days post tamoxifen injection. Error bars represent ± SD. The p values were determined by Wilcoxon non-parametric statistical test (* P< 0,05, ** P<0,01, *** P< 0,001).

B) Expression analysis by qPCR of lysozyme1 (Lyz1) in murine colon samples isolated from wild type and *Lgr5-eGFP-CreERT2-Apc*$^{fl/fl}$ mice (n = 1), eight days after the first tamoxifen injection. Rplp0 expression was used as normalizing control. Error bars represent ± SD.

C) Immunohistochemical staining using anti-lysozyme1 (Lyz1) on colonic samples of wild type and *Villin-Eed*$^{fl/fl}$ mice (n = 1) fifteen days after the first tamoxifen injection.

3.7 Loss of PRC1.1 rescues the effects of PRC2 inactivation during secretory lineage commitment

Removal of PCGF1/2/4-containing complexes in the small intestine is associated with intestinal stem cell exhaustion, loss of H2AK119ub1 deposition and a massive transcriptional derepression of Polycomb target genes, suggesting that the combined activity of cPRC1 and PRC1.1 reproduces the effects of RING1A/B loss of function [145] (reference to a section of Annachiara Delvecchio's PhD thesis).

Considering the current model of Polycomb recruitment positing EED in the middle of PCGF1 and cPRC1 activities, and bearing in mind that loss of EED abrogates cPRC1 engagement, we asked whether the combined removal of EED and PRC1.1 was able to phenocopy what observed in PCGF1/2/4 tKO mice.

To address this question, we crossed *PCGF1*$^{fl/fl}$ mice with the EED$^{fl/fl}$ allele under the *Villin- CreERT2* promoter. *Villin-Eed/Pcgf1*$^{fl/fl}$ mice were injected with tamoxifen for four consecutive days per week and sacrificed both at seven and fifteen days after the first injection. This treatment was intended to prevent expansion of potential escaper crypts that had avoided Cre activation, as we observed counterselection of PRC2 inactivation at day fifteen in mice exposed with the conventional regimen (Fig. 3.23A, B).

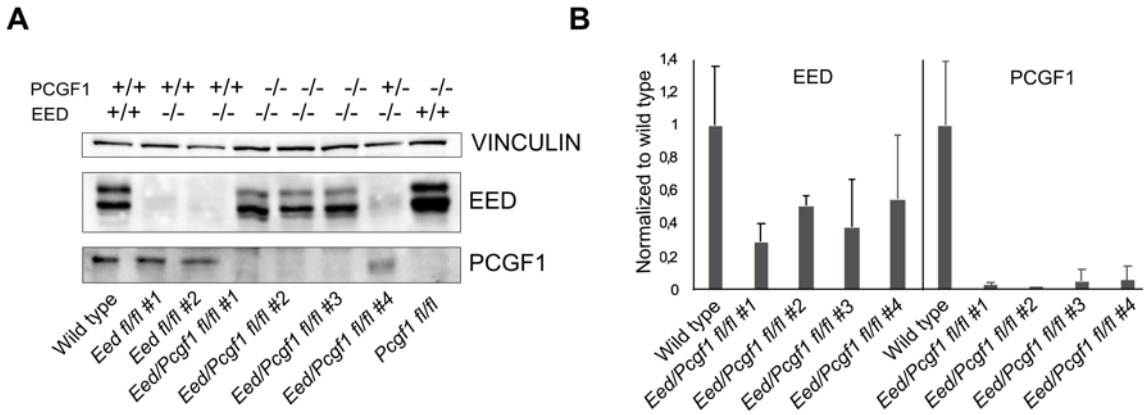

Fig. 3.23 EED inactivation is counterselected in *Villin-Eed/Pcgf1*$^{fl/fl}$ mice over time

A) Western blot analysis representing EED and PCGF1 levels, correlated with the relative mouse genotypes, fifteen days after Cre recombinase activation induced with the conventional tamoxifen regimen in *Villin-Eed*$^{fl/fl}$, *Villin-Eed/Pcgf1*$^{fl/fl}$ and *Villin-Pcgf1*$^{fl/fl}$ mice (n = 2, n = 4, n = 1). Vinculin was used as loading control.

B) Expression analysis by qPCR of EED and PCGF1 in *Villin-Eed/Pcgf1*$^{fl/fl}$ mice (n = 4) fifteen days after Cre recombinase induction by using the classical tamoxifen regimen. Rplp0 expression was used as normalizing control. Error bars represent ± SD.

Efficient ablation of EED and PCGF1 activities was confirmed by Western blot and qPCR analysis on small intestinal crypts at both time points (Fig. 3.24A- C).

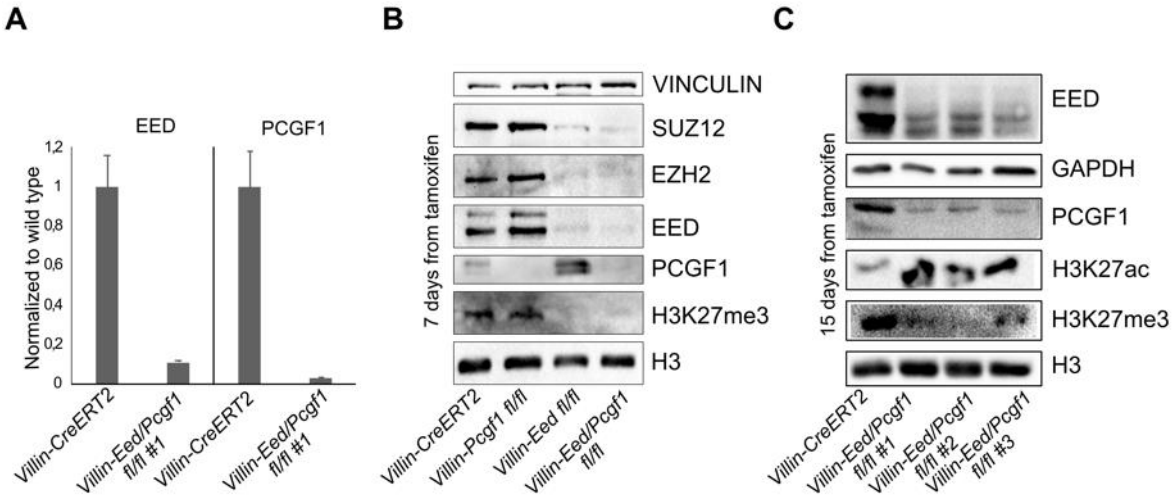

Fig. 3.24 Efficient inactivation of EED and PCGF1 activities *in vivo*

A) Expression analysis by qPCR of EED and PCGF1 in *Villin-Eed/Pcgf1*$^{fl/fl}$ mice (n = 1) seven days following the first tamoxifen injection. Rplp0 expression was used as normalizing control. Error bars represent ± SD.

B) PRC2 subunits (SUZ12, EZH2, EED), PCGF1 and H3K27me3 levels determined by Western blot analysis seven days post tamoxifen administration in the indicated mice (n = 1). Vinculin and histone H3 were used as loading controls.

C) EED, PCGF1, H3K27ac and H3K27me3 levels determined by Western blot analysis fifteen days after Cre recombinase activation using a boost of tamoxifen in *Villin-Eed/Pcgf1* $^{fl/fl}$ mice (n = 3). GAPDH and histone H3 were used as loading controls.

Histological analysis revealed that loss of PCGF1 function in the EED null background rescues the proliferative defects observed upon PRC2 inactivation, as well as the accumulation of intermediated cells, since the number of goblet cells was restored to physiological levels and Paneth cells were normally detected at the crypt bottom (Fig. 3.25A, B).

Such effects were not due to an independent effect of PRC1.1 in secretory lineage commitment as Alcian Blue staining and immunohistochemistry for lysozyme1 in intestines depleted of PCGF1 activity were similar to their wild type counterpart (Fig.3.25A).

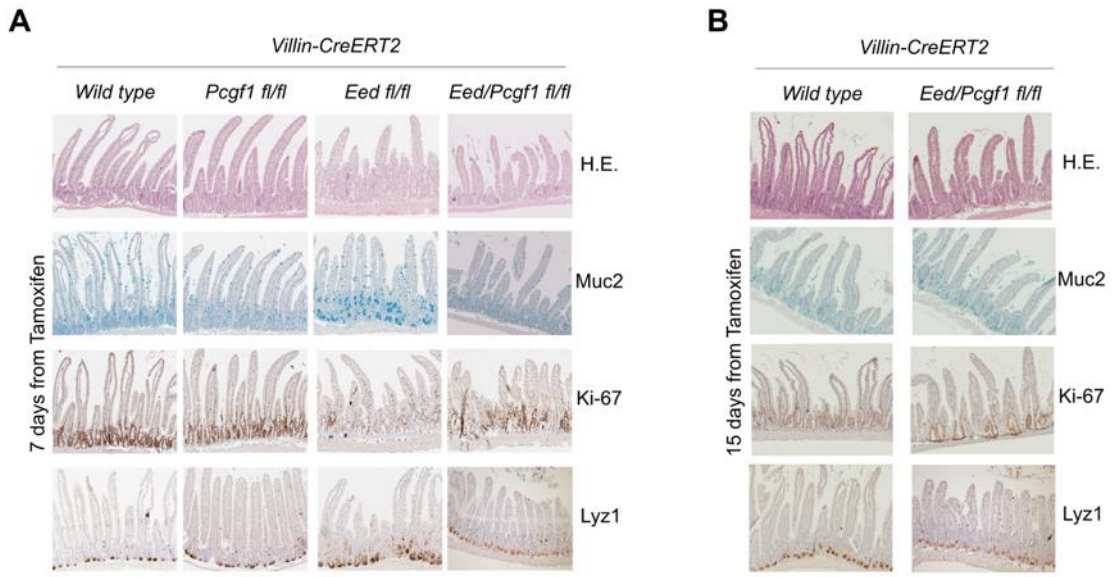

Fig. 3.25 Loss of PCGF1 normalizes the number of secretory cells in the EED null background

A) Haematoxylin and eosin (H.E.) staining, Alcian Blue staining and immunohistochemical staining using anti-Ki67 and anti-lysozyme1 on intestinal sections prepared from the indicated *Villin-CreERT2* mice (n = 1) seven days post Cre recombinase activation.

B) Haematoxylin and eosin (H.E.), Alcian Blue staining and immunohistochemical staining using anti-Ki67 and anti-lysozyme1 on intestinal sections prepared from the indicated *Villin-CreERT2* mice (n = 1) fifteen days after the first tamoxifen injection.

These morphological analyses not only demonstrated that EED/PCGF1 removal was phenotypically uncoupled from PCGF1/2/4 inactivation, but added also another layer of complexity in Polycomb-mediated regulation of secretory cell fate.

3.8 EED/PCGF1 loss restricts the intestinal secretory compartment via *Cdkn2a*-independent mechanisms

To shed light into these observations, we performed RNA-seq analysis on intestinal samples collected seven days after knocking out EED and PCGF1, finding a strong transcriptional upregulation and few downregulated genes (Fig. 3.26A).

It is well established that both PRC1 and PRC2 are direct repressors of the Ink4a-Arf (*Cdkn2a*) locus, and that transcriptional reactivation of p16 (Ink4a) and p19 (Arf) is one of the main mechanisms behind several PcG-related loss-of-function phenotypes.

Our previous work demonstrated that PRC2 loss prevents intestinal epithelial regeneration after whole body irradiation in a *Cdkn2a*-dependent manner [144], but that removal of EED in a *Cdkn2a* null background is unable to revert the defects in lineage skewing.

To address whether the restored number of secretory cells in *Eed/Pcgf* $^{fl/fl}$ mice was related to the transcriptional activity of the *Cdkn2a* locus, we evaluated expression levels of p16 and p19. Our RNA-seq data revealed that combined removal of EED and PCGF1 promoted a strong transcriptional reactivation of *Cdkn2a*, even higher of that occurring upon EED loss (Fig. 3.26B).

Overall, these results further confirmed that the effects observed in lineage skewing following combined ablation of EED and PCGF1 were *Cdkn2a*-independent.

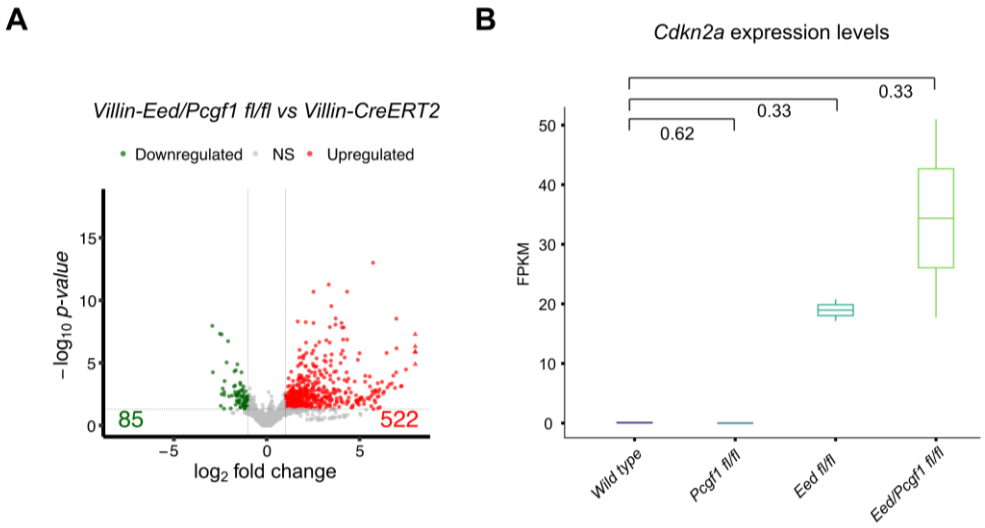

Fig. 3.26 Combined loss of EED and PCGF1 restores the secretory compartment independently from *Cdkn2a*

A) Volcano plots of –log10 (p value) against log2 fold change representing the differences in gene expression, related to RNA-seq analysis, between wild type and *Villin-Eed/Pcgf1*$^{fl/fl}$ small intestinal crypts (n = 2) seven days post-tamoxifen injection.

B) Boxplot displaying FPKM values of *Cdkn2a* transcriptional levels in the indicated mice (n = 2) seven days after Cre recombinase activation. The p values were determined by Wilcoxon non-parametric statistical test.

3.9 Inactivation of EED/PCGF1-containing complexes attenuates interferon and NF-κB activities

By performing Gene Ontology analysis of the differentially expressed genes, we evaluated the transcriptional effects induced by removal of *Eed/Pcgf1*-containing complexes respect

to PRC2 inactivation alone. The most affected biological processes in *Eed/Pcgf1 dKO* intestinal crypts were development and morphogenesis, consistent with the classical Polycomb signature and foremost with PRC2 inactivation (Fig. 3.27A, Fig. 3.21B). Despite that, we did not observe the active antiviral response detected in EED null mice (Fig. 3.21B).

To identify the molecular mechanism behind these transcriptional differences, we scanned the signaling pathways determinants for interferon (IFN) activity.

Studies performed in NF-κB-deficient cells have revealed that the initial steps of the type I IFN response depend on concurrent NF-κB activation [208] and that, in absence of NF-κB, the rapid IFN-β expression is prevented, reducing the propagation of antiviral signals in the epithelium [209].

Taking these findings into consideration, we evaluated the expression levels of some components of the NF-κB pathway. Following PRC2 inactivation, we detected a strong upregulation of the *Tnfrsf12a* gene, also known as Tumor Necrosis Factor-like weak inducer of apoptosis (TWEAK), which acts as activator of the non-canonical NF-κB pathway in diverse cell types. Moreover, the gene *Irf−7*, whose promoter contains an NF-κB response element [210], underwent transcriptional activation upon EED removal. In absence of both EED and PCGF1, the expression levels of *Tnfrsf12a* and *Irf-7* were similar to their wild type counterpart, suggesting a potential role of NF-κB activity in the observed phenotypes. In support of this hypothesis, we observed an opposite transcriptional pattern for *Usp7*, which has been recently identified as a negative regulator of the NF-κB signaling pathway [211] (Fig. 3.27B).

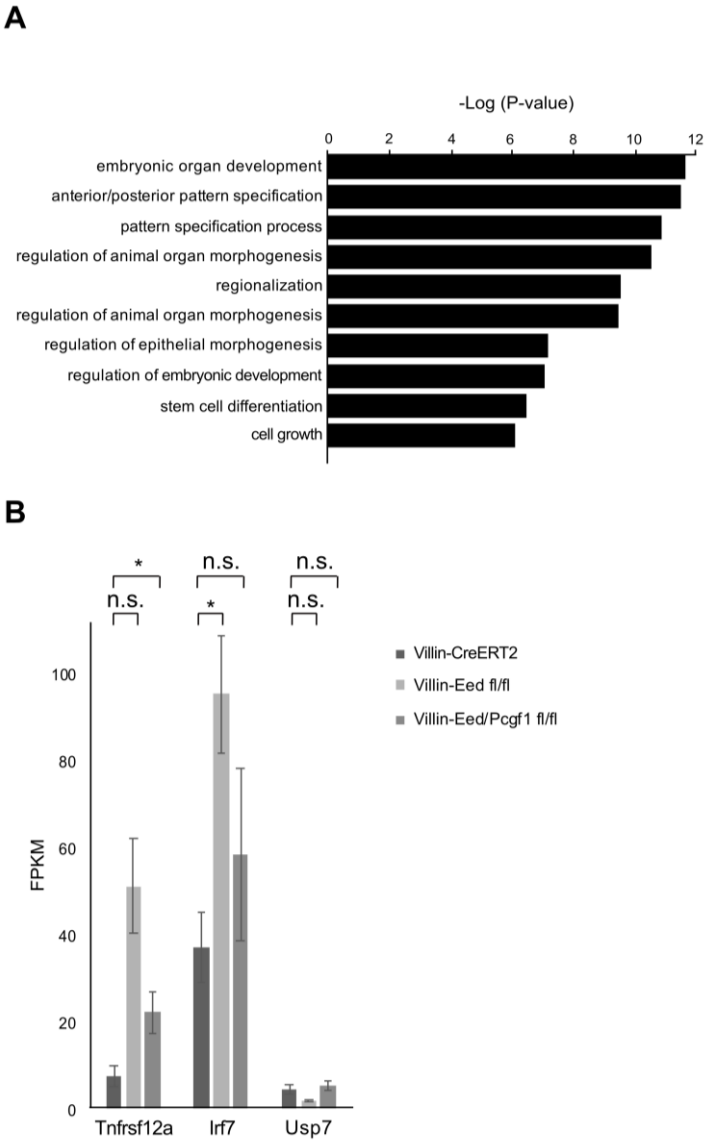

Fig. 3.27 Loss of PCGF1 restores the impairment in interferon and NF-κB signaling pathways induced by PRC2 inactivation

A) Bar plot of affected biological processes in *Eed/Pcgf1 dKO* intestinal crypts.

B) Bar plots showing the expression levels obtained from RNA-seq analyses performed in wild type, *Villin-Eed* $^{fl/fl}$ and *Villin-Eed/Pcgf1*$^{fl/fl}$ intestinal crypts (n = 2) for a set of genes involved in the NF-κB pathway, seven days post tamoxifen injection. Error bars represent ± SD. The p values were determined by Wilcoxon non-parametric statistical test (* P< 0,05, ** P<0,01, *** P< 0,001).

3.10 Future perspectives and ongoing characterization

3.10.1 Explore the molecular and epigenetic mechanisms implied in the restriction of the secretory compartment upon intestinal-specific loss of EED/PCGF1-containing complexes

To date, we show that *in vivo* PRC2 regulates secretory lineage choices without involving cPRC1 and that this function is accomplished also through the activity of PCGF1-containing complexes. To untangle this intricate network, our phenotypic results should be complemented with *in vitro* and genome-wide analyses.

Considering that PRC2 inactivation produces different outcomes in ESCs and intestinal cells, employing *EED/PCGF1 dKO* ESCs to unravel the functional crosstalk between PRC2 and PRC1.1 is discouraging.

By performing *ex vivo*-derived organoids, we will be able to demonstrate whether the effects of PRC2 in skewing towards the secretory lineage are cell-autonomous and unrelated to the activity of the immune system. Moreover, we will take advantage of this tool to perform RNA-sequencing analyses in absence of EED, both alone and in combination with PCGF1.

Crypts depleted of PRC2 activity are impaired in organoids formation post-*ex vivo* isolation, preventing any type of validation. To overcome this limit, we are planning to induce EED knockout *in vitro* at different time points from plating. This will be useful to establish the perfect timing of collection prior RNA isolation and sequencing.

Considering that EED/PCGF1 depleted intestines are more similar to the wild type counterpart, at least at the cellular level, we envision that they should be proficient in organoid formation.

The generated data will help us to focus our attention to a more limited number of transcriptional changes, as the *in vivo* context is not free from contamination effects, which can represent a bias.

In vitro results will be coupled with single-cell RNA sequencing analyses performed on small intestinal crypts dissociated at the single cell level. This experiment will be useful to identify the transcriptional landscape of specific intestinal subpopulations, helping us in tracing the molecular link connecting cell choices with the activity of EED/PCGF1-containing complexes. In particular, by tracing gene expression profiles at the single cell level, we envision to resolve the intricate network by which PRC2 and PRC1.1 play opposite functions in secretory lineage commitment. Finally, this could be helpful to potentially define the unclear role of NF-κB in determining intestinal fate choices by interacting with Polycomb complexes.

3.10.2 Evaluate the biochemical and biological relevance of vPRC1/CBX7-containing complexes

By performing genome-wide studies and mass-spectrometry analyses, we identified that the residual chromatin occupancy of CBX7 occurring upon cPRC1 inactivation, both in the intestinal epithelium and in the mESC model, invaded vPRC1-bound sites.

Considering that removal of vPRC1 complexes strongly compromises H2AK119ub1 deposition and RING1B occupancy [134], it would be interesting to evaluate the impact of CBX7 loss in PRC1 catalytic activity and recruitment. To this purpose, we will take advantage of *Cbx7 KO* and *Pcgf2/4-Cbx7 tKO* ESC lines, which have been already generated in our laboratory for this study. By coupling ChIP and RNA-seq analyses, we will explore whether vPRC1/CBX7-containing complexes are functional and whether CBX7 has a potential role in Polycomb-mediated transcriptional identity.

Moreover, it would be interesting to address whether the biochemical assembly of vPRC1/CBX7 complexes is sensitive to quantitative perturbations of Polycomb components. By overexpressing CBX7 in ESCs, both wild type and cPRC1 depleted, we will evaluate whether the interaction with PCGF1 and PCGF6 is enhanced through IP-mass spectrometry analyses.

The generated results will be useful to better characterize the role of CBX7 in clinical contexts, such as cancer, where its activity is often deregulated [174].

4. DISCUSSION

4.1 Variant PRC1 subcomplexes compensate for H2AK119ub1 deposition and gene repression in the adult intestine

Using Cre-dependent conditional knockout mouse models abrogating the activity of single variant PRC1 subcomplexes, we had the opportunity to deeply investigate the independent roles of PCGF1, 3/5 and 6 in the intestinal epithelium. In particular, we were able to explore their functions during intestinal homeostasis, since the inactivation of both RING1A and RING1B disrupts all PRC1 activities, preventing any kind of analysis.

To achieve tissue specificity, we used the *AhCre* promoter, which is expressed in all the small intestine (with the exception of Paneth cells) and spares the colonic epithelium. The use of this transgene has been a matter of debate, especially in stress conditions, where β-naphthoflavone-mediated gene deletion can produce side effects [212].

Keeping this in mind, we envision to validate our observations also in the *Villin-CreERT2* background, which targets all intestinal epithelial cells, although our results suggest that the effects achieved with the *AhCre* transgene are faithfully reproduced with the *Villin-CreERT2* model.

By performing morphological and genome-wide analyses (ChIP-seq, RNA-seq) *in vivo*, we found that inactivation of single variant PRC1 subcomplexes preserved intestinal homeostasis and resulted in the compensation of H2AK119ub1 deposition and gene repression.

Although the regulation of Polycomb activity could be more challenging in adult differentiated tissues, these *in vivo* results are partially consistent with the mouse embryonic stem cell model, which represents the most used system to study PcG function.

In mouse embryonic stem cells, loss of PCGF1 does not affect cell viability, but has the largest effect on H2AK119ub1 deposition at PRC1-bound sites, leading also to a specific and substantial reduction in H3K27me3 levels and resulting in the reactivation of hundreds of Polycomb target genes [134]. In the intestinal epithelium, PCGF1 is the most expressed PCGF protein, displaying a large co-occupancy with RING1B targets. Despite that, we observed normal spatial H2AK119ub1 deposition as well as H3K27me3 levels following intestinal-specific ablation of PRC1.1 activity, suggesting that different mechanisms of compensation occur among variant PRC1 complexes in absence of distinct PCGF functions *in vivo*.

Similar to ESCs, loss of PRC1.3/5-containing complexes severely reduced H2AK119ub1 deposition at intergenic regions in the intestinal epithelium. Moreover, among vPRC1

subcomplexes, those containing PCGF3 and PCGF5 were the only one producing a major reactivation of Polycomb targets, despite transcriptional changes were minimal compared to those observed in *RING1A/B dKO* mice [145].

Our laboratory has already demonstrated that loss of PCGF3/5-PRC1 complexes counteracts H2AK119ub1 accumulation in absence of BAP1 [142], the deubiquitinating enzyme part of the Polycomb Repressive-Deubiquitinase Complex (PR-DUB). Such dependency is maintained in BAP1 null tumors addicted to hyper-H2AK119ub1 accumulation. Despite we did not address the relationship between BAP1 and PCGF3/5 activity *in vivo*, it would be interesting deepen this epigenetic link to render PRC1.3/5 complexes an attractive target for all those tumors in which BAP1 activity is suppressed.

Finally, PCGF6 seems to cover different functions in stem vs differentiated cells.

Although occupancy of PCGF6 and RING1B largely overlap in ESCs, we found that only a small subset of RING1B targets was decorated also by PCGF6 *in vivo*. This could explain the lack of phenotypic effects upon intestinal-specific inactivation of PRC1.6 and the robust derepression of germ cell-related genes observed in *Pcgf6 KO* ESC [115], which is due to the specific loss of H2AK119ub1 deposition at these targets.

4.2 Canonical PRC1 preserves RING1B occupancy *in vivo,* without affecting gene repression

It has been proposed that canonical PRC1, which is recruited to chromatin via recognition of PRC2-dependent H3K27me3, promotes Polycomb-mediated gene repression [128,201]. Nevertheless, we found that conditional removal of both PCGF2 and PCGF4, which ablates cPRC1 activity, had no transcriptional effects *in vivo*. This observation is consistent with previous reports in ESCs, where it has been demonstrated that PRC2 loss produces very few transcriptional changes [136], but disagrees with the diffuse gene upregulation occurring when EED activity is depleted *in vivo*.

Moreover, by analyzing RING1B occupancy and H2AK119ub1 levels upon cPRC1 removal in the intestinal epithelium, we found that the vast majority of RING1B binding was lost without affecting the global PRC1 catalytic activity, in accordance with previous studies performed in ESC [134].

Overall, these findings raise several questions about the functional relevance of cPRC1 complexes and the significance of their recruitment to PRC2-bound sites. One explanation may be that cPRC1 complexes are involved in long-range interactions between Polycomb repressed domains [72,73], acting as a “seal” for variant PRC1-dependent gene repression, as previously suggested [213].

Transcriptional control is crucial during cellular differentiation and development, where Polycomb activity constrains the transcriptional activation of genes that have to be kept silent. This is consistent with the crucial role of canonical PRC1 during the embryonic development [94, 96] and with its dispensability in more differentiated contexts, as demonstrated by our analyses in the intestinal epithelium.

4.3 vPRC1 complexes contribute to CBX7 binding upon combined loss of PCGF2 and PCGF4

Among the chromobox protein family, CBX2, 4, 6, 7 and 8 have been shown to take part of the PRC1 complex, providing distinct functions. In ESCs, CBX7 is the main CBX protein incorporated into the cPRC1 complex and is involved in the reading recognition of H3K27me3. CBX7 expression is downregulated during ESC differentiation, preceding the upregulation of CBX2, CBX4, and CBX8, which are directly repressed by CBX7.

Unexpectedly, we found that removal of cPRC1 activity, both in the intestinal epithelium and in mESCs, did not ablate CBX7 occupancy, preserving a residual binding. Moreover, it was *de novo* redistributed across vPRC1-bound sites when PCGF2 and PCGF4 were removed *in vivo*. In line with this, genome wide and mass-spectrometry analyses in mESCs revealed that, among the vPRC1-associated PCGF proteins, CBX7 preferentially interacted with PCGF1 and PCGF6.

Indeed, we observed that the additional removal of PRC1.1 and PRC1.6 in *Pcgf2/4 dKO* ESCs (*Pcgf1/2/4/6 qKO*) prevented CBX7 recruitment to chromatin, similarly to what observed in absence of PRC2-dependent H3K27me3 deposition.

Proteomic studies of CBX7 immuno-purifications from mESCs could better define the composition of vPRC1-CBX7 complexes, particularly whether other cPRC1 members (i.e., PHC 1-3 subunits) or PRC1.1/6 accessory proteins (for example, KDM2B or MGA) are included. Moreover, the generated results could help in identifying the mechanisms by which these complexes are recruited to PcG loci.

Since the assembly of the different Polycomb subcomplexes is context- and tissue-specific, mass-spectrometry analyses from PCGF4 immuno-purifications in small intestinal crypts are needed, in order to identify which of the five CBX subunits is prevalently associated to cPRC1 *in vivo*. This would be crucial to determine whether vPRC1 promiscuously contains CBX7 or other CBXs in the intestinal epithelium. Moreover, by performing PCGF1/6 immunoprecipitation coupled with mass spectrometry (IP/MS) on small intestinal crypts, we could translate the interaction with cPRC1 subunits to the *in vivo* context.

Collectively, our data reveal for the first time a relationship between vPRC1-associated PCGF proteins and CBX7, twisting the classical biochemical nomenclature of Polycomb complexes. However, this promiscuity is not new, as CBX6 has been showed to associate with PCGF6 in the mouse ESC model [214].

Although we did not deepen the biological relevance of such biochemical link, it could not be excluded that vPRC1 complexes containing CBX7 play a potential role in the maintenance of cell identity. It has been demonstrated that CBX7-bound genes, decorated by high levels of RING1B and H2AK119ub1, are strongly repressed and associated with cell differentiation choices during early development [56]. Moreover, several reports support the oncogenic role of CBX7 in a variety of tumors, as it mediates the transcriptional control of cell proliferation, apoptosis and self-renewal [174].

Of course, the mechanisms of CBX7 activity have not been completely elucidated yet. As a member of Polycomb complexes, CBX7 not only acts independently of PRC1 but mediates gene repression together with PRC1 as a whole and PCR2. These phenomena require further studies as they could provide evidence for the clinical prognostic value and help in the identification of new therapeutic targets against cancer.

4.4 cPRC1 is not involved in PRC2-dependent effects on intestinal lineage skewing

To confirm our previous findings in the *AhCre* model, we analyzed the role of PRC2 activity in the intestinal compartment by eliminating the structural subunit EED under the control of the *Villin-CreERT2* promoter.

Despite differences in intestinal targeting exist between the *AhCre* and the *Villin-CreERT2* transgenes, our data revealed identical outcomes following EED inactivation in both models. Indeed, we found that PRC2 activity was required for the maintenance of cell proliferation in the TA compartment, as previously found using *in vitro* systems [215], and for preserving secretory lineage commitment.

By confronting the effects produced by combined loss of PCGF2/4 with EED inactivation, we demonstrated that cPRC1 activity was not involved in the PRC2-mediated control of intestinal lineage skewing. This was due to diffuse transcriptional changes following H3K27me3 loss, which were not reproduced by cPRC1 activity on its own. Furthermore, these functions occurred independently from PRC1 catalysis, as H2AK119ub1 deposition was globally maintained in EED null intestines, suggesting that the extent of overlap and redundancy between the two Polycomb complexes is context-dependent.

Despite we did not evaluate whether PRC2 inactivation impinges with the chromatin binding of PCGF2 and PCGF4, our genome-wide analyses revealed a similar displacement

of RING1B across PRC1-bound loci in EED null mice and cPRC1 depleted intestines. This observation is in line with the current model of Polycomb recruitment, supporting the requirement of H3K27me3 deposition for cPRC1 engagement to chromatin domains occupied by PRC2.

Such results still raise important question about the functional role of cPRC1 complex, as they are in sharp contrast with the requirement of PCGF2/4 activities during development. Similar to EED-deficient embryos, which fail to complete gastrulation, combined removal of PCGF2 and PCGF4 during embryonic development results in lethality at dpc 9.5.

Moreover, our observations confirm that the mouse embryonic stem cell model partially recaps the mechanisms by which PcG control transcriptional silencing *in vivo*. Despite removal of cPRC1 activity is associated with similar effects in both adult tissues and ESCs, genetic inactivation of PRC2 produces different outcomes. Indeed, PRC2 activity is dispensable for self-renewal of ESCs, but seems to be crucial for adult tissue integrity. In this context, it has still to be determined whether the accumulation of secretory cells observed upon EED removal relies on failure of differentiation. Considering the direct role of PRC2 in controlling cell cycle progression, the impaired capability of progenitor cells to properly mature could stuck them in the differentiation process, without fulfilling their half-life timing. This hypothesis is supported by other studies performed in different adult compartments. For example, PRC2 is required to maintain bone marrow long-term hematopoietic stem cells, as loss of EED severely impairs HSC viability and their ability to differentiate into mature blood cells [216].

Taking together, our results suggest that the outcomes derived from PcG loss-of-function rely not only on the functional nature of the deregulated genes but also on the cellular context in which this occurs.

4.5 Removal of PCGF1 rescues the increase of intermediate cells upon EED loss

The extensive characterization of PcG function in the adult intestine, carried out in our laboratory during the last years, has revealed that distinct Polycomb activities must act together to reproduce the biological function of RING1A/B loss *in vivo*.

By combinedly removing PCGF1/2/4, which share a subset of strongly repressed target genes in the intestinal epithelium, we found that the stem cell pool was exhausted and that H2AK119ub1 deposition was lost, concomitant with a global transcriptional derepression. These results, reminiscent of the catalytic inactivation of PRC1, are not mimicked by the ESC model. Indeed, we have previously showed that, despite preserving H2AK119ub1 deposition at repressed sites, the PCGF1/2/4 module was dispensable for ESC viability [43].

Again, these data add another layer of complexity to the mechanisms used by Polycomb components to preserve transcriptional identity in different cellular contexts.

Considering the hierarchy of PcG recruitment to chromatin, we hypothesized that EED/PCGF1-containing complexes could have covered the biological functions of the PCGF1/2/4 unit. Since PRC2 inactivation disengages the downstream cPRC1, we decided to delete EED along with PRC1.1 in order to address whether similarities with PCGF1/2/4 removal could exist.

Morphological analyses of *Eed/Pcgf1 dKO* mice revealed that the homeostasis of the intestinal epithelium was preserved and that stem cells were actively proliferating, suggesting that the model of PRC1-PRC2 consequentiality could not explain the observed effects on PCGF1/2/4-mediated transcriptional silencing.

Leaving aside the relationship with the PCGF1/2/4 module, we showed that removal of EED/PCGF1-containing complexes unexpectedly rescued the expansion of the secretory compartment occurring upon PRC2 inactivation. The histological and transcriptional analyses of *Pcgf1 KO* mice failed to justify the counteraction to EED activity. Indeed, the number of secretory cells and the pathways involved in their differentiation were not affected upon single loss of PCGF1.

However, the interaction between PRC1.1 and PRC2 in intestinal lineage choices could open a debate in oncogenic conditions where PRC2 function is altered.

EZH2 overexpression has been reported in solid tumor types and in hematologic malignancies (i.e., B cell lymphomas), leading to the development of different EZH2 inhibitors for cancer treatment. Potential side effects of these chemical drugs in the intestinal epithelium have not been evaluated yet and our results raise the possibility that PRC2 inactivation could alter intestinal differentiation programs also in patients receiving EZH2 inhibitors. Moreover, it would be interesting to address whether PCGF1 activity is enhanced when PRC2 function is pharmacologically suppressed, since it could synergize in altering proper maturation of intestinal secretory cells.

Since our results showed that loss of PCGF1 is able to restore intestinal homeostasis in the context of PRC2 inactivation, we propose that PCGF1 inhibitors could help in overcoming potential side effects arising in cancer patients exposed to EZH2-targeted therapies.

4.6 Deletion of EED/PCGF1-containing complexes preserves secretory lineage commitment independently from *Cdkn2a* transcriptional reactivation

Studies performed in ESCs and embryonic fibroblasts [217] have demonstrated that Polycomb complexes act as transcriptional regulators of the *Cdkn2a* (alias Ink4-Arf) locus, by maintaining the deposition of repressive histone marks.

Our extensive analysis *in vivo* revealed that both PRC1 and PRC2 kept this locus silent also in the intestinal compartment. PCGF proteins, indistinctly associated with variant or canonical PRC1 complexes, occupied *Cdkn2a*, where they deposited similar levels of H2AK119ub1. Despite removal of single PCGF activities resulted in the upregulation of p16 and p19, the two cell cycle regulators encoded by *Cdkn2a*, the extent of transcriptional reactivation was lesser compared to EED loss, as it produced a 20-fold increase in Ink4-Arf expression levels.

Nevertheless, by inactivating PRC2 in a *Cdkn2a* null background we have previously demonstrated that the defects in secretory lineage commitment were not rescued, revealing that the observed increase of intermediate cells was unrelated to Ink4-Arf reactivation [144]. Considering this, we evaluated the activity of the *Cdkn2a* locus upon combined loss of EED and PCGF1 finding the highest expression levels, probably due to the additive effects of PRC1 and PRC2 on its transcriptional control.

Although our studies are far from explaining the mechanisms by which EED and PCGF1 act in concert to regulate intestinal lineage skewing, our data exclude the transcriptional activity of *Cdkn2a* from this scenario.

4.7 Loss of PRC1.1 counteracts the activation of the NF-κB signaling pathway induced by PRC2 inactivation

By analyzing the transcriptional profiles of $Eed^{fl/fl}$ mice, we revealed that loss of PRC2 function promoted the activation of the type I interferon (IFN) response, which was not due to an active recruitment of inflammatory cells. Indeed, staining of colonic samples as well as gene signature revealed the absence of Cd45-expressing cells, suggesting that the initiation of these molecular pathways was an intrinsic property of the intestinal epithelium. A plethora of studies indicate that IFN acts to amplify DNA-damage responses. Consistent with this, we detected a strong upregulation of p53 target genes in EED mutant crypts, which could be reinforced by the direct evaluation of sensitive molecular markers of DNA damage (i.e, γH2AX) in the intestinal epithelium.

Another possibility is that pathways different from p53 trigger the observed epithelial cell-intrinsic IFN response. For example, it has been proposed that NF-κB activity regulates

intestinal mucous secretion, potentially leading to the accumulation of secretory progenitors induced by EED loss. Indeed, several cytokines and chemokines enhance the transcription of mucin genes through activation of the NF-κB pathway via the Ras-mitogen-activated protein kinase (MAPK) as well as the PI3K/AKT cascades [218, 219].

Moreover, by removing PCGF1 in the EED null background, we observed that the number of secretory cells was rescued, coupled with the suppression of the IFN response and the NF-κB signaling pathway induced by PRC2 inactivation. These observations further strengthen a potential role of NF-κB in determining intestinal lineage choices, as proposed in different works [220, 221].

Despite further experiments are needed to define the molecular circuitries linking PRC2 and PRC1.1 activities with secretory lineage commitment, our preliminary analyses propose a role of the non-canonical NF-κB cascade, as genes involved in the classical activation of this signaling pathway are transcriptionally unchanged in $Eed^{fl/fl}$ and $Eed/Pcgf1^{fl/fl}$ mice.

We strongly believe that uncovering these molecular mechanisms will be clinically relevant, in light of the protective role that mucus-secreting cells play during inflammatory bowel diseases [222].

REFERENCES

1. Mohammad, H. P., & Baylin, S. B. (2010). Linking cell signaling and the epigenetic machinery. *Nature Biotechnology* (Vol. 28, Issue 10). https://doi.org/10.1038/nbt1010-1033
2. Marshall, O. J., & Brand, A. H. (2017). Chromatin state changes during neural development revealed by in vivo cell-type specific profiling. *Nature Communications*, *8*(1). https://doi.org/10.1038/s41467-017-02385-4
3. Ho, L., & Crabtree, G. R. (2010). Chromatin remodelling during development. *Nature* (Vol. 463, Issue 7280). https://doi.org/10.1038/nature08911
4. Perino, M., & Veenstra, G. J. C. (2016). Chromatin Control of Developmental Dynamics and Plasticity. *Developmental Cell* (Vol. 38, Issue 6). https://doi.org/10.1016/j.devcel.2016.08.004
5. Piunti, A., & Shilatifard, A. (2021). The roles of Polycomb Repressive Complexes in mammalian development and cancer. *Nature Reviews Molecular Cell Biology* (Vol. 22, Issue 5). https://doi.org/10.1038/s41580-021-00341-1
6. Keller, G. (2005). Embryonic stem cell differentiation: Emergence of a new era in biology and medicine. *Genes and Development* (Vol. 19, Issue 10). https://doi.org/10.1101/gad.1303605
7. Murry, C. E., & Keller, G. (2008). Differentiation of embryonic stem cells to clinically relevant populations: lessons from embryonic development. *Cell* (Vol. 132, Issue 4). https://doi.org/10.1016/j.cell.2008.02.008
8. Barker, N. (2014). Adult intestinal stem cells: Critical drivers of epithelial homeostasis and regeneration. *Nature Reviews Molecular Cell Biology* (Vol. 15, Issue 1). https://doi.org/10.1038/nrm3721
9. Simons, B. D., & Clevers, H. (2011). Strategies for homeostatic stem cell self-renewal in adult tissues. *Cell* (Vol. 145, Issue 6). https://doi.org/10.1016/j.cell.2011.05.033
10. McKenzie Duncan, I. (1982). Polycomblike: A gene that appears to be required for the normal expression of the bithorax and antennapedia gene complexes of Drosophila melanogaster. *Genetics* (Vol. 102, Issue 1). https://doi.org/10.1093/genetics/102.1.49
11. Jürgens, G. (1985). A group of genes controlling the spatial expression of the bithorax complex in Drosophila. *Nature* (Vol. 316, Issue 6024). https://doi.org/10.1038/316153a0

12. Lewis, E. B. (1978). A gene complex controlling segmentation in Drosophila. *Nature* (Vol. 276, Issue 5688). https://doi.org/10.1038/276565a0
13. Gao, Z., Zhang, J., Bonasio, R., Strino, F., Sawai, A., Parisi, F., Kluger, Y., & Reinberg, D. (2012). PCGF homologs, CBX proteins, and RYBP define functionally distinct PRC1 family complexes. *Molecular Cell* (Vol. 45, Issue 3). https://doi.org/10.1016/j.molcel.2012.01.002
14. Li, Z., Cao, R., Wang, M., Myers, M. P., Zhang, Y., & Xu, R. M. (2006). Structure of a Bmi-1-Ring1B Polycomb group ubiquitin ligase complex. *Journal of Biological Chemistry* (Vol. 281 Issue 29). https://doi.org/10.1074/jbc.M602461200
15. Buchwald, G., Van Der Stoop, P., Weichenrieder, O., Perrakis, A., Van Lohuizen, M., & Sixma, T. K. (2006). Structure and E3-ligase activity of the Ring-Ring complex of Polycomb proteins Bmi1 and Ring1b. *EMBO Journal* (Vol. 25, Issue 11). https://doi.org/10.1038/sj.emboj.7601144
16. Bentley, M. L., Corn, J. E., Dong, K. C., Phung, Q., Cheung, T. K., & Cochran, A. G. (2011). Recognition of UbcH5c and the nucleosome by the Bmi1/Ring1b ubiquitin ligase complex. *EMBO Journal* (Vol. 30, Issue 16). https://doi.org/10.1038/emboj.2011.243
17. Wang, R., Taylor, A. B., Leal, B. Z., Chadwell, L. V., Ilangovan, U., Robinson, A. K., Schirf, V., Hart, P. J., Lafer, E. M., Demeler, B., Hinck, A. P., McEwen, D. G., & Kim, C. A. (2010). Polycomb group targeting through different binding partners of RING1B C-terminal domain. *Structure* (Vol. 18, Issue 8). https://doi.org/10.1016/j.str.2010.04.013
18. Levine, S. S., Weiss, A., Erdjument-Bromage, H., Shao, Z., Tempst, P., & Kingston, R. E. (2002). The core of the Polycomb Repressive Complex is compositionally and functionally conserved in flies and humans. *Molecular and Cellular Biology* (Vol. 22, Issue 17). https://doi.org/10.1128/mcb.22.17.6070-6078.2002
19. Shao, Z., Raible, F., Mollaaghababa, R., Guyon, J. R., Wu, C. T., Bender, W., & Kingston, R. E. (1999). Stabilization of chromatin structure by PRC1, a Polycomb complex. *Cell* (Vol. 98, Issue 1). https://doi.org/10.1016/S0092-8674(00)80604-2
20. McGinty, R. K., Henrici, R. C., & Tan, S. (2014). Crystal structure of the PRC1 ubiquitylation module bound to the nucleosome. *Nature* (Vol. 514, Issue 7524). https://doi.org/10.1038/nature13890
21. Kalashnikova, A. A., Porter-Goff, M. E., Muthurajan, U. M., Luger, K., & Hansen, J. C. (2013). The role of the nucleosome acidic patch in modulating higher order

chromatin structure. *Journal of the Royal Society Interface* (Vol. 10, Issue 82). https://doi.org/10.1098/rsif.2012.1022

22. Ciferri, C., Lander, G. C., Maiolica, A., Herzog, F., Aebersold, R., & Nogales, E. (2012). Molecular architecture of human Polycomb Repressive Complex 2. *ELife*, (Vol. 1). https://doi.org/10.7554/eLife.00005
23. Chen, S., Jiao, L., Shubbar, M., Yang, X., & Liu, X. (2018). Unique structural platforms of Suz12 dictate distinct classes of PRC2 for chromatin binding. *Molecular Cell* (Vol. 69, Issue 5). https://doi.org/10.1016/j.molcel.2018.01.039
24. Beringer, M., Pisano, P., Di Carlo, V., Blanco, E., Chammas, P., Vizán, P., Gutiérrez, A., Aranda, S., Payer, B., Wierer, M., & Di Croce, L. (2016). EPOP functionally links Elongin and Polycomb in pluripotent stem cells. *Molecular Cell* (Vol. 64, Issue 4). https://doi.org/10.1016/j.molcel.2016.10.018
25. Liefke, R., Karwacki-Neisius, V., & Shi, Y. (2016). EPOP interacts with Elongin BC and USP7 to modulate the chromatin landscape. *Molecula Cell* (Vol. 64, Issue 4). https://doi.org/10.1016/j.molcel.2016.10.019
26. Zhang, Z., Jones, A., Sun, C. W., Li, C., Chang, C. W., Joo, H. Y., Dai, Q., Mysliwiec, M. R., Wu, L. C., Gou, Y., Yang, W., Liu, K., Pawlik, K. M., Erdjument-Bromage, H., Tempst, P., Lee, Y., Min, J., Townes, T. M., & Wang, H. (2011). PRC2 complexes with JARID2, MTF2, and esPRC2p48 in ES cells to modulate ES cell pluripotency and somatic cell reprograming. *Stem Cells* (Vol. 29, Issue 2). https://doi.org/10.1002/stem.578
27. Ragazzini, R., Pérez-Palacios, R., Baymaz, I. H., Diop, S., Ancelin, K., Zielinski, D., Michaud, A., Givelet, M., Borsos, M., Aflaki, S., Legoix, P., Jansen, P. W. T. C., Servant, N., Torres-Padilla, M. E., Bourc'his, D., Fouchet, P., Vermeulen, M., & Margueron, R. (2019). EZHIP constrains Polycomb Repressive Complex 2 activity in germ cells. *Nature Communications* (Vol. 10, Issue 1). https://doi.org/10.1038/s41467-019-11800-x
28. Jain, S. U., Do, T. J., Lund, P. J., Rashoff, A. Q., Diehl, K. L., Cieslik, M., Bajic, A., Juretic, N., Deshmukh, S., Venneti, S., Muir, T. W., Garcia, B. A., Jabado, N., & Lewis, P. W. (2019). PFA ependymoma-associated protein EZHIP inhibits PRC2 activity through a H3 K27M-like mechanism. *Nature Communications* (Vol. 10, Issue 1). https://doi.org/10.1038/s41467-019-09981-6
29. Chan, H. L., Beckedorff, F., Zhang, Y., Garcia-Huidobro, J., Jiang, H., Colaprico, A., Bilbao, D., Figueroa, M. E., LaCava, J., Shiekhattar, R., & Morey, L. (2018). Polycomb Complexes associate with enhancers and promote oncogenic

transcriptional programs in cancer through multiple mechanisms. *Nature Communications* (Vol. 9, Issue 1). https://doi.org/10.1038/s41467-018-05728-x

30. Bracken, A. P., Dietrich, N., Pasini, D., Hansen, K. H., & Helin, K. (2006). Genome-wide mapping of Polycomb target genes unravels their roles in cell fate transitions. *Genes and Development* (Vol. 20, Issue 9). https://doi.org/10.1101/gad.381706
31. Mendenhall, E. M., Koche, R. P., Truong, T., Zhou, V. W., Issac, B., Chi, A. S., Ku, M., & Bernstein, B. E. (2010). GC-rich sequence elements recruit PRC2 in mammalian ES cells. *PLoS Genetics* (Vol. 6, Issue 12). https://doi.org/10.1371/journal.pgen.1001244
32. Saxonov, S., Berg, P., & Brutlag, D. L. (2006). A genome-wide analysis of CpG dinucleotides in the human genome distinguishes two distinct classes of promoters. *Proceedings of the National Academy of Sciences of the United States of America* (Vol. 103, Issue 5). https://doi.org/10.1073/pnas.0510310103
33. Schübeler, D. (2015). Function and information content of DNA methylation. *Nature* (Vol. 517, Issue 7534). https://doi.org/10.1038/nature14192
34. Bartke, T., Vermeulen, M., Xhemalce, B., Robson, S. C., Mann, M., & Kouzarides, T. (2010). Nucleosome-interacting proteins regulated by DNA and histone methylation. *Cell* (Vol. 143, Issue 3). https://doi.org/10.1016/j.cell.2010.10.012
35. Sánchez, C., Sánches, I., Demmers, J. A. A., Rodriguez, P., Strouboulis, J., & Vidal, M. (2007). Proteomics analysis of Ring1B/Rnf2 interactions identifies a novel complex with the Fbxl10/Jhdm1B histone demethylase and the Bcl6 interacting corepressor. *Molecular and Cellular Proteomics* (Vol. 6, Issue 5). https://doi.org/10.1074/mcp.M600275-MCP200
36. Shin Voo, K., Carlone, D. L., Jacobsen, B. M., Flodin, A., & Skalnik, D. G. (2000). Cloning of a mammalian transcriptional activator that binds unmethylated CpG motifs and shares a CXXC domain with DNA methyltransferase, human trithorax, and methyl-CpG binding domain protein 1. *Molecular and Cellular Biology* (Vol. 20, Issue 6). https://doi.org/10.1128/mcb.20.6.2108-2121.2000
37. Farcas, A. M., Blackledge, N. P., Sudbery, I., Long, H. K., McGouran, J. F., Rose, N. R., Lee, S., Sims, D., Cerase, A., Sheahan, T. W., Koseki, H., Brockdorff, N., Ponting, C. P., Kessler, B. M., & Klose, R. J. (2012). KDM2B links the Polycomb Repressive Complex 1 (PRC1) to recognition of CpG islands. *ELife* (Vol. 1). https://doi.org/10.7554/eLife.00205
38. Li, H., Liefke, R., Jiang, J., Kurland, J. V., Tian, W., Deng, P., Zhang, W., He, Q., Patel, D. J., Bulyk, M. L., Shi, Y., & Wang, Z. (2017). Polycomb-like proteins link

the PRC2 complex to CpG islands. *Nature* (Vol. 549, Issue 7671). https://doi.org/10.1038/nature23881

39. Kassis, J. A., & Brown, J. L. (2013). Polycomb Group response elements in Drosophila and vertebrates. *Advances in Genetics* (Vol. 81). https://doi.org/10.1016/B978-0-12-407677-8.00003-8
40. Bernstein, B. E., Mikkelsen, T. S., Xie, X., Kamal, M., Huebert, D. J., Cuff, J., Fry, B., Meissner, A., Wernig, M., Plath, K., Jaenisch, R., Wagschal, A., Feil, R., Schreiber, S. L., & Lander, E. S. (2006). A bivalent chromatin structure marks key developmental genes in embryonic stem cells. *Cell* (Vol. 125, Issue 2). https://doi.org/10.1016/j.cell.2006.02.041
41. Boyer, L. A., Tong, I. L., Cole, M. F., Johnstone, S. E., Levine, S. S., Zucker, J. P., Guenther, M. G., Kumar, R. M., Murray, H. L., Jenner, R. G., Gifford, D. K., Melton, D. A., Jaenisch, R., & Young, R. A. (2005). Core transcriptional regulatory circuitry in human embryonic stem cells. *Cell* (Vol. 122, Issue 6). https://doi.org/10.1016/j.cell.2005.08.020
42. Loh, Y. H., Wu, Q., Chew, J. L., Vega, V. B., Zhang, W., Chen, X., Bourque, G., George, J., Leong, B., Liu, J., Wong, K. Y., Sung, K. W., Lee, C. W. H., Zhao, X. D., Chiu, K. P., Lipovich, L., Kuznetsov, V. A., Robson, P., Stanton, L. W., … Ng, H. H. (2006). The Oct4 and Nanog transcription network regulates pluripotency in mouse embryonic stem cells. *Nature Genetics* (Vol. 38, Issue 4). https://doi.org/10.1038/ng1760
43. Scelfo, A., Fernández-Pérez, D., Tamburri, S., Zanotti, M., Lavarone, E., Soldi, M., Bonaldi, T., Ferrari, K. J., & Pasini, D. (2019). Functional landscape of PCGF proteins reveals both RING1A/B-dependent-and RING1A/B-independent-specific activities. *Molecular Cell*, (Vol. 74, Issue 5). https://doi.org/10.1016/j.molcel.2019.04.002
44. Stielow, B., Finkernagel, F., Stiewe, T., Nist, A., & Suske, G. (2018). MGA, L3MBTL2 and E2F6 determine genomic binding of the non-canonical Polycomb Repressive Complex PRC1.6. *PLoS Genetics* (Vol.14, Issue 1). https://doi.org/10.1371/journal.pgen.1007193
45. Ren, X., & Kerppola, T. K. (2011). REST interacts with Cbx proteins and regulates Polycomb Repressive Complex 1 occupancy at RE1 elements. *Molecular and Cellular Biology* (Vol. 31, Issue10). https://doi.org/10.1128/mcb.05088-11
46. Herranz, N., Pasini, D., Díaz, V. M., Francí, C., Gutierrez, A., Dave, N., Escrivà, M., Hernandez-Muñoz, I., Di Croce, L., Helin, K., García de Herreros, A., & Peiró, S. (2008). Polycomb Complex 2 is required for E-cadherin repression by the Snail1

transcription factor. *Molecular and Cellular Biology* (Vol. 28, Issue 15). https://doi.org/10.1128/mcb.00323-08

47. Dietrich, N., Lerdrup, M., Landt, E., Agrawal-Singh, S., Bak, M., Tommerup, N., Rappsilber, J., Södersten, E., & Hansen, K. (2012). REST-mediated recruitment of Polycomb Repressor Complexes in mammalian cells. *PLoS Genetics*, (Vol. 8, Issue 3). https://doi.org/10.1371/journal.pgen.1002494
48. Jeon, Y., Lee, J.T. (2011). YY1 tethers Xist RNA to the inactive X nucleation center. *Cell* (Vol. 146, Issue 1). https://doi.org/10.1016/j.cell.2011.06.026
49. Almeida, M., Pintacuda, G., Masui, O., Koseki, Y., Gdula, M., Cerase, A., Brown, D., Mould, A., Innocent, C., Nakayama, M., Schermelleh, L., Nesterova, T. B., Koseki, H., & Brockdorff, N. (2017). PCGF3/5-PRC1 initiates Polycomb recruitment in X chromosome inactivation. *Science* (Vol. 356, Issue 6342). https://doi.org/10.1126/science.aal2512
50. Pintacuda, G., Wei, G., Roustan, C., Kirmizitas, B. A., Solcan, N., Cerase, A., Castello, A., Mohammed, S., Moindrot, B., Nesterova, T. B., & Brockdorff, N. (2017). hnRNPK recruits PCGF3/5-PRC1 to the Xist RNA B-repeat to establish Polycomb-mediated chromosomal silencing. *Molecular Cell* (Vol. 68, Issue 5). https://doi.org/10.1016/j.molcel.2017.11.013
51. Somarowthu, S., Legiewicz, M., Chillón, I., Marcia, M., Liu, F., & Pyle, A. M. (2015). HOTAIR forms an intricate and modular secondary structure. *Molecular Cell* (Vol. 58, Issue 2). https://doi.org/10.1016/j.molcel.2015.03.006
52. Portoso, M., Ragazzini, R., Brenčič, Ž., Moiani, A., Michaud, A., Vassilev, I., Wassef, M., Servant, N., Sargueil, B., & Margueron, R. (2017). PRC2 is dispensable for HOTAIR-mediated transcriptional repression. *The EMBO Journal* (Vol. 36, Issue 8). https://doi.org/10.15252/embj.201695335
53. Amândio, A.R., Necsulea, A., Joye, E., Mascrez, B., Duboule, D. (2016). Hotair is dispensible for mouse development. *PLoS Genetics* (Vol. 12, Issue 12). https://doi.org/10.1371/journal.pgen.1006232
54. Yap, K.L., Li, S., Muñoz-Cabello, A.M., Raguz, S., Zeng, L., Mujtaba, S., Gil, J., Walsh, M.J., Zhou, M.M. (2010). Molecular interplay of the noncoding RNA ANRIL and methylated histone H3 lysine 27 by Polycomb CBX7 in transcriptional silencing of INK4a. *Molecular Cell* (Vol. 38, Issue 5). https://doi.org/10.1016/j.molcel.2010.03.021
55. Zhao, J., Ohsumi, T.K., Kung, J.T., Ogawa, Y., Grau, D.J., Sarma, K., Song, J.J., Kingston, R.E., Borowsky, M., Lee, J.T. (2010). Genome-wide identification of

polycomb-associated RNAs by RIP-seq. *Mol Cell* (Vol. 40, Issue 6). https://doi.org/10.1016/j.molcel.2010.12.011

56. Morey, L., Pascual, G., Cozzuto, L., Roma, G., Wutz, A., Benitah, S. A., & Di Croce, L. (2012). Nonoverlapping functions of the Polycomb group Cbx family of proteins in embryonic stem cells. *Cell Stem Cell* (Vol. 10, Issue 1). https://doi.org/10.1016/j.stem.2011.12.006
57. Taherbhoy, A. M., Huang, O. W., & Cochran, A. G. (2015). BMI1-RING1B is an autoinhibited RING E3 ubiquitin ligase. *Nature Communications* (Vol. 6). https://doi.org/10.1038/ncomms8621
58. Rose, N. R., King, H. W., Blackledge, N. P., Fursova, N. A., Ember, K. J., Fischer, R., Kessler, B. M., & Klose, R. J. (2016). RYBP stimulates PRC1 to shape chromatin-based communication between Polycomb Repressive Complexes. *ELife* (Vol. 5). https://doi.org/10.7554/eLife.18591
59. Margueron, R., Justin, N., Ohno, K., Sharpe, M. L., Son, J., Drury, W. J., Voigt, P., Martin, S. R., Taylor, W. R., De Marco, V., Pirrotta, V., Reinberg, D., & Gamblin, S. J. (2009). Role of the Polycomb protein EED in the propagation of repressive histone marks. *Nature* (Vol. 461, Issue 7265). https://doi.org/10.1038/nature08398
60. Lee, C. H., Yu, J. R., Kumar, S., Jin, Y., LeRoy, G., Bhanu, N., Kaneko, S., Garcia, B. A., Hamilton, A. D., & Reinberg, D. (2018). Allosteric activation dictates PRC2 activity independent of its recruitment to chromatin. *Molecular Cell* (Vol. 70, Issue 3). https://doi.org/10.1016/j.molcel.2018.03.020
61. Ku, M., Koche, R. P., Rheinbay, E., Mendenhall, E. M., Endoh, M., Mikkelsen, T. S., Presser, A., Nusbaum, C., Xie, X., Chi, A. S., Adli, M., Kasif, S., Ptaszek, L. M., Cowan, C. A., Lander, E. S., Koseki, H., & Bernstein, B. E. (2008). Genomewide analysis of PRC1 and PRC2 occupancy identifies two classes of bivalent domains. *PLoS Genetics* (Vol. 4, Issue 10). https://doi.org/10.1371/journal.pgen.1000242
62. Zhao, J., Wang, M., Chang, L., Yu, J., Song, A., Liu, C., Huang, W., Zhang, T., Wu, X., Shen, X., Zhu, B., & Li, G. (2020). RYBP/YAF2-PRC1 complexes and histone H1-dependent chromatin compaction mediate propagation of H2AK119ub1 during cell division. *Nature Cell Biology* (Vol. 22, Issue 4). https://doi.org/10.1038/s41556020-0484-1
63. Cooper, S., Dienstbier, M., Hassan, R., Schermelleh, L., Sharif, J., Blackledge, N. P., DeMarco, V., Elderkin, S., Koseki, H., Klose, R., Heger, A., & Brockdorff, N. (2014). Targeting Polycomb to pericentric heterochromatin in embryonic stem cells

reveals a role for H2AK119u1 in PRC2 recruitment. *Cell Reports* (Vol. 7, Issue 5). https://doi.org/10.1016/j.celrep.2014.04.012

64. Blackledge, N. P., Farcas, A. M., Kondo, T., King, H. W., McGouran, J. F., Hanssen, L. L. P., Ito, S., Cooper, S., Kondo, K., Koseki, Y., Ishikura, T., Long, H. K., Sheahan, T. W., Brockdorff, N., Kessler, B. M., Koseki, H., & Klose, R. J. (2014). Variant PRC1 complex-dependent H2A ubiquitylation drives PRC2 recruitment and Polycomb domain formation. *Cell* (Vol. 157, Issue 6). https://doi.org/10.1016/j.cell.2014.05.004
65. Tavares, L., Dimitrova, E., Oxley, D., Webster, J., Poot, R., Demmers, J., Bezstarosti, K., Taylor, S., Ura, H., Koide, H., Wutz, A., Vidal, M., Elderkin, S., & Brockdorff, N. (2012). RYBP-PRC1 complexes mediate H2A ubiquitylation at Polycomb target sites independently of PRC2 and H3K27me3. *Cell* (Vol. 148, Issue 4). https://doi.org/10.1016/j.cell.2011.12.029
66. Kasinath, V., Beck, C., Sauer, P., Poepsel, S., Kosmatka, J., Faini, M., Toso, D., Aebersold, R., & Nogales, E. (2021). JARID2 and AEBP2 regulate PRC2 in the presence of H2AK119ub1 and other histone modifications. *Science* (Vol. 371, Issue 6527). https://doi.org/10.1126/science.abc3393
67. Kalb, R., Latwiel, S., Baymaz, H. I., Jansen, P. W. T. C., Müller, C. W., Vermeulen, M., & Müller, J. (2014). Histone H2A monoubiquitination promotes histone H3 methylation in Polycomb repression. *Nature Structural and Molecular Biology* (Vol. 21, Issue 6). https://doi.org/10.1038/nsmb.2833
68. Plys, A. J., Davis, C. P., Kim, J., Rizki, G., Keenen, M. M., Marr, S. K., & Kingston, R. E. (2019). Phase separation of Polycomb-Repressive Complex 1 is governed by a charged disordered region of CBX2. *Genes and Development* (Vol. 33, Issue 13–14). https://doi.org/10.1101/gad.326488.119
69. Tatavosian, R., Kent, S., Brown, K., Yao, T., Duc, H. N., Huynh, T. N., Zhen, C. Y., Ma, B., Wang, H., & Ren, X. (2019). Nuclear condensates of the Polycomb protein chromobox 2 (CBX2) assemble through phase separation. *Journal of Biological Chemistry* (Vol. 294, Issue 5). https://doi.org/10.1074/jbc.RA118.006620
70. Seif, E., Kang, J. J., Sasseville, C., Senkovich, O., Kaltashov, A., Boulier, E. L., Kapur, I., Kim, C. A., & Francis, N. J. (2020). Phase separation by the polyhomeotic sterile alpha motif compartmentalizes Polycomb Group proteins and enhances their activity. *Nature Communications* (Vol. 11, Issue 1). https://doi.org/10.1038/s41467020-19435-z

71. Kim, C. A., Gingery, M., Pilpa, R. M., & Bowie, J. U. (2002). The SAM domain of polyhomeotic forms a helical polymer. *Nature Structural Biology* (Vol. 9, Issue 6). https://doi.org/10.1038/nsb802
72. Isono, K., Endo, T. A., Ku, M., Yamada, D., Suzuki, R., Sharif, J., Ishikura, T., Toyoda, T., Bernstein, B. E., & Koseki, H. (2013). SAM domain polymerization links subnuclear clustering of PRC1 to gene silencing. *Developmental Cell* (Vol. 26, Issue 6). https://doi.org/10.1016/j.devcel.2013.08.016
73. Saurin, A. J., Shiels, C., Williamson, J., Satijn, D. P. E., Otte, A. P., Sheer, D., & Freemont, P. S. (1998). The human Polycomb Group Complex associates with pericentromeric heterochromatin to form a novel nuclear domain. *Journal of Cell Biology* (Vol. 142, Issue 4). https://doi.org/10.1083/jcb.142.4.887
74. Francis, N. J., Follmer, N. E., Simon, M. D., Aghia, G., & Butler, J. D. (2009). Polycomb proteins remain bound to chromatin and DNA during DNA replication in vitro. *Cell* (Vol. 137, Issue 1). https://doi.org/10.1016/j.cell.2009.02.017
75. Lo, S. M., Follmer, N. E., Lengsfeld, B. M., Madamba, E. V., Seong, S., Grau, D. J., & Francis, N. J. (2012). A bridging model for persistence of a Polycomb Group protein complex through DNA replication in vitro. *Molecular Cell* (Vol. 46, Issue 6). https://doi.org/10.1016/j.molcel.2012.05.038
76. Hansen, K. H., Bracken, A. P., Pasini, D., Dietrich, N., Gehani, S. S., Monrad, A., Rappsilber, J., Lerdrup, M., & Helin, K. (2008). A model for transmission of the H3K27me3 epigenetic mark. *Nature Cell Biology* (Vol. 10, Issue 11). https://doi.org/10.1038/ncb1787
77. Petruk, S., Sedkov, Y., Johnston, D. M., Hodgson, J. W., Black, K. L., Kovermann, S. K., Beck, S., Canaani, E., Brock, H. W., & Mazo, A. (2012). TrxG and PcG proteins but not methylated histones remain associated with DNA through replication. *Cell* (Vol. 150, Issue 5). https://doi.org/10.1016/j.cell.2012.06.046
78. Coleman, R. T., & Struhl, G. (2017). Causal role for inheritance of H3K27me3 in maintaining the off state of a Drosophila HOX gene. *Science* (Vol. 356, Issue 6333). https://doi.org/10.1126/science.aai8236
79. Alabert, C., Barth, T. K., Reverón-Gómez, N., Sidoli, S., Schmidt, A., Jensen, O., Imhof, A., & Groth, A. (2015). Two distinct modes for propagation of histone PTMs across the cell cycle. *Genes and Development* (Vol. 29, Issue 6). https://doi.org/10.1101/gad.256354.114
80. Reverón-Gómez, N., González-Aguilera, C., Stewart-Morgan, K. R., Petryk, N., Flury, V., Graziano, S., Johansen, J. V., Jakobsen, J. S., Alabert, C., & Groth, A. (2018). Accurate recycling of parental histones reproduces the histone modification

landscape during DNA replication. *Molecular Cell* (Vol. 72, Issue 2). https://doi.org/10.1016/j.molcel.2018.08.010

81. Escobar, T. M., Oksuz, O., Saldaña-Meyer, R., Descostes, N., Bonasio, R., & Reinberg, D. (2019). Active and repressed chromatin domains exhibit distinct nucleosome segregation during DNA replication. *Cell* (Vol. 179, Issue 4). https://doi.org/10.1016/j.cell.2019.10.009
82. Dahl, J. A., Jung, I., Aanes, H., Greggains, G. D., Manaf, A., Lerdrup, M., Li, G., Kuan, S., Li, B., Lee, A. Y., Preissl, S., Jermstad, I., Haugen, M. H., Suganthan, R., Bjørås, M., Hansen, K., Dalen, K. T., Fedorcsak, P., Ren, B., & Klungland, A. (2016). Broad histone H3K4me3 domains in mouse oocytes modulate maternal-to-zygotic transition. *Nature* (Vol. 537, Issue 7621). https://doi.org/10.1038/nature19360
83. Liu, X., Wang, C., Liu, W., Li, J., Li, C., Kou, X., Chen, J., Zhao, Y., Gao, H., Wang, H., Zhang, Y., Gao, Y., & Gao, S. (2016). Distinct features of H3K4me3 and H3K27me3 chromatin domains in pre-implantation embryos. *Nature* (Vol. 537, Issue 7621). https://doi.org/10.1038/nature19362
84. Zheng, H., Huang, B., Zhang, B., Xiang, Y., Du, Z., Xu, Q., Li, Y., Wang, Q., Ma, J., Peng, X., Xu, F., & Xie, W. (2016). Resetting epigenetic memory by reprogramming of histone modifications in mammals. *Molecular Cell* (Vol. 63, Issue 6). https://doi.org/10.1016/j.molcel.2016.08.032
85. Wright, S. J. (1999). Sperm nuclear activation during fertilization. *Current topics in developmental biology* (Vol. 46). https://doi.org/10.1016/s0070-2153(08)60328-2
86. Torres-Padilla, M. E., Bannister, A. J., Hurd, P. J., Kouzarides, T., & Zernicka-Goetz, M. (2006). Dynamic distribution of the replacement histone variant H3.3 in the mouse oocyte and preimplantation embryos. *International Journal of Developmental Biology* (Vol. 50, Issue 5). https://doi.org/10.1387/ijdb.052073mt
87. Posfai, E., Kunzmann, R., Brochard, V., Salvaing, J., Cabuy, E., Roloff, T. C., Liu, Z., Tardat, M., van Lohuizen, M., Vidal, M., Beaujean, N., & Peters, A. H. F. M. (2012). Polycomb function during oogenesis is required for mouse embryonic development. *Genes and Development* (Vol. 26, Issue 9). https://doi.org/10.1101/gad.188094.112
88. Faust, C., Schumacher, A., Holdener, B., & Magnuson, T. (1995). The eed mutation disrupts anterior mesoderm production in mice. *Development* (Vol. 121, Issue 2). https://doi.org/10.1242/dev.121.2.273
89. O'Carroll, D., Erhardt, S., Pagani, M., Barton, S. C., Surani, M. A., & Jenuwein, T. (2001). The Polycomb-group gene Ezh2 is required for early mouse development.

Molecular and Cellular Biology (Vol. 21, Issue 13). https://doi.org/10.1128/mcb.21.13.4330-4336.2001

90. Pasini, D., Bracken, A. P., Jensen, M. R., Denchi, E. L., & Helin, K. (2004). Suz12 is essential for mouse development and for EZH2 histone methyltransferase activity. *EMBO Journal* (Vol. 23, Issue 20). https://doi.org/10.1038/sj.emboj.7600402
91. Ezhkova, E., Lien, W. H., Stokes, N., Pasolli, H. A., Silva, J. M., & Fuchs, E. (2011). EZH1 and EZH2 cogovern histone H3K27 trimethylation and are essential for hair follicle homeostasis and wound repair. *Genes and Development* (Vol. 25, Issue 5). https://doi.org/10.1101/gad.2019811
92. Voncken, J. W., Roelen, B. A. J., Roefs, M., De Vries, S., Verhoeven, E., Marino, S., Deschamps, J., & Van Lohuizen, M. (2003). Rnf2 (Ring1b) deficiency causes gastrulation arrest and cell cycle inhibition. *Proceedings of the National Academy of Sciences of the United States of America* (Vol. 100, Issue 5). https://doi.org/10.1073/pnas.0434312100
93. Del Mar Lorente, M., Marcos-Gutierrez, C., Perez, C., Schoorlemmer, J., Ramirez, A., Magin, T., & Vidal, M. (2000). Loss- and gain-of-function mutations show a Polycomb group function for Ring1A in mice. *Development* (Vol. 127, Issue 23). https://doi.org/10.1242/dev.127.23.5093
94. Van der Lugt, N. M. T., Domen, J., Linders, K., Van Roon, M., Robanus-Maandag, E., Te Riele, H., Van der Valk, M., Deschamps, J., Sofroniew, M., Van Lohuizen, M., & Berns, A. (1994). Posterior transformation, neurological abnormalities, and severe hematopoietic defects in mice with a targeted deletion of the bmi-1 proto-oncogene. *Genes and Development* (Vol. 8, Issue 7). https://doi.org/10.1101/gad.8.7.757
95. Akasaka, T., Kanno, M., Balling, R., Mieza, M. A., Taniguchi, M., & Koseki, H. (1996). A role for mel-18, a Polycomb group-related vertebrate gene, during the anteroposterior specification of the axial skeleton. *Development* (Vol. 122, Issue 5). https://doi.org/10.1242/dev.122.5.1513
96. Akasaka, T., van Lohuizen, M., van der Lugt, N., Mizutani-Koseki, Y., Kanno, M., Taniguchi, M., Vidal, M., Alkema, M., Berns, A., Koseki, H. (2001). Mice doubly deficient for the Polycomb Group genes Mel18 and Bmi1 reveal synergy and requirement for maintenance but not initiation of Hox gene expression. *Development* (Vol. 128, Issue 9). https://doi.org/10.1242/dev.128.9.1587
97. Pirity, M. K., Locker, J., & Schreiber-Agus, N. (2005). Rybp/DEDAF is required for early postimplantation and for central nervous system development. *Molecular*

and Cellular Biology (Vol. 25, Issue 16). https://doi.org/10.1128/mcb.25.16.7193-7202.2005

98. Fukuda, T., Tokunaga, A., Sakamoto, R., & Yoshida, N. (2011). Fbxl10/Kdm2b deficiency accelerates neural progenitor cell death and leads to exencephaly. *Molecular and Cellular Neuroscience* (Vol. 46, Issue 3). https://doi.org/10.1016/j.mcn.2011.01.001
99. Liu, B., Liu, Y. F., Du, Y. R., Mardaryev, A. N., Yang, W., Chen, H., Xu, Z. M., Xu, C. Q., Zhang, X. R., Botchkarev, V. A., Zhang, Y., & Xu, G. L. (2013). Cbx4 regulates the proliferation of thymic epithelial cells and thymus function. *Development* (Vol. 140, Issue 4). https://doi.org/10.1242/dev.085035
100. Coré, N., Bel, S., Gaunt, S. J., Aurrand-Lions, M., Pearce, J., Fisher, A., & Djabali, M. (1997). Altered cellular proliferation and mesoderm patterning in Polycomb-M33-deficient mice. *Development* (Vol. 124, Issue 3). https://doi.org/10.1242/dev.124.3.721
101. Boyer, L. A., Plath, K., Zeitlinger, J., Brambrink, T., Medeiros, L. A., Lee, T. I., Levine, S. S., Wernig, M., Tajonar, A., Ray, M. K., Bell, G. W., Otte, A. P., Vidal, M., Gifford, D. K., Young, R. A., & Jaenisch, R. (2006). Polycomb complexes repress developmental regulators in murine embryonic stem cells. *Nature* (Vol. 441, Issue 7091). https://doi.org/10.1038/nature04733
102. Lee, T. I., Jenner, R. G., Boyer, L. A., Guenther, M. G., Levine, S. S., Kumar, R. M., Chevalier, B., Johnstone, S. E., Cole, M. F., Isono, K. ichi, Koseki, H., Fuchikami, T., Abe, K., Murray, H. L., Zucker, J. P., Yuan, B., Bell, G. W., Herbolsheimer, E., Hannett, N. M., … Young, R. A. (2006). Control of developmental regulators by Polycomb in human embryonic stem cells. *Cell* (Vol. 125, Issue 2). https://doi.org/10.1016/j.cell.2006.02.043
103. Hammachi, F., Morrison, G. M., Sharov, A. A., Livigni, A., Narayan, S., Papapetrou, E. P., O'Malley, J., Kaji, K., Ko, M. S. H., Ptashne, M., & Brickman, J. M. (2012). Transcriptional activation by Oct4 is sufficient for the maintenance and induction of pluripotency. *Cell Reports* (Vol. 1, Issue 2). https://doi.org/10.1016/j.celrep.2011.12.002
104. Obier, N., Lin, Q., Cauchy, P., Hornich, V., Zenke, M., Becker, M., & Müller, A. M. (2015). Polycomb protein EED is required for silencing of pluripotency genes upon ESC differentiation. *Stem Cell Reviews and Reports* (Vol. 11, Issue 1). https://doi.org/10.1007/s12015-014-9550-z
105. Nichols, J., Zevnik, B., Anastassiadis, K., Niwa, H., Klewe-Nebenius, D., Chambers, I., Schöler, H., & Smith, A. (1998). Formation of pluripotent stem cells

in the mammalian embryo depends on the POU transcription factor Oct4. *Cell* (Vol. 95, Issue 3). https://doi.org/10.1016/S0092-8674(00)81769-9

106. Niwa, H., Miyazaki, J. I., & Smith, A. G. (2000). Quantitative expression of Oct-3/4 defines differentiation, dedifferentiation or self-renewal of ES cells. *Nature Genetics* (Vol. 24, Issue 4). https://doi.org/10.1038/74199
107. Avilion, A. A., Nicolis, S. K., Pevny, L. H., Perez, L., Vivian, N., & Lovell-Badge, R. (2003). Multipotent cell lineages in early mouse development depend on SOX2 function. *Genes and Development* (Vol. 17, Issue 1). https://doi.org/10.1101/gad.224503
108. Masui, S., Nakatake, Y., Toyooka, Y., Shimosato, D., Yagi, R., Takahashi, K., Okochi, H., Okuda, A., Matoba, R., Sharov, A. A., Ko, M. S. H., & Niwa, H. (2007). Pluripotency governed by Sox2 via regulation of Oct3/4 expression in mouse embryonic stem cells. *Nature Cell Biology* (Vol. 9, Issue 6). https://doi.org/10.1038/ncb1589
109. Chen, X., Xu, H., Yuan, P., Fang, F., Huss, M., Vega, V. B., Wong, E., Orlov, Y. L., Zhang, W., Jiang, J., Loh, Y. H., Yeo, H. C., Yeo, Z. X., Narang, V., Govindarajan, K. R., Leong, B., Shahab, A., Ruan, Y., Bourque, G., … Ng, H. H. (2008). Integration of external signaling pathways with the core transcriptional network in embryonic Stem Cells. *Cell* (Vol. 133, Issue 6). https://doi.org/10.1016/j.cell.2008.04.043
110. Endoh, M., Endo, T. A., Endoh, T., Fujimura, Y. I., Ohara, O., Toyoda, T., Otte, A. P., Okano, M., Brockdorff, N., Vidal, M., & Koseki, H. (2008). Polycomb group proteins Ring1A/B are functionally linked to the core transcriptional regulatory circuitry to maintain ES cell identity. *Development* (Vol. 135, Issue 8). https://doi.org/10.1242/dev.014340
111. Pasini, D., Bracken, A. P., Jensen, M. R., Denchi, E. L., & Helin, K. (2004). Suz12 is essential for mouse development and for EZH2 histone methyltransferase activity. *EMBO Journal* (Vol. 23, Issue 20). https://doi.org/10.1038/sj.emboj.7600402
112. Chamberlain, S. J., Yee, D., & Magnuson, T. (2008). Polycomb Repressive Complex 2 is dispensable for maintenance of embryonic stem cell pluripotency. *Stem Cells* (Vol. 26, Issue 6). https://doi.org/10.1634/stemcells.2008-0102
113. Shen, X., Liu, Y., Hsu, Y. J., Fujiwara, Y., Kim, J., Mao, X., Yuan, G. C., & Orkin, S. H. (2008). EZH1 mediates methylation on histone H3 lysine 27 and complements EZH2 in maintaining stem cell identity and executing pluripotency. *Molecular Cell* (Vol. 32, Issue 4). https://doi.org/10.1016/j.molcel.2008.10.016

114. van Mierlo, G., Dirks, R. A. M., De Clerck, L., Brinkman, A. B., Huth, M., Kloet, S. L., Saksouk, N., Kroeze, L. I., Willems, S., Farlik, M., Bock, C., Jansen, J. H., Deforce, D., Vermeulen, M., Déjardin, J., Dhaenens, M., & Marks, H. (2019). Integrative proteomic profiling reveals PRC2-dependent epigenetic crosstalk maintains ground-state pluripotency. *Cell Stem Cell* (Vol. 24, Issue 1). https://doi.org/10.1016/j.stem.2018.10.017

115. Endoh, M., Endo, T. A., Shinga, J., Hayashi, K., Farcas, A., Ma, K. W., Ito, S., Sharif, J., Endoh, T., Onaga, N., Nakayama, M., Ishikura, T., Masui, O., Kessler, B. M., Suda, T., Ohara, O., Okuda, A., Klose, R., & Koseki, H. (2017). PCGF6-PRC1 suppresses premature differentiation of mouse embryonic stem cells by regulating germ cell-related genes. *ELife* (Vol. 6). https://doi.org/10.7554/eLife.21064

116. Leeb, M., Pasini, D., Novatchkova, M., Jaritz, M., Helin, K., & Wutz, A. (2010). Polycomb complexes act redundantly to repress genomic repeats and genes. *Genes and Development* (Vol. 24, Issue 3). https://doi.org/10.1101/gad.544410

117. Leeb, M., & Wutz, A. (2007). Ring1B is crucial for the regulation of developmental control genes and PRC1 proteins but not X inactivation in embryonic cells. *Journal of Cell Biology* (Vol. 178, Issue 2). https://doi.org/10.1083/jcb.200612127

118. Hisada, K., Sánchez, C., Endo, T. A., Endoh, M., Román-Trufero, M., Sharif, J., Koseki, H., & Vidal, M. (2012). RYBP represses endogenous retroviruses and preimplantation- and germ line-specific genes in mouse embryonic stem cells. *Molecular and Cellular Biology* (Vol. 32, Issue 6). https://doi.org/10.1128/mcb.06441-11

119. Qin, J., Whyte, W. A., Anderssen, E., Apostolou, E., Chen, H. H., Akbarian, S., Bronson, R. T., Hochedlinger, K., Ramaswamy, S., Young, R. A., & Hock, H. (2012). The polycomb group protein L3mbtl2 assembles an atypical PRC1-family complex that is essential in pluripotent stem cells and early development. *Cell Stem Cell* (Vol. 11, Issue 3). https://doi.org/10.1016/j.stem.2012.06.002

120. Peng, J. C., Valouev, A., Swigut, T., Zhang, J., Zhao, Y., Sidow, A., & Wysocka, J. (2009). Jarid2/Jumonji coordinates control of PRC2 enzymatic activity and target gene occupancy in pluripotent cells. *Cell* (Vol. 139, Issue 7). https://doi.org/10.1016/j.cell.2009.12.002

121. Pasini, D., Cloos, P. A. C., Walfridsson, J., Olsson, L., Bukowski, J. P., Johansen, J. V., Bak, M., Tommerup, N., Rappsilber, J., & Helin, K. (2010). JARID2 regulates binding of the Polycomb Repressive Complex 2 to target genes in ES cells. *Nature* (Vol. 464, Issue 7286). https://doi.org/10.1038/nature08788

122. Walker, E., Chang, W. Y., Hunkapiller, J., Cagney, G., Garcha, K., Torchia, J., Krogan, N. J., Reiter, J. F., & Stanford, W. L. (2010). Polycomb-like 2 associates with PRC2 and regulates transcriptional networks during mouse embryonic stem cell self-renewal and differentiation. *Cell Stem Cell* (Vol. 6, Issue 2). https://doi.org/10.1016/j.stem.2009.12.014
123. Ballaré, C., Lange, M., Lapinaite, A., Martin, G. M., Morey, L., Pascual, G., Liefke, R., Simon, B., Shi, Y., Gozani, O., Carlomagno, T., Benitah, S. A., & Di Croce, L. (2012). Phf19 links methylated Lys36 of histone H3 to regulation of Polycomb activity. *Nature Structural and Molecular Biology* (Vol. 19, Issue 12). https://doi.org/10.1038/nsmb.2434
124. Brookes, E., De Santiago, I., Hebenstreit, D., Morris, K. J., Carroll, T., Xie, S. Q., Stock, J. K., Heidemann, M., Eick, D., Nozaki, N., Kimura, H., Ragoussis, J., Teichmann, S. A., & Pombo, A. (2012). Polycomb associates genome-wide with a specific RNA polymerase II variant, and regulates metabolic genes in ESCs. *Cell Stem Cell* (Vol. 10, Issue 2). https://doi.org/10.1016/j.stem.2011.12.017
125. Mikkelsen, T. S., Ku, M., Jaffe, D. B., Issac, B., Lieberman, E., Giannoukos, G., Alvarez, P., Brockman, W., Kim, T. K., Koche, R. P., Lee, W., Mendenhall, E., O'Donovan, A., Presser, A., Russ, C., Xie, X., Meissner, A., Wernig, M., Jaenisch, R., … Bernstein, B. E. (2007). Genome-wide maps of chromatin state in pluripotent and lineage-committed cells. *Nature* (Vol. 448, Issue 7153). https://doi.org/10.1038/nature06008
126. Alder, O., Lavial, F., Helness, A., Brookes, E., Pinho, S., Chandrashekran, A., Arnaud, P., Pombo, A., O'Neill, L., & Azuara, V. (2010). Ring1B and Suv39h1 delineate distinct chromatin states at bivalent genes during early mouse lineage commitment. *Development* (Vol. 137, Issue 15). https://doi.org/10.1242/dev.048363
127. Schuettengruber, B., Chourrout, D., Vervoort, M., Leblanc, B., & Cavalli, G. (2007). Genome regulation by Polycomb and Trithorax proteins. *Cell* (Vol. 128, Issue 4). https://doi.org/10.1016/j.cell.2007.02.009
128. Simon, J. A., & Kingston, R. E. (2009). Mechanisms of Polycomb gene silencing: knowns and unknowns. *Nature Reviews Molecular Cell Biology* (Vol. 10, Issue 10). https://doi.org/10.1038/nrm2763
129. Cloos, P. A. C., Christensen, J., Agger, K., & Helin, K. (2008). Erasing the methyl mark: histone demethylases at the center of cellular differentiation and disease. *Genes and Development* (Vol. 22, Issue 9). https://doi.org/10.1101/gad.1652908

130. Lan, F., Nottke, A. C., & Shi, Y. (2008). Mechanisms involved in the regulation of histone lysine demethylases. *Current Opinion in Cell Biology* (Vol. 20, Issue 3). https://doi.org/10.1016/j.ceb.2008.03.004
131. Mohn, F., Weber, M., Rebhan, M., Roloff, T. C., Richter, J., Stadler, M. B., Bibel, M., & Schübeler, D. (2008). Lineage-specific Polycomb targets and de novo DNA methylation define restriction and potential of neuronal progenitors. *Molecular Cell* (Vol. 30, Issue 6). https://doi.org/10.1016/j.molcel.2008.05.007
132. Cui, K., Zang, C., Roh, T. Y., Schones, D. E., Childs, R. W., Peng, W., & Zhao, K. (2009). Chromatin signatures in multipotent human hematopoietic stem cells indicate the fate of bivalent genes during differentiation. *Cell Stem Cell* (Vol. 4, Issue 1). https://doi.org/10.1016/j.stem.2008.11.011
133. Marks, H., Kalkan, T., Menafra, R., Denissov, S., Jones, K., Hofemeister, H., Nichols, J., Kranz, A., Francis Stewart, A., Smith, A., & Stunnenberg, H. G. (2012). The transcriptional and epigenomic foundations of ground state pluripotency. *Cell* (Vol. 149, Issue 3). https://doi.org/10.1016/j.cell.2012.03.026
134. Fursova, N. A., Blackledge, N. P., Nakayama, M., Ito, S., Koseki, Y., Farcas, A. M., King, H. W., Koseki, H., & Klose, R. J. (2019). Synergy between Variant PRC1 complexes defines Polycomb-mediated gene repression. *Molecular Cell* (Vol. 74, Issue 5). https://doi.org/10.1016/j.molcel.2019.03.024
135. Blackledge, N. P., Fursova, N. A., Kelley, J. R., Huseyin, M. K., Feldmann, A., & Klose, R. J. (2020). PRC1 catalytic activity is central to Polycomb system function. *Molecular Cell* (Vol. 77, Issue 4). https://doi.org/10.1016/j.molcel.2019.12.001
136. Tamburri, S., Lavarone, E., Fernández-Pérez, D., Conway, E., Zanotti, M., Manganaro, D., & Pasini, D. (2020). Histone H2AK119 mono-ubiquitination is essential for Polycomb-mediated transcriptional repression. *Molecular Cell* (Vol. 77, Issue 4). https://doi.org/10.1016/j.molcel.2019.11.021
137. Huseyin, M. K., & Klose, R. J. (2021). Live-cell single particle tracking of PRC1 reveals a highly dynamic system with low target site occupancy. *Nature Communications* (Vol. 12, Issue 1). https://doi.org/10.1038/s41467-021-21130-6
138. Zhen, C. Y., Tatavosian, R., Huynh, T. N., Duc, H. N., Das, R., Kokotovic, M., Grimm, J. B., Lavis, L. D., Lee, J., Mejia, F. J., Li, Y., Yao, T., & Ren, X. (2016). Live-cell single-molecule tracking reveals co-recognition of H3K27me3 and DNA targets polycomb Cbx7-PRC1 to chromatin. *ELife* (Vol. 5). https://doi.org/10.7554/elife.17667
139. Dobrinić, P., Szczurek, A. T., & Klose, R. J. (2021). PRC1 drives Polycomb-mediated gene repression by controlling transcription initiation and burst

frequency. *Nature Structural and Molecular Biology* (Vol. 28, Issue 10). https://doi.org/10.1038/s41594-021-00661-y

140. Lehmann, L., Ferrari, R., Vashisht, A. A., Wohlschlegel, J. A., Kurdistani, S. K., & Careys, M. (2012). Polycomb Repressive Complex 1 (PRC1) disassembles RNA polymerase II preinitiation complexes. *Journal of Biological Chemistry* (Vol. 287, Issue 43). https://doi.org/10.1074/jbc.M112.397430
141. Dellino, G. I., Schwartz, Y. B., Farkas, G., McCabe, D., Elgin, S. C. R., & Pirrotta, V. (2004). Polycomb silencing blocks transcription initiation. *Molecular Cell* (Vol. 13, Issue 6). https://doi.org/10.1016/S1097-2765(04)00128-5
142. Conway, E., Rossi, F., Fernandez-Perez, D., Ponzo, E., Ferrari, K. J., Zanotti, M., Manganaro, D., Rodighiero, S., Tamburri, S., & Pasini, D. (2021). BAP1 enhances Polycomb repression by counteracting widespread H2AK119ub1 deposition and chromatin condensation. *Molecular Cell* (Vol. 81, Issue 17). https://doi.org/10.1016/j.molcel.2021.06.020
143. Campagne, A., Lee, M. K., Zielinski, D., Michaud, A., Le Corre, S., Dingli, F., Chen, H., Shahidian, L. Z., Vassilev, I., Servant, N., Loew, D., Pasmant, E., Postel-Vinay, S., Wassef, M., & Margueron, R. (2019). BAP1 complex promotes transcription by opposing PRC1-mediated H2A ubiquitylation. *Nature Communications* (Vol. 10, Issue 1). https://doi.org/10.1038/s41467-018-08255-x
144. Chiacchiera, F., Rossi, A., Jammula, S., Zanotti, M., & Pasini, D. (2016). PRC2 preserves intestinal progenitors and restricts secretory lineage commitment. *The EMBO Journal* (Vol. 35, Issue 21). https://doi.org/10.15252/embj.201694550
145. Chiacchiera, F., Rossi, A., Jammula, S., Piunti, A., Scelfo, A., Ordóñez-Morán, P., Huelsken, J., Koseki, H., & Pasini, D. (2016). Polycomb Complex PRC1 preserves intestinal stem cell identity by sustaining Wnt/β-Catenin transcriptional activity. *Cell Stem Cell* (Vol. 18, Issue 1). https://doi.org/10.1016/j.stem.2015.09.019
146. Jadhav, U., Nalapareddy, K., Saxena, M., O'Neill, N. K., Pinello, L., Yuan, G. C., Orkin, S. H., & Shivdasani, R. A. (2016). Acquired tissue-specific promoter bivalency is a basis for PRC2 necessity in adult cells. *Cell* (Vol. 165, Issue 6). https://doi.org/10.1016/j.cell.2016.04.031
147. Santos, A. J. M., Lo, Y. H., Mah, A. T., & Kuo, C. J. (2018). The intestinal stem cell niche: homeostasis and adaptations. *Trends in Cell Biology* (Vol. 28, Issue 12). https://doi.org/10.1016/j.tcb.2018.08.001
148. Tian, H., Biehs, B., Warming, S., Leong, K. G., Rangell, L., Klein, O. D., & De Sauvage, F. J. (2011). A reserve stem cell population in small intestine renders

Lgr5-positive cells dispensable. *Nature* (Vol. 478, Issue 7368). https://doi.org/10.1038/nature10408

149. Van Es, J. H., Sato, T., Van De Wetering, M., Lyubimova, A., Yee Nee, A. N., Gregorieff, A., Sasaki, N., Zeinstra, L., Van Den Born, M., Korving, J., Martens, A. C. M., Barker, N., Van Oudenaarden, A., & Clevers, H. (2012). Dll1 + secretory progenitor cells revert to stem cells upon crypt damage. *Nature Cell Biology* (Vol. 14, Issue 10). https://doi.org/10.1038/ncb2581
150. Schmitt, M., Schewe, M., Sacchetti, A., Feijtel, D., van de Geer, W. S., Teeuwssen, M., Sleddens, H. F., Joosten, R., van Royen, M. E., van de Werken, H. J. G., van Es, J., Clevers, H., & Fodde, R. (2018). Paneth cells respond to inflammation and contribute to tissue regeneration by acquiring stem-like features through SCF/c-Kit signaling. *Cell Reports* (Vol. 24, Issue 9). https://doi.org/10.1016/j.celrep.2018.07.085
151. Yu, S., Tong, K., Zhao, Y., Balasubramanian, I., Yap, G. S., Ferraris, R. P., Bonder, E. M., Verzi, M. P., & Gao, N. (2018). Paneth cell multipotency induced by Notch activation following injury. *Cell Stem Cell* (Vol. 23, Issue 1). https://doi.org/10.1016/j.stem.2018.05.002
152. Tetteh, P. W., Basak, O., Farin, H. F., Wiebrands, K., Kretzschmar, K., Begthel, H., Van Den Born, M., Korving, J., De Sauvage, F., Van Es, J. H., Van Oudenaarden, A., & Clevers, H. (2016). Replacement of lost Lgr5-positive stem cells through plasticity of their enterocyte-lineage daughters. *Cell Stem Cell* (Vol. 18, Issue 2). https://doi.org/10.1016/j.stem.2016.01.001
153. Howitt, M. R., Lavoie, S., Michaud, M., Blum, A. M., Tran, S. V., Weinstock, J. V., Gallini, C. A., Redding, K., Margolskee, R. F., Osborne, L. C., Artis, D., & Garrett, W. S. (2016). Tuft cells, taste-chemosensory cells, orchestrate parasite type 2 immunity in the gut. *Science* (Vol. 351, Issue 6279). https://doi.org/10.1126/science.aaf1648
154. Gerbe, F., Sidot, E., Smyth, D. J., Ohmoto, M., Matsumoto, I., Dardalhon, V., Cesses, P., Garnier, L., Pouzolles, M., Brulin, B., Bruschi, M., Harcus, Y., Zimmermann, V. S., Taylor, N., Maizels, R. M., & Jay, P. (2016). Intestinal epithelial tuft cells initiate type 2 mucosal immunity to helminth parasites. *Nature* (Vol. 529, Issue 7585). https://doi.org/10.1038/nature16527
155. Kretzschmar, K., & Clevers, H. (2017). Wnt/β-catenin signaling in adult mammalian epithelial stem cells. *Developmental Biology* (Vol. 428, Issue 2). https://doi.org/10.1016/j.ydbio.2017.05.015

156. van Es, J. H., Jay, P., Gregorieff, A., van Gijn, M. E., Jonkheer, S., Hatzis, P., Thiele, A., van den Born, M., Begthel, H., Brabletz, T., Taketo, M. M., & Clevers, H. (2005). Wnt signalling induces maturation of Paneth cells in intestinal crypts. *Nature Cell Biology* (Vol. 7, Issue 4). https://doi.org/10.1038/ncb1240

157. Sato, T., Van Es, J. H., Snippert, H. J., Stange, D. E., Vries, R. G., Van Den Born, M., Barker, N., Shroyer, N. F., Van De Wetering, M., & Clevers, H. (2011). Paneth cells constitute the niche for Lgr5 stem cells in intestinal crypts. *Nature* (Vol. 469, Issue 7330). https://doi.org/10.1038/nature09637

158. De Lau, W., Barker, N., & Clevers, H. (2007). WNT signaling in the normal intestine and colorectal cancer. *Frontiers in Bioscience* (Vol. 12, Issue 2). https://doi.org/10.2741/2076

159. He, X. C., Zhang, J., Tong, W. G., Tawfik, O., Ross, J., Scoville, D. H., Tian, Q., Zeng, X., He, X., Wiedemann, L. M., Mishina, Y., & Li, L. (2004). BMP signaling inhibits intestinal stem cell self-renewal through suppression of Wnt-β-catenin signaling. *Nature Genetics* (Vol. 36, Issue 10). https://doi.org/10.1038/ng1430

160. Qi, Z., Li, Y., Zhao, B., Xu, C., Liu, Y., Li, H., Zhang, B., Wang, X., Yang, X., Xie, W., Li, B., Han, J. D. J., & Chen, Y. G. (2017). BMP restricts stemness of intestinal Lgr5+ stem cells by directly suppressing their signature genes. *Nature Communications* (Vol. 8). https://doi.org/10.1038/ncomms13824

161. Guruharsha, K. G., Kankel, M. W., & Artavanis-Tsakonas, S. (2012). The Notch signalling system: recent insights into the complexity of a conserved pathway. *Nature Reviews Genetics* (Vol. 13, Issue 9). https://doi.org/10.1038/nrg3272

162. Sancho, R., Cremona, C. A., & Behrens, A. (2015). Stem cell and progenitor fate in the mammalian intestine: Notch and lateral inhibition in homeostasis and disease. *EMBO Reports*. (Vol. 16, Issue 5). https://doi.org/10.15252/embr.201540188

163. Citri, A., & Yarden, Y. (2006). EGF-ERBB signalling: towards the systems level. *Nature Reviews Molecular Cell Biology* (Vol. 7, Issue 7). https://doi.org/10.1038/nrm1962

164. Threadgill, D. W., Dlugosz, A. A., Hansen, L. A., Tennenbaum, T., Lichti, U., Yee, D., LaMantia, C., Mourton, T., Herrup, K., Harris, R. C., Barnard, J. A., Yuspa, S. H., Coffey, R. J., & Magnuson, T. (1995). Targeted disruption of mouse EGF receptor: effect of genetic background on mutant phenotype. *Science* (Vol. 269, Issue 5221). https://doi.org/10.1126/science.7618084

165. Pivetti, S., Fernandez-Perez, D., D'Ambrosio, A., Barbieri, C.M., Manganaro, D., Rossi, A., Barnabei, L., Zanotti, M., Scelfo, A., Chiacchiera, F., Pasini, D. (2019). Loss of PRC1 activity in different stem cell compartments activates a common

transcriptional program with cell type-dependent outcomes. *Science Advances* (Vol. 5, Issue 5). https://doi.org/10.1126/sciadv.aav1594

166. Jacobs, J. J. L., Scheijen, B., Voncken, J. W., Kieboom, K., Berns, A., & Van Lohuizen, M. (1999). Bmi-1 collaborates with c-Myc in tumorigenesis by inhibiting c-Myc- induced apoptosis via INK4a/ARF. *Genes and Development* (Vol. 13, Issue 20). https://doi.org/10.1101/gad.13.20.2678
167. Dietrich, N., Bracken, A. P., Trinh, E., Schjerling, C. K., Koseki, H., Rappsilber, J., Helin, K., & Hansen, K. H. (2007). Bypass of senescence by the Polycomb group protein CBX8 through direct binding to the INK4A-ARF locus. *EMBO Journal* (Vol. 26, Issue 6). https://doi.org/10.1038/sj.emboj.7601632
168. Nakamura, S., Oshima, M., Yuan, J., Saraya, A., Miyagi, S., Konuma, T., Yamazaki, S., Osawa, M., Nakauchi, H., Koseki, H., & Iwama, A. (2012). Bmi1 confers resistance to oxidative stress on hematopoietic stem cells. *PLoS ONE* (Vol. 7, Issue 5). https://doi.org/10.1371/journal.pone.0036209
169. Hu, T., Kitano, A., Luu, V., Dawson, B., Hoegenauer, K. A., Lee, B. H., & Nakada, D. (2019). Bmi1 suppresses adipogenesis in the hematopoietic stem cell niche. *Stem Cell Reports* (Vol. 13, Issue 3). https://doi.org/10.1016/j.stemcr.2019.05.027
170. Di Foggia, V., Zhang, X., Licastro, D., Gerli, M. F. M., Phadke, R., Muntoni, F., Mourikis, P., Tajbakhsh, S., Ellis, M., Greaves, L. C., Taylor, R. W., Cossu, G., Robson, L. G., & Marino, S. (2014). Bmi1 enhances skeletal muscle regeneration through MT1-mediated oxidative stress protection in a mouse model of dystrophinopathy. *Journal of Experimental Medicine* (Vol. 211, Issue 13). https://doi.org/10.1084/jem.20140317
171. Burgold, T., Spreafico, F., De Santa, F., Totaro, M. G., Prosperini, E., Natoli, G., & Testa, G. (2008). The histone H3 lysine 27-specific demethylase Jmjd3 is required for neural commitment. *PLoS ONE* (Vol. 3, Issue 8). https://doi.org/10.1371/journal.pone.0003034
172. Testa, G. (2011). The time of timing: how Polycomb proteins regulate neurogenesis. *BioEssays* (Vol. 33, Issue 7). https://doi.org/10.1002/bies.201100021
173. Grindheim, J. M., Nicetto, D., Donahue, G., & Zaret, K. S. (2019). PRC2 proteins EZH1 and EZH2 regulate timing of postnatal hepatocyte maturation and fibrosis by repressing gene expression at promoter regions in euchromatin in mice. *Gastroenterology* (Vol. 156, Issue 6). https://doi.org/10.1053/j.gastro.2019.01.041
174. Li, J., Ouyang, T., Li, M., Hong, T., Alriashy, M. H. S., Meng, W., & Zhang, N. (2021). CBX7 is dualistic in cancer progression based on its function and molecular

interactions. *Frontiers in Genetics* (Vol. 12). https://doi.org/10.3389/fgene.2021.740794

175. Zhang, Y., Liu, T., Yuan, F., Garcia-Martinez, L., Lee, K. D., Stransky, S., Sidoli, S., Verdun, R. E., Zhang, Y., Wang, Z., & Morey, L. (2021). The Polycomb protein RING1B enables estrogen-mediated gene expression by promoting enhancer-promoter interaction and R-loop formation. *Nucleic Acids Research* (Vol. 49, Issue 17). https://doi.org/10.1093/nar/gkab723
176. Oksenberg, N., & Ahituv, N. (2013). The role of AUTS2 in neurodevelopment and human evolution. *Trends in Genetics* (Vol. 29, Issue 10). https://doi.org/10.1016/j.tig.2013.08.001
177. Astolfi, A., Fiore, M., Melchionda, F., Indio, V., Bertuccio, S. N., & Pession, A. (2019). BCOR involvement in cancer. *Epigenomics* (Vol. 11, Issue 7). https://doi.org/10.2217/epi-2018-0195
178. Varambally, S., Dhanasekaran, S. M., Zhou, M., Barrette, T. R., Kumar-Sinha, C., Sanda, M. G., Ghosh, D., Pienta, K. J., Sewalt, R. G. A. B., Rubin, M. A., & Chinnaiyan, A. M. (2002). The Polycomb group protein EZH2 is involved in progression of prostate cancer. *Nature* (Vol. 419, Issue 6907). https://doi.org/10.1038/nature01075
179. Morin, R. D., Johnson, N. A., Severson, T. M., Mungall, A. J., An, J., Goya, R., Paul, J. E., Boyle, M., Woolcock, B. W., Kuchenbauer, F., Yap, D., Humphries, R. K., Griffith, O. L., Shah, S., Zhu, H., Kimbara, M., Shashkin, P., Charlot, J. F., Tcherpakov, M., … Marra, M. A. (2010). Somatic mutations altering EZH2 (Tyr641) in follicular and diffuse large B-cell lymphomas of germinal-center origin. *Nature Genetics* (Vol. 42, Issue 2). https://doi.org/10.1038/ng.518
180. Helin, K., & Dhanak, D. (2013). Chromatin proteins and modifications as drug targets. *Nature* (Vol. 502, Issue 7472). https://doi.org/10.1038/nature12751
181. Lee, W., Teckie, S., Wiesner, T., Ran, L., Prieto Granada, C. N., Lin, M., Zhu, S., Cao, Z., Liang, Y., Sboner, A., Tap, W. D., Fletcher, J. A., Huberman, K. H., Qin, L. X., Viale, A., Singer, S., Zheng, D., Berger, M. F., Chen, Y., … Chi, P. (2014). PRC2 is recurrently inactivated through EED or SUZ12 loss in malignant peripheral nerve sheath tumors. *Nature Genetics* (Vol. 46, Issue 11). https://doi.org/10.1038/ng.3095
182. Ireland, H., Kemp, R., Houghton, C., Howard, L., Clarke, A. R., Sansom, O. J., & Winton, D. J. (2004). Inducible Cre-mediated control of gene expression in the murine gastrointestinal tract: effect of loss of β-Catenin. *Gastroenterology* (Vol. 126, Issue 5). https://doi.org/10.1053/j.gastro.2004.03.020

183. Barker, N., Van Es, J. H., Kuipers, J., Kujala, P., Van Den Born, M., Cozijnsen, M., Haegebarth, A., Korving, J., Begthel, H., Peters, P. J., & Clevers, H. (2007). Identification of stem cells in small intestine and colon by marker gene Lgr5. *Nature* (Vol. 449, Issue 7165). https://doi.org/10.1038/nature06196
184. Soriano, P. (1999). Generalized lacZ expression with the ROSA26 Cre reporter strain. *Nature Genetics* (Vol. 21, Issue 1). https://doi.org/10.1038/5007
185. El Marjou, F., Janssen, K. P., Chang, B. H. J., Li, M., Hindie, V., Chan, L., Louvard, D., Chambon, P., Metzger, D., & Robine, S. (2004). Tissue-specific and inducible Cre-mediated recombination in the gut epithelium. *Genesis* (Vol. 39, Issue 3). https://doi.org/10.1002/gene.20042
186. Lavarone, E., Barbieri, C. M., & Pasini, D. (2019). Dissecting the role of H3K27 acetylation and methylation in PRC2 mediated control of cellular identity. *Nature Communications* (Vol. 10, Issue 1). https://doi.org/10.1038/s41467-019-09624-w
187. Picelli, S., Faridani, O. R., Björklund, Å. K., Winberg, G., Sagasser, S., & Sandberg, R. (2014). Full-length RNA-seq from single cells using Smart-seq2. *Nature Protocols* (Vol. 9, Issue 1). https://doi.org/10.1038/nprot.2014.006
188. Faust, G.G., Hall, I.M. (2014). SAMBLASTER: fast duplicate marking and structural variant read extraction. *Bioinformatics* (Vol. 30, Issue 17). https://doi.org/10.1093/bioinformatics/btu314
189. Liao, Y., Smyth, G.K., Shi, W. (2014). featureCounts: an efficient general purpose program for assigning sequence reads to genomic features. *Bioinformatics* (Vol. 30, Issue 7). https://doi.org/10.1093/bioinformatics/btt656
190. Love, M.I., Huber, W., Anders, S. (2014). Moderated estimation of fold change and dispersion for RNA-seq data with DESeq2. *Genome Biology* (Vol. 15, Issue 12). https://doi.org/10.1186/s13059-014-0550-8
191. Zhu, A., Ibrahim, J.G., Love, M.I. (2019). Heavy-tailed prior distributions for sequence count data: removing the noise and preserving large differences. *Bioinformatics* (Vol. 35, Issue 12). https://doi.org/10.1093/bioinformatics/bty895
192. Ignatiadis, N., Klaus, B., Zaugg, J.B., Huber, W. (2016). Data-driven hypothesis weighting increases detection power in genome-scale multiple testing. *Nature Methods* (Vol. 13, Issue 7). https://doi.org/10.1038/nmeth.3885
193. Yu, G., Wang, L.G., Han, Y., He, Q.Y. (2012). clusterProfiler: an R package for comparing biological themes among gene clusters. *OMICS* (Vol. 16, Issue 5). https://doi.org/10.1089/omi.2011.0118
194. Ferrari, K. J., Scelfo, A., Jammula, S. G., Cuomo, A., Barozzi, I., Stützer, A., Fischle, W., Bonaldi, T., & Pasini, D. (2014). Polycomb-dependent H3K27me1 and

H3K27me2 regulate active transcription and enhancer fidelity. *Molecular Cell* (Vol. 53, Issue 1). https://doi.org/10.1016/j.molcel.2013.10.030

195. Chen, S., Zhou, Y., Chen, Y., Gu, J. (2018) fastp: an ultra-fast all-in-one FASTQ preprocessor. *Bioinformatics* (Vol. 34, Issue 17). https://doi.org/10.1093/bioinformatics/bty560
196. Langmead, B., Trapnell, C., Pop, M., Salzberg, S.L. (2009). Ultrafast and memory-efficient alignment of short DNA sequences to the human genome. *Genome Biology* (Vol.10, Issue 3). https://doi.org/10.1186/gb-2009-10-3-r25
197. Zhang, Y., Liu, T., Meyer, C.A. et al. (2008). Model-based analysis of ChIP-seq. *Genome Biology* (Vol. 9, Issue 9). https://doi.org/10.1186/gb-2008-9-9-r137
198. Zhu, L.J., Gazin, C., Lawson, N.D., Pagès, H., Lin, S.M., Lapointe, D.S., Green, M.R. (2010). ChIPpeakAnno: a bioconductor package to annotate ChIP-seq and ChIP-chip data. *BMC Bioinformatics* (Vol. 11). https://doi.org/10.1186/1471-2105-11-237
199. Ramírez, F., Ryan, D.P., Grüning, B., Bhardwaj, V., Kilpert, F., Richter, A.S., Heyne, S., Dündar, F., Manke, T. (2016) deepTools2: a next generation web server for deep-sequencing data analysis. *Nucleic Acids Research* (Vol. 44, Issue W1). https://doi.org/10.1093/nar/gkw257
200. Orlando, D.A., Chen, M.W., Brown, V.E., Solanki, S., Choi, Y.J., Olson, E.R., Fritz, C.C., Bradner, J.E., Guenther, M.G. (2014). Quantitative ChIP-Seq normalization reveals global modulation of the epigenome. *Cell Reports* (Vol. 9, Issue 3). https://doi.org/10.1016/j.celrep.2014.10.018
201. Schuettengruber, B., Bourbon, H. M., Di Croce, L., & Cavalli, G. (2017). Genome regulation by Polycomb and Trithorax: 70 Years and Counting. *Cell* (Vol. 171, Issue 1). https://doi.org/10.1016/j.cell.2017.08.002
202. O'Loghlen, A., Muñoz-Cabello, A.M., Gaspar-Maia, A., Wu, H.A., Banito, A., Kunowska N., Racek T., Pemberton, H.N., Beolchi, P., Lavial, F., Masui, O., Vermeulen, M., Carroll, T., Graumann, J., Heard, E., Dillon, N., Azuara, V., Snijders, A.P., Peters, G., Bernstein, E., Gil, J. (2012). MicroRNA regulation of Cbx7 mediates a switch of Polycomb orthologs during ESC differentiation. *Cell Stem Cell* (Vol. 10, Issue 1). https://doi.org/10.1016/j.stem.2011.12.004
203. Bernstein, E., Duncan, E.M., Masui, O., Gil, J., Heard, E., Allis, C.D. (2006). Mouse Polycomb proteins bind differentially to methylated histone H3 and RNA and are enriched in facultative heterochromatin. *Molecular and Cellular Biology* (Vol. 26, Issue 7). https://doi.org/10.1128/MCB.26.7.2560-2569.2006

204. Calvert, R., Bordeleau, G., Grondin, G., Vezina, A., Ferrari, J. (1988). On the presence of intermediate cells in the small intestine. *The Anatomical Record*. (Vol. 220, Issue 3). https://doi.org/10.1002/ar.1092200310
205. Shorning, B.Y., Zabkiewicz, J., McCarthy, A., Pearson, H.B., Winton, D.J., Sansom, O.J., Ashworth, A., Clarke, A.R. (2009). Lkb1 deficiency alters goblet and Paneth cell differentiation in the small intestine. *PLoS One* (Vol. 4, Issue 1). https://doi.org/10.1371/journal.pone.0004264
206. Kamal, M., Wakelin, D., Ouellette, A.J., Smith, A., Podolsky, D.K., Mahida, Y.R. (2001). Mucosal T cells regulate Paneth and intermediate cell numbers in the small intestine of T. spiralis-infected mice. *Clinical & Experimental Immunology* (Vol. 126, Issue 1). https://doi.org/10.1046/j.1365-2249.2001.01589.x
207. López-Arribillaga, E., Yan, B., Lobo-Jarne, T., Guillén, Y., Menéndez, S., Andreu, M., Bigas, A., Iglesias, M., Espinosa, L. (2021). Accumulation of Paneth cells in early colorectal adenomas is associated with beta-catenin signaling and poor patient prognosis. *Cells* (Vol. 10, Issue 11). https://doi.org/10.3390/cells10112928
208. Bertolusso, R., Tian, B., Zhao, Y., Vergara, L., Sabree, A., Iwanaszko, M., et al. (2014). Dynamic cross talk model of the epithelial innate immune response to double-stranded RNA stimulation: coordinated dynamics emerging from cell-level noise. *PLoS One* (Vol. 9, Issue 4). https://doi.org/10.1371/journal.pone.0093396
209. Moschonas, A., Ioannou, M., Eliopoulos, A.G. (2012) CD40 stimulates a "feed-forward" NF-κB–driven molecular pathway that regulates IFN-β expression in carcinoma cells. *Journal of Immunology* (Vol. 188, Issue 11). https://doi.org/10.4049/jimmunol.1200133
210. Lu, R., Moore, P.A., Pitha, P.M. (2002). Stimulation of IRF-7 gene expression by tumor necrosis factor alpha: requirement for NFkappa B transcription factor and gene accessibility. *Journal of Biological Chemistry* (Vol. 277, Issue 19). https://doi.org/10.1074/jbc.M111440200
211. Li, T., Guan, J., Li, S., Zhang, X., Zheng, X. (2014). HSCARG downregulates NF-κB signaling by interacting with USP7 and inhibiting NEMO ubiquitination. *Cell Death & Disease*. https://doi.org/10.1038/cddis.2014.197
212. Murata, K., Jadhav, U., Madha, S., van Es, J., Dean, J., Cavazza, A., Wucherpfennig, K., Michor, F., Clevers, H., Shivdasani, R.A. (2020). Ascl2-dependent cell dedifferentiation drives regeneration of ablated intestinal stem cells. *Cell Stem Cell* (Vol. 26, Issue 3). https://doi.org/10.1016/j.stem.2019.12.011
213. Ogiyama, Y., Schuettengruber, B., Papadopoulos, G.L., Chang, J.M., Cavalli, G. (2018). Polycomb-dependent chromatin looping contributes to gene silencing

during Drosophila development. *Molecular Cell* (Vol. 71, Issue 1). https://doi.org/10.1016/j.molcel.2018.05.032

214. Santanach, A., Blanco, E., Jiang, H., Molloy, K.R., Sansó, M., LaCava, J., Morey, L., Di Croce, L. (2017). The Polycomb group protein CBX6 is an essential regulator of embryonic stem cell identity. *Nature Communications* (Vol. 8, Issue 1). https://doi.org/10.1038/s41467-017-01464-w
215. Benoit, Y.D., Lepage, M.B., Khalfaoui, T., Tremblay, E., Basora, N., Carrier, J.C., Gudas, L.J., Beaulieu, J.F. (2012). Polycomb Repressive Complex 2 impedes intestinal cell terminal differentiation. *Journal of Cell Science* (Vol. 125, Issue 14). https://doi.org/10.1242/jcs.102061
216. Xie, H., Xu, J., Hsu, J.H., Nguyen, M., Fujiwara, Y., Peng, C., Orkin, S.H. (2014). Polycomb Repressive Complex 2 regulates normal hematopoietic stem cell function in a developmental-stage-specific manner. *Cell Stem Cell* (Vol. 14, Issue 1). https://doi.org/10.1016/j.stem.2013.10.001
217. Bracken, A.P., Kleine-Kohlbrecher, D., Dietrich, N., Pasini, D., Gargiulo, G., Beekman, C., Theilgaard-Mönch, K., Minucci, S., Porse, B.T., Marine, J.C., Hansen, K.H., Helin, K. (2007). The Polycomb group proteins bind throughout the INK4A-ARF locus and are disassociated in senescent cells. *Genes Dev*. (Vol. 21, Issue 5). https://doi: 10.1101/gad.415507.
218. Li, J.D., Feng, W., Gallup, M., Kim, J.H., Gum, J., Kim, Y., Basbaum, C. (1998). Activation of NF-kappaB via a Src-dependent Ras-MAPK-pp90rsk pathway is required for Pseudomonas aeruginosa-induced mucin overproduction in epithelial cells. *Proceedings of the National Academy of Sciences U S A* (Vol. 95, Issue 10). https://doi.org/10.1073/pnas.95.10.5718
219. Ahn, D.H., Crawley, S.C., Hokari, R., Kato, S., Yang, S.C., Li, J.D., Kim, Y.S. (2005). TNF-alpha activates MUC2 transcription via NF-kappaB but inhibits via JNK activation. *Cellular Physiology and Biochemistry* (Vol. 15, Issue 1–4). https://doi.org/10.1159/000083636
220. Brischetto, C., Krieger, K., Klotz, C., Krahn, I., Kunz, S., Kolesnichenko, M., Mucka, P., Heuberger, J., Scheidereit, C., Schmidt-Ullrich, R. (2021). NF-κB determines Paneth versus goblet cell fate decision in the small intestine. *Development*. https://doi.org/10.1242/dev.199683
221. Liu, Y., Peng, J., Sun, T., Li, N., Zhang, L., Ren, J., Yuan, H., Kan, S., Pan, Q., Li, X., Ding, Y., Jiang, M., Cong, X., Tan, M., Ma, Y., Fu, D., Cai, S., Xiao, Y., Wang, X., Qin, J. (2017) Epithelial EZH2 serves as an epigenetic determinant in experimental colitis by inhibiting TNFα-mediated inflammation and apoptosis.

Proc Natl Acad Sci U S A (Vol. 114, Issue 19). https://doi: 10.1073/pnas.1700909114.

222. Johansson, M.E. (2014). Mucus layers in inflammatory bowel disease. *Inflammatory Bowel Diseases* (Vol. 20, Issue 11). https://doi.org/10.1097/MIB.0000000000000117

APPENDIX: COLLABORATIONS

The present work, unravelling Polycomb activity in the intestinal epithelium, is part of a huge project that has been performed in collaboration with my colleague Annachiara Del Vecchio, who performed most of the experiments regarding the activity of vPRC1 complexes. Moreover, she contributed to characterize the *Eed*$^{fl/fl}$ and *Eed/Pcgf1*$^{fl/fl}$ phenotypes by performing ChIP and histological techniques.

For what concerns the experiments performed in mESCs, MS-MS analysis of PCGF1-interacting proteins has been carried out by my colleague Eleonora Ponzo.

An enormous work has been performed by the bioinformatician Daniel Fernandez Perez, who analyzed all the generated genome-wide data.

ACKNOWLEDGEMENTS

I would like to thank my supervisor Prof. Diego Pasini for giving me the opportunity to work on these challenging but exciting projects, encouraging me to do my best and supporting my professional growth.

A special thank goes to Prof. Fulvio Chiacchiera, who taught me most of the *in vivo* techniques and strongly motivated me during the first year of my PhD.

I would like to thank all my colleagues, both present and former members, for these four years in which we shared not only “science”, but also life experiences and laughs.

I would like to thank also Karin Ferrari, who helped me to solve scientific problems and give me a lot of personal support.

Among my colleagues, a special thank goes to Simone and Eleonora, trusted friends inside and outside the laboratory.

Thanks to my family, a source of support and good advices. You taught me to be wise, responsible, loyal and always ready to bring out my strengths, but also my vulnerabilities.

Finally, thanks to Manuel, you are the best man in the world and during this last year you shared with me all the moments of this PhD. You are everything to me.